2009

THE USE OF A TRI-AXIAL ACCELEROMETER TO MEASURE CHANGES IN LOWER EXTREMITY FATIGUE DURING FUNCTIONAL ACTIVITY

Kristin Morgan
Virginia Commonwealth University

THE USE OF A TRI-AXIAL ACCELEROMETER TO MEASURE CHANGES IN LOWER EXTREMITY FATIGUE DURING FUNCTIONAL ACTIVITY

A thesis submitted in partial fulfillment of the requirements for the degree of Master of Science at Virginia Commonwealth University

By

Kristin Denise Morgan
Bachelor of Science, Duke University, 2007

Director: Peter Pidcoe, Ph.D., P.T., Assistant Professor, Department of Physical Therapy
Co-Director: Gerald Miller, Ph.D., Chair, Department of Biomedical Engineering

Virginia Commonwealth University
Richmond, Virginia
August 11, 2009

ACKNOWLEDGEMENT

I would like to acknowledge Reebok for sponsoring the footwear used by the participants in this study. I would like to thank Dr. Pidcoe for his help and direction with this project. I additionally would like to thank the Dean's Office for their advice, guidance, and financial support. And finally, I would like to thank my parents for supporting me through this entire process and my brother, Eric, for being a positive role model and encouraging me to keep at it.

TABLE OF CONTENTS

LIST OF TABLES

LIST OF FIGURES

LIST OF ABBREVIATIONS AND DEFINITIONS

vertical Ground Reaction Forces (vGRF): It is the vertical component of the ground reaction forces produced by the supporting surface, which in this case is the forceplate.

Center of Pressure (COP): It is the geometric center of the vertical force distribution on the plantar surface of the foot or the point location of the resultant ground reaction force (GRF) vector in the plane of the ground at which the GRF vector is considered to apply.

Center of Mass (COM): It is the point in a system of particles where the systems concentrated mass acts through.

Time to Stabilization (TTS): The time it takes for the individual to stabilize which is defined in this study as one standard deviation difference between the baseline and output mean.

Time to Peak (TTP): Is the time it takes to reach the maximum or peak value that is being studied.

ABSTRACT

THE USE OF A TRI-AXIAL ACCELEROMETER TO MEASURE CHANGES IN LOWER EXTREMITY FATIGUE DURING FUNCTIONAL ACTIVITY

By Kristin Morgan

A thesis submitted in partial fulfillment of the requirements for the degree of Master of Science at Virginia Commonwealth University

Virginia Commonwealth University, 2009

Director: Peter Pidcoe, Ph.D., P.T., Associate Professor, Department of Physical Therapy
Co-Director: Gerald Miller, Ph.D., Chair, Department of Biomedical Engineering

In 2004, the National Collegiate Athletic Association reported ankle sprain as the most frequent injury in soccer, basketball, and volleyball players. Further research found an increased likelihood with fatigue. Measuring fatigue during functional activities has been a longstanding problem. In this study, changes in ankle biomechanics were measured using a tri-axial accelerometer embedded in the shoe as subjects (n=12) performed a fatiguing activity. Data were collected from the accelerometer and from established devices that are considered the industry gold standard. Several kinetic and kinematic accelerometer derived variables were highly correlated with these standards (r^2>0.90) and were associated with changes in fatigue. The tri-axial accelerometer in this configuration may be suitable for monitoring fatigue during the performance of functional activities.

Chapter 1 - Introduction

Ankle sprains are one of the most common injuries physically active individuals experience. Residual symptoms, like pain or swelling, are reported by 20-50% of these individuals.[5-7] Recurrent ankle sprains occur 18 to 42% of the time.[1-4] Repeated ankle sprains residual symptoms can have large clinical ramifications; specifically, osteoarthritis and articular degeneration.[8, 9] There are also occupational health considerations for recurrent ankle instability. This has been shown to prevent 6% of patients suffering ankle sprain from returning to their occupation. Thirteen to 15% of patients remain occupationally handicapped from at least 9 months to 6.5 years following their injury.[10, 11]

In 2004, the National Collegiate Athletic Association (NCAA) revealed that the most frequent injury reported by both men and women soccer, basketball, and volleyball players is a sprained ankle.[12] Furthermore, the majority of ankle sprains (85%) are due to lateral ankle inversions. Ankle inversions are often the end result of exaggerated, overextensions of the ankle that lead to damage of the ankle ligaments. In sports like soccer, basketball and volleyball where quick changes of direction are needed, these injuries are not only more likely to occur but have a high chance of reoccurring. Studies also found that these injuries were more likely to occur toward the latter stages of the activities when the athletes are fatigued.

Muscle fatigue is one of many factors found to possibly affect ankle control during landing as it believed to impair postural control (stability).[13,14] Postural stability is involved in both static and dynamic movements. Without postural stability, activities such as walking, running, and even standing would be extremely difficult. Given that postural stability is involved in a broad range of motions, it impacts the lives of people of all ages from young athletes to the elderly. Hence, due to fatigues affects on postural and ankle control and stability, it is important to understand what measurements can be made to observe these changes in ankle stability.

This descriptional study will investigate the changes in ankle stability that result from quadriceps muscle fatigue during a landing event. Vertical ground reaction forces (vGRF), lower extremity kinematics, and lower extremity kinetics will be recorded to evaluate changes in the landing biomechanics associated with fatigue. Previous studies have identified biomechanical variables of interests that are important to landing events.[15] These variables include peak vGRF, vGRF impulse, time to stabilization, (maximum) hip, knee and ankle flexion, and force impulse about the hip, knee and ankle. These can be measured using kinetic and kinematic sensors.

Forceplates (kinetic sensors) measure ground reaction force. This is the force the floor (or forceplate) produces when a falling object makes contact.[15] To assist in the analysis of these data, the force is typically broken into 3 absolute referenced axes components; a vertical axis, an anterior-posterior axis, and a medial-lateral axis. Each axis is orthogonal to the others. There are also 3 moments that can be measured; one around each axis. The vGRF is often linked to injury potential. Jump landing forces from level surface high jumps can reach 6.2 times body weight

during the impact phase (first 200ms) of landing.[16] Forces this high can lead to injury. To control these forces and minimize the risk for injury, joint flexion and joint moments are generated.[17]

Motion systems (kinematic sensors) are designed to measure positional changes of the objects to which they are attached. In studies of this type, these are typically used to measure subject limb movements to reconstruct the jumping event in an animation. These data provide a means of comparing performance changes as fatigue develops and often illustrate observable changes. These data also provide objective measures of joint excursions. The combination of kinematic data with kinetic data allows joint torques and forces to be computed using inverse dynamic methods. This provides detailed objective data on each of the lower extremity joints during landing and can be used to evaluate the progressive potential for injury during an imposed fatigue protocol.

Forceplates and kinematic sensors are the well-established gold standard for biomechanical performance measures. In addition to these sensors, the current research is exploring the measurement capabilities of a tri-axial accelerometer mounted in the shoe of the landing foot. It is hoped that this device will provide a simpler method of monitoring fatigue associated changes that increase the potential for injury. Correlations between the forceplate, kinematic sensor data, and the accelerometer data will be performed. Strong correlations between these devices would help to establish the accelerometer as a biomechanical measurement device that could be implanted into a shoe to signal fatigue in athletes prior to injury.

Ankle and Ankle Stability

Many studies have been interested on the role of ankle ligaments on ankle joint stability .[18] In the ankle, the bones and ligaments are responsible for static stability and muscles and tendons are responsible for dynamic stability.[19] To study ankle joint stability or even lower leg joint stability, one must know the various parts that make up the ankle and understand the roles these parts play in ankle stability.

The ankle is often described as having two joints, talocrural and the subtalar ankle joints. [19] The talocrural joint consists of the medial malleolus of the tibia, the lateral malleolus of the fibula of the leg and talus bone of the foot. This joint connects the leg and foot and is involved in ankle dorsiflexion and plantar flexion. [19] The subtalar joint consists of the talus and calcaneus bones and is involved in ankle eversion and inversion. [19] However, these joints alone cannot maintain static ankle stability without the aid of the ankle ligaments.

The major ligaments in the ankle are the anterior talofibular and the calcaneofibular ligament. Both of these ligaments reside on the lateral side of the ankle. The anterior talofibular ligament connects the lateral malleolus to the talus and becomes taut during motions of plantarflexion and inversion. The cancaneofibular ligament connects the fibular malleolus to the calcaneus and becomes taut during motions of dorsiflexion and inversion. Stability during normal range of motion is the responsibility of these two ligaments as a way to protect the ankle joint.[19]

Ankle joints and ligaments play a role in static ankle stability, while skeletal muscles provide dynamic stability and control movements related to postural balance and locomotion. Control of postural balance and locomotion is done through concentric, eccentric, and isometric

muscle contractions.[20] Eccentric contractions are contractions where the muscle lengthens often acting to oppose a movement or motion (decelerate motion). The other dynamic stabilizers are ankle tendons. Ankle tendons, such as the peroneous longus tendon and the peroneus brevis tendon, connect muscles to bones transmitting the muscles forces across the ankle joint. [19] These tendons span underneath the foot, connecting to the big and little toe. [19]

Structurally the foot is divided into three parts: the forefoot, midfoot and hindfoot portions. The forefoot includes the metatarsals and phalanges, the midfoot contains the tarsal bones and the hindfoot contains the talus and calcaneus.

In the forefoot, the phalanges make up the first three bones for all of the toes except the big toe where they make up the first two bones. Behind the phalanges are the metatarsals and they are the five longer bones in the foot.

The midfoot includes a collection of odd-shaped tarsal bones: the navicular, cuboid, and the three cuneiform bones. The tarsal bones are a collection of seven bones that link the ankle and the foot. Since they are linked, it means the bones have to coordinate the activities of the ankle and foot. Together these bones must ensure mobility as well as provide stability during all weight-bearing events. In order to serve this purpose, each tarsal bone must serve a different function.

The three cuneiform bones are another collection of bones with a very special purpose. These three bones stretch across the arch of the foot as indicated by their names: medial, intermediate and lateral cuneiforms. While they do participate and withstand the impact and loading forces associated with the foot, they have more of a role as the stabilizing portion of the foot.

Due to the size of the foot and the major weight-bearing role it plays, it is only logical that the various bones work together to withstand the force of the load. This is the case with the calcaneus, navicular and talus bones, which make up the hindfoot. These three work together to diffuse the weight of the body throughout the foot. Since the talus connects the ankle and the foot, it transmits forces from the ankle to the other bones in the foot. The calcaneus, which is commonly known as the heel, is the largest bone in the foot and it withstands and transmits significant forces, specifically from the hind to the forefoot. The navicular is wedged in between the talus and three cuneiform and serves to transmit the forces from the talus to them.

When discussing the foot, ankle, and even postural stability, one must also consider the notion of postural strategies. Postural strategy refers to the control actions employed to maintain body balance.[21] Ankle and hip strategies are essential elements of postural strategies.[22,23] The hip strategy resolves the actions of the joints in the lower leg extremity while the multi-chained unit of the hip serves as a pivot point. This strategy implies that adjustments for stability or balance are segmented actions. The ankle strategy (secondary role) functions like an inverted pendulum where all of the adjustments are made at the ankle and the rest of the body above the ankle acts as a single, connected rigid body. [21] These dual strategies highlight the role that the joints of the lower leg extremity, especially the ankle, play in postural stability.

Fatigue

Neuromuscular fatigue is defined as the decreased capacity of muscle fibers to absorb energy and produce force.[24] Previous research has studied the effects of muscle fatigue which have reported that (muscle) fatigue leads to decreased motor control performance, decreased

balance skill and decreased proprioception .[25] All of these effects are associated with lower extremity muscle fatigue and are related to maintaining stability/balance.

Lower extremity fatigue can be induced in a number of ways. It is typically accomplished via a sustained isometric muscle contraction or repeated concentric/eccentric muscle contractions in a constrained time period. Christina, White and Gilchrest[26] performed a study where they induced muscle fatigue through exhaustive running. Exhaustive running was chosen as a fatiguing measure because it had been reported that running induced muscle fatigue and leads to changes in ankle landing forces and motions that can result in injury.[27] The results from their study found that fatigue led to an increase in loading rate, peak magnitudes, and ankle joint in running. [27] Although their running fatigue protocol produced the above results, they acknowledged that they could not be certain which of these changes were truly a result of the lower extremity fatigue. [26] This result highlighted the importance of selecting an appropriate fatiguing protocol for the extremity and/or joint in question.

Since this study is interested in the biomechanics of the landing events of the ankle, a fatiguing protocol that included a series of squats and jump landings was chosen. Squats were used to induce fatigue in the quadriceps muscles. Inducing fatigue in the quadriceps instead of other muscle groups in the lower extremity will exhibit the appropriate changes (characteristics) in landing biomechanics sought, which are lower extremity ground reaction forces, lower extremity joint kinematics and lower extremity joint kinetics. Previous researchers have studied the differences between fatiguing the hamstrings and the quadriceps.[28] One such study isolated hamstring and quadriceps fatigue through landing actions. It was observed that hamstring fatigue resulted in decreased peak impact knee flexion moments, peak ankle dorsiflexion, and

increased internal tibial rotation at peak knee flexion. However, the quadriceps fatigue that resulted from this landing motion caused an increase in peak ankle dorsiflexion moments, a decrease in peak knee extension moments, delayed peak knee flexion and delayed subtalar peak inversion moment .[28] Since quadriceps fatigue will be induced through the fatiguing protocol, involving a series of squats and jump landings, these changes may also be observed in this study.

Accelerometers

In the 1950s accelerometers became a viable option for capturing dynamic movement.[29,30] Initially the accelerometers were uni-axial, bulky and expensive. Teramoto et al. used uni-axial accelerometers to measure shock attenuation in female runners.[31] Two uni-axial accelerometers were placed at the forehead and on the tibia to determine shock attenuation at these locations. The researchers fatigued the runners using a protocol that included a series of concentric and eccentric contractions on a commercial exercise device followed by a one-minute run on a treadmill.[31] The accelerometers measured impact accelerations that were then used to calculate shock attenuations. These results revealed an increase in both the head and leg accelerations from the non-fatigued to fatigued states as accelerations increased from 1.12 +/- 0.33 to 1.47 +/- 0.86 g's for the head and from 3.96+/- 0.78 to 4.95+/-0.47 g's in the leg.[31] These results also indicated an increase in shock attenuation for the transition from the non-fatigued to fatigued state. However, only significant changes were observed for the leg accelerations and the shock attenuations.[31]

Accelerometer technology has continued to improve with the development of smaller, lighter and relatively inexpensive devices. Accelerometers have evolved from measuring accelerations in only one direction to three. The ability of the tri-axial accelerometer to measure

accelerations in three directions enables the device to estimate dynamic functions at different joints.[32,33] Capturing the dynamic functions of joints means that it is possible to monitor and analyze joint movement during every phase of motion. Henriksen and Moe-Nilssen[34] studied the reliability of such accelerometers for gait analysis. The results indicated that the accelerometer was able to reproduce the same results on the same subject group on two different days with respect to step, stride length, and cadence. The validation of the accelerometer output data was established by comparing its performance to established forceplate and kinematic sensor systems.

Alderton and Moritz[21] looked at the correlation between the forceplate and tri-accelerometer in an investigation of one-legged postural control during muscle fatigue. The study observed females postural stability pre and post a fatiguing exercise. The fatiguing exercise involved performing calf raises until they could no longer perform any more. Forceplates were used to measure center-of-pressure velocity and amplitude in the medial/lateral and anterior/posterior direction, while a trunk accelerometer measured accelerations in the medial/lateral and anterior/posterior direction.[21] The results showed significant increase in trunk acceleration and center-of-pressure amplitude in both directions, and a significant decrease in center-of-pressure velocity in both directions.[21] Further analysis of the results concluded that there was a moderate correlation between forceplate center-of-pressure measurements and trunk accelerometer accelerations. While moderate correlations were reported between the trunk accelerometer and the forceplate, Alderton and Mortiz did acknowledge that the trunk accelerometer was better for measuring changes at the hip and trunk. Since the trunk accelerometer was able to measure changes at the trunk that correlated to changes at the

forceplate, the placement of the tri-axial accelerometer in the shoe should be effective for identifying such changes at the ankle.

The improvements to accelerometers, especially the evolution of the tri-axial accelerometer, have lead to the development of a portable device that is able to collect the same data as the foot switches, kinematic sensors, and forceplates. Due to these improvements more applications for the accelerometer have been created. Some examples have included measuring changes in gait and balance in the elderly to provide fall risk assessment[35], determining the energy expenditure during physical activity[36], and overall body movements. In this study, a tri-axial accelerometer will be used to monitor changes in the foot associated with fatigue that may predispose someone to ankle injury.

Accelerometer Placement

Bates, Ostering & Sawhill[37] stated that the feet form the human body's force transfer interface and offer more leverage for improving athletic performance than any other part of the body. For instance the forces generated from muscle contractions are transferred to the foot upon contact with the ground.[37] The foot, which can aid in stability, mainly serves as the weight-bearing load of the body and, as the weight-bearing structure, it has to withstand the impact due to various forms of locomotion as well as the normal forces associated with standing.[38] This study is interested in the movements at the ankle/foot joint with respect to fatigue. In addition to capturing these movements with the traditional forceplate, a tri-axial accelerometer was placed in the heel of the shoe to see if it was able to capture important features associated with the performance of proximal joints.

The forces experienced by the forceplate are the reaction forces between the individuals shoe and the forceplate surface. A limitation of the forceplate is that it cannot produce information about the distribution of forces on the foot.[39] The bones of the hindfoot transmit forces exerted on and by the body. [38] The hope is that the placement of an accelerometer at the heel of the foot will measure these forces during the jump landing event. However, the drawback here is that the accelerometer measures the accelerations experienced at the heel of the foot inside the shoe. These differ from the forces at the shoe-floor interface. Despite the discrepancies in the measurement locations, it is anticipated that the accelerations experience by the accelerometer in the shoe will pick up the same forces and movements exerted on the forceplate allowing a correlation to be drawn between the two devices.

Accelerometer and Time to Stabilization

Prior research has found that fatigue has an effect on postural stability. In attempts to maintain postural stability, individuals modify hip and ankle strategies. While it is unclear why individuals adopt one strategy over the other, this study focuses on changes at and around the ankle/foot joint. The placement of the accelerometer in the heel of the shoe will provide information about the dynamic movements occurring at the ankle/foot joint. A convenient way to measure the dynamic (ankle) stability is through the time-to-stabilization (TTS). Dynamic stability is defined as maintaining the center-of-mass over the base of support as this base of support is moving or perturbed by an external force applied to the body.[40] To successfully complete the jump landing / fatigue protocol, the subject must land the jump without falling meaning they must maintain their balance or rather maintain their center of mass over the base of support, their foot. The time it takes for the subject to become stable is defined as the time to

stabilization. Researchers Brown and Mynark[40] studied the effects of chronic ankle sprains on ankle stability by measuring how long it took for the individuals to stabilize following tibial nerve stimulation. A study by Shaw et al.[13] examined the effect of fatigue on time to stabilization for volleyball players as they performed jump landing task with and without an ankle brace. Both the Brown and Mynark and Shaw et al. studies found that TTS increased fatigue. Wikstrom studied the effects of fatigue on time to stabilization in healthy males and found TTS decreased with increasing fatigue.[41]

The study by Shaw et. al. [13] examined the effect of fatigue on time to stabilization for volleyball players as they performed jump landing task with and without an ankle brace. This study was motivated by the report that (during athletic competition) fatigue may alter neuromuscular control and may decrease the body's ability to maintain stability.[42,43] Jump and landing activities account for 79 to 87% of all lateral ankle sprains. [13] Thus using jump landings to fatigue individuals, such as in this study, is a type of functional fatigue. Wikstrom identified time to stabilization as a functional measure of joint kinesthesia and position and because of this can be used to assess the functional effects of fatigue on neuromuscular control and dynamic stability. [41]

Impaired strength of ankle muscles and proprioceptive function of ankle ligaments may be attributed to functional ankle instability.[44] Impaired proprioception of the ankle ligaments, damages the sensory receptors decreasing the communication between the joint movement and position and the afferent pathways.[44,45] The stimulation of mechanoreceptors produces increased afferent signaling and peroneal response.[46] The response of peroneus muscle is needed to aid in the dynamic stability and control movements related to postural balance and locomotion. Shaw

et al. study was motivated by the report that (during athletic competition) fatigue may alter neuromuscular control and may decrease the body's ability to maintain stability. [42,43] And in this study, the dynamic functional measurement of time to stability will be used to assess the effects of (neuromuscular control on) postural control and stability due to fatigue at the ankle.

Forceplate and Center of Pressure (COP)

Single leg jump test challenge the dynamic postural control system and aid in the understanding of dynamic postural stability.[44] It is during these times of postural instability (i.e. jump tests) that the forceplate measures changes in center of pressure position. [44] The center of pressure (COP) is defined as the geometric center of the vertical force distribution on the plantar surface of the foot or the point location of the resultant ground reaction force (GRF) vector in the plane of the ground at which the GRF vector is considered to apply.[47] In the case of jump landings, the COP is the theoretical point between the foot and the forceplate where all of the weighted averages of all forces are centered. The COP controls the body's center of mass (COM) and is responsible for restoring equilibrium forces.[48,49] The ankle muscles produce these restoring equilibrium forces and, detailing the change in the COP, will provide information about the control strategies needed for stability.[50] The COP is a variable of interest because it is surmised that changes in balance that may require control strategies can be deduced from COP displacement and velocity. The COP path length measures the amount of biomechanical adjustments made at the ankle/foot. [48] Longer COP path lengths mean more adjustments and movements were made at the ankle/foot to stabilize the COM and maintain balance. Harringe et al.[51] measured COP path length in gymnast with lower back pain and lower extremity injury on hard and foam surfaces. That study entailed dividing the gymnasts into four groups (non-injured,

lower back pain only, lower extremity injury only, and multiple injury) and measuring the COP path length in quiet stance on both hard and foam surfaces with their eyes opened and closed. These results showed an increase in COP path length for all groups on the foam surface with the lower back pain group recording the largest COP path length. [51] The longer COP path length in the lower back pain group was believed to be a result of stiffening of the spine that required a more focused ankle strategy to maintain balance. [51]

COP path length was also used to evaluate the difference in balance between bare-foot and high-heeled women. [48] The women's COP was measured using a two waist-pulling system to determine perturbed differences. The first waist-pulling system used falling masses of 1, 2, and 3 kg to perturb the subjects and the other system involved the use of an air cylinder compressor. [48] The results from this study saw the COP path length increase with an increase in masses when comparing high heels to bare feet. In fact, there was a 200% increase in COP path length reported for the high-heeled group versus the barefoot group.

Both of these studies show that a lack of stability, whether it be the result of injury (lower back pain and lower extremity injury) or unstable base (high heels), represents a decrease in postural control and an increase in possible injury or fall. [48] The lack of postural control was expressed as increased COP path length. Thus, in this study, the force plate will also be used to measure COP path length, area and velocity to investigate postural control, the underlying ankle strategy used to maintain balance and stability and the COP's role in postural control strategies[50] at the ankle with the onset of fatigue.

Measurements

A study by Madigan and Pidcoe[15] observed changes in landing biomechanics with fatigue. Many of the variables of interest mentioned above (vGRF, vGRF Impulse, joint flexion and moments) are variables he studied, with the exception of time to stabilization and center-of-pressure. Time-to-stabilization is an additional measurement used to understand dynamic stability. Many studies have used forceplates to calculate time-to-stabilization[13,40,41]; however, with the addition of the accelerometer, this device can also be used to calculate this variable.

Center-of-pressure analysis will also be used for stability measurement. Forceplates are the gold standard for center-of-pressure measurements and thus this study will rely on the forceplate for those calculations.

According to Adlerton and Mortiz, forceplates and accelerometers are valuable tools to measure different aspects of balance control[21] and in this study these devices will be used to observe changes in balance control with fatigue.

Summary

This is a descriptive study investigating how fatigue effects lower extremity biomechanics during landing. It is hoped that accelerometer data will be sensitive to these changes and therefore be capable of monitoring fatigue. Since fatigue is associated with the potential for injury, this device may have commercial application. The goals of this study are outlined below in the research questions and associated research hypotheses.

Research Questions

R1: Will medial-lateral time-to-stabilization (during landing) increase as a result of quadriceps muscle fatigue?

R2: Will joint torque (during landing) proximal and distal to the knee increase as a result of quadriceps muscle fatigue?

R3: Will accelerometer data provide a useful and simpler metric in the measurement of kinetic and kinematic markers associated with lower extremity fatigue?

Research Hypotheses

H1: Medial-lateral time-to-stabilization (TTS) during the impact phase of landing (0 to 200ms) will increase with lower extremity fatigue.

Previous research has shown that the time to stabilization is larger in individuals who possess chronic ankle injuries or are fatigued.[13,40] Both studies reported significant increase in TTS in the anterior/posterior direction. An increase in medial lateral TTS is expected based on those studies results. The time to stabilization information will allow us to better understand the effects of fatigue on dynamic stability[41] and establish the accelerometer as a viable tool for measuring and studying dynamic stability.

H2: Ankle and hip joint torque during the impact phase of landing (0 to 200ms) will increase with quadriceps muscle (knee joint) fatigue.

Fatigue decreases the muscles ability to produce force and therefore decreases the capacity of muscle fibers to absorb energy.[2] The decreased ability of lower extremity muscles to produce force can lead to increased joint movement during landing.[41] Muscle force production is directly related to torque since the muscle acts through a moment arm to create rotation at the joint. As the quadriceps muscle fatigues, it will be less able to support the loads presented during landing.

These loads will have to be transferred to proximal and distal joints. A study by Nyland found that quadriceps fatigue led to increased ankle torque production.[28] This transfer of load distally may overload the ankle joint and increase the potential for injury. According to Robinovitch et al., stability recovery is dependent upon the magnitude and velocity at which lower extremity torques can be developed.[52] They observed how decreases in torque magnitude and time to development led to higher incident of falls in the elderly. [52] This study is designed to induce quadriceps muscle fatigue. A compensatory increase in ankle torque is expected.

H3a: Accelerometer magnitude will be correlated with translational kinetic data during landing.

H3b: Accelerometer rotational derivatives along an anterior-posterior foot axis will be correlated with rotational kinetic data during landing.

Accelerometers are able to obtain force (kinetic) and position/orientation (kinematic) data. Correlations between these measures and fatigue state may provide a useful tool capable of warning the wearer of changes in the potential for injury.

Operational Definitions

Vertical Ground Reaction Forces (vGRF): It is the vertical component of the ground reaction forces produced by the supporting surface, which in this case is the forceplate.

Time to Stabilization (TTS): The time it takes for the individual to stabilize which is defined in this study as one standard deviation difference between the baseline and output mean.

Center-of-pressure (COP): It is the geometric center of the vertical force distribution on the plantar surface of the foot or the point location of the resultant ground reaction force (GRF) vector in the plane of the ground at which the GRF vector is considered to apply

Center of mass (COM): It is the point in a system of particles where the systems concentrated mass acts through.

Chapter 2 - Methods

The purpose of this study is to investigate how ankle stability is affected by quadriceps muscle fatigue and if a tri-axial accelerometer can be used to monitor these changes. Madigan and Pidcoe[15] conducted a similar study that observed changes in landing biomechanics at the onset of fatigue. Madigan and Pidcoe's study reported a decrease in vertical Ground Reaction Forces (vGRF) and increased lower extremity joint flexion during landing with quadriceps muscle fatigue.[15] In that study, quadriceps muscle fatigue was induced by participation in a single leg squat fatiguing protocol combined with repeated single leg landing events. In the present study, a similar fatigue protocol is employed. Biomechanic performance metrics are taken using a tri-axial accelerometer, forceplate, and kinematic sensors.

Subjects

Subjects were recruited from a sample of convenience and volunteered to participate in this study. Consent to participate in the study was obtained from each participant. Twelve subjects (seven males, five females) participated (mean weight 69.5 +/- 9.1kg and mean height 160.8+/-6.8cm, 25.7+/-4.6years). It is important to note that while thirteen subjects performed the jump landing fatigue protocol, the accelerometer analysis data only included nine subjects due to equipment malfunction.

The malfunction being that a broken wire created an open ended input resulting in cross talk that contaminated a channel of data. These results are noted and discussed separately in later sections of this document.

Fatigue Landing Activity/Fatigue Protocol

Prior to performing the fatigue protocol, subjects were fitted with shoes that had a tri-axial accelerometer (Analog Devices model ADXL330, +/-3g, 3 –axis, 300mV/g sensitivity, and bandwidth range 0.5-1600Hz in X,Y and 0.5-550Hz in Z direction) mounted in the heel of the right shoe. Sport shoes were donated by ReeBok and were sized to fit each participant. The accelerometer was oriented so that the X axis (Ax) was aligned in the medial/lateral direction of the foot, the Y axis (Ay) was aligned in the fore/aft direction of the foot, and the Z direction (Az) was aligned with vertical. Each subject also had a kinematic sensors (Motion Monitor™, Innovative Sports Training, Inc) placed on their person to monitor their movement during the landing activity. These sensors were capable of measuring 6 DOF kinematic data at a sampling rate of 100Hz per channel. Sensors were placed at the following four locations: the sacrum (base of the spine), the outside of the right thigh, the right shank on the tibia bone, and one interwoven into the laces of their right shoe. Anatomical landmarks were recorded using standard methods to define each body segment. These data were used to reconstruct a geometric representation of the trunk and right lower extremity of the subject.

After being properly fit with shoes and sensors, each subject was asked to stand in an anatomically neutral position. Baseline data were recorded on which to standardize future movements. Next, each subject began the fatigue protocol. The fatigue protocol involved a

series of single leg squats followed by a single jump landing event. The subject began the fatigue protocol standing on the left edge of a 9 inch high stool (23cm) on his/her right leg. Arms were crossed against the chest to minimize upper extremity movement. The stool was positioned directly behind the forceplate to the right of center. From this position, a forward jump would result in a centered landing on the forceplate. Standing in the correct experimental position (as seen in Figure 1), the subject proceeded to perform the fatiguing protocol. This consisted of 3 squats; squatting low enough each time so that the heel of the free leg (left leg) made light contact with the ground. The squats were then immediately followed by a jump onto the center of the forceplate. The subject was instructed to land solely on the right leg. They were also asked to avoid a multiple contact landing (e.g. a hop) and to hold that position for 1 second. The end of the jump landing event marked the completion of one full cycle of the fatiguing protocol. The subject was asked to repeat the cycle as many times as possible, stopping when they felt that the next landing would result in a fall. Landings were monitored by a spotter to avoid the potential for injury.

Figure 1: Fatigue Protocol Subject Set Up

Data Collection

In addition to the kinematic and accelerometer data, ground reaction forces (GRF) were collected during each jump landing event (Bertec forceplate model FP4060-NC,0.44N/mV sensitivity in the X,Y direction and 0.89N/mV in the Y and a 500Hz Bandwidth). The GRF (and accelerometer) data were sampled at 1000Hz per channel. The data collection window was five seconds and it was stored in a circular buffer. The forceplate triggered the end of an activity and collected an additional three seconds of data. Thus resulting in a data stored stream of two seconds pre and three seconds post trigger. The total number of jumps varied across individuals since each subject was defining their own end point. All data were collected synchronously

through the MotionMonitor™ computer system. Following each experiment, data were exported for offline processing.

The accelerometer was powered by a regulated 3.0V DC supply. This resulted in a linear scaling factor of 0.300V per G (gravity). The multiplication of the number of G's by the gravitational constant (9.81m/s^2) was used in the accelerometer calculations given below.

$$G's = \frac{(V_{out} - 1.50V)}{0.300V} \qquad \text{Equation 1}$$

$$Magnitude\ of\ G's = \sqrt{(X_g)^2 + (Y_g)^2 + (Z_g)^2} \qquad \text{Equation 2}$$

$$Acceleration\ (m/s^2) = (\text{Magnitude of G's}) \times (9.81\text{m/s}^2) \qquad \text{Equation 3}$$

The tri-axial accelerometer was used to determine force and orientation data. Force was determined by scaling the acceleration data by the mass of the subject. Orientation (or angle with respect to horizontal) was calculated using the law of cosines. Orientation data were used to assess changes in rotation during the landing event. All accelerometer data were adjusted for offset based on the baseline data collected in anatomical position at the start of each experiment.

Data Analysis

Data analysis focused primarily on the impact phase of the landing event. The impact phase as defined by Madigan and Pidcoe[15] was the first 200 ms (milliseconds) after contact with the forceplate. They found that defining an impact phase provided a consistent landing interval for all subjects and as Lees[53] observed most of the impact, absorption, and downward body deceleration occurred during this 200ms period. Thus, in this study, the peak vGRF, vGRF impulse (accelerometer impulse) were analyzed over a 200 ms impact period.

Forceplate data

The forceplate measured the ground reaction forces and torques. Three biomechanical variables of interests were dependent upon vertical Ground Reaction Force (vGRF) data: the peak vGRF and the vGRF impulse. The peak vGRF was determined to be the peak vGRF during the impact phase after each landing force had been normalized by the subject's weight. The vGRF impulse was calculated based on norms using the subject's height and weight. The vGRF was then integrated over the 200ms impact period to obtain the impulse. This numerical integration was performed using the MATLAB™ "trapz" sub-routine.

The forceplate was also used to calculate the overall excursion path length for the COP. The excursion path length is cumulative distance between sequential COP points in the medial/lateral and anterior/posterior directions. The magnitude of the distances/path lengths in the medial/lateral and anterior/posterior directions were used to obtain the overall excursion path length for the center of pressure. In addition to the COP path length, the COP area was determined for the 200ms impact period.

Kinematic Sensor data

The kinematic sensors provided temporal and positional data at the sacrum, right thigh, right shank, and right foot. From these sensors, maximum joint excursions, sacrum movement (jump height), joint impulse and net muscle moment (joint torque) about the lower extremity joints were obtained.

The kinematic sensors were also used to measure joint flexion at the hip, knee and ankle during landing. Maximum joint flexion and time to maximum joint flexion were calculated during the first 500ms after landing. Joint flexion data were analyzed up to 500ms after landing

since subjects continue to fall and bend after the 200ms impact phase in an attempt to further decelerate and control the landing. The maximum joint flexion was determined as the largest joint flexion generated during the first 500ms of landing minus the baseline flexion values.

The joint impulse at the hip, knee and ankle was calculated from the normed (joint) force by integrating this force over the 200ms impact period. This is consistent with the method used to compute the vGRF impulse. Jump height was recorded as the maximum sacral height achieved during the flight phase of the jump. Kinematic data were analyzed in both the sagittal and frontal planes.

Accelerometer data

The accelerometer was placed in the heel of the shoe with an approximate orientation aligning the Z axis to a superior-inferior subject axis, the Y axis to an anterior-posterior subject axis, and the X axis to a medial-lateral subject axis as shown in Figure 2. These data were adjusted to compensate for any misalignment by applying an orientation matrix. This matrix was defined from data collected during anatomical baseline. In this static anatomical position, X and Y readings should be zero and the Z reading should equal 1G. The tri-axial accelerometer data was used to determine impact phase properties that included time-to-stabilization.

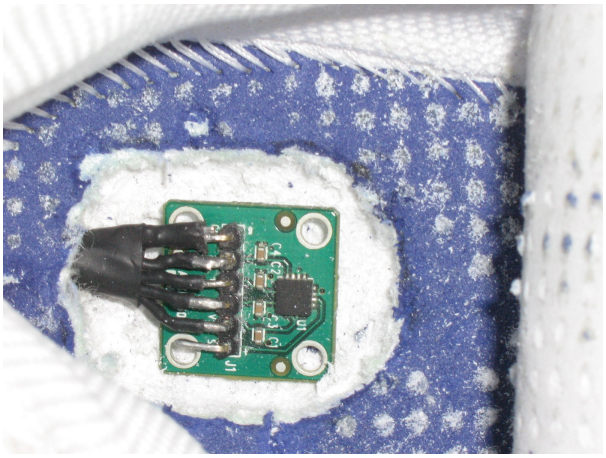

Figure 2: Orientation of Tri-axial Accelerometer in Shoe

vGRF → The vertical ground force impulse was calculated from the accelerometer output (G's) in the Z direction. Like the vGRF impulse data, the vertical ground force impulse was determined by integrating the vertical ground force impulse in the Z direction over the 200ms impact period.

TTS → The time-to-stabilization in the medial/lateral direction and the anterior/posterior direction were each calculated using the same criteria. First, an average baseline accelerometer output was calculated from the stationary baseline data. These were considered offset and were subtracted from all subsequent measures. The standard deviation was computed to establish boundaries for a measure of stability. During landing, each subject's accelerometer data was evaluated and compared to a one standard deviation envelope. TTS was defined as the point when this signal stayed within the envelope. These measures were compared to similar measures from the forceplate to assess the overall validity of the accelerometer measurements.

Data Transition Methodologies for Accelerometer Data

Figure 3a depicts typical accelerometer data for a jump landing. The raw voltage readings are from the X-axis which was orientated in the medial/lateral foot direction. These data were sampled at 1000Hz and each trial lasted 5s. The data collection program (Motion Monitor™) utilized a circular buffer which allowed the end of each collection cycle to be triggered by initial contact. This "landing" was defined to be aligned with the 2s time mark. The acceleration signature prior to this 2s is a result of airborne movement prior to landing. The second accelerometer burst in this figure (at approximately 4s) shows the subject stepping off of the forceplate. Figure 3b is an extraction of the first 500ms of data following landing (the 2s mark of Figure 3a). During the first 200ms of this interval major oscillations are observed followed by a relatively slow decay to a steady state. In figure 3c the ordinate has been scaled by the magnitude of the acceleration vector, mag (a). With figure 3d the steady state ordinate value has been subtracted. This figure also contains the standard deviation envelope used to determine the TTS.

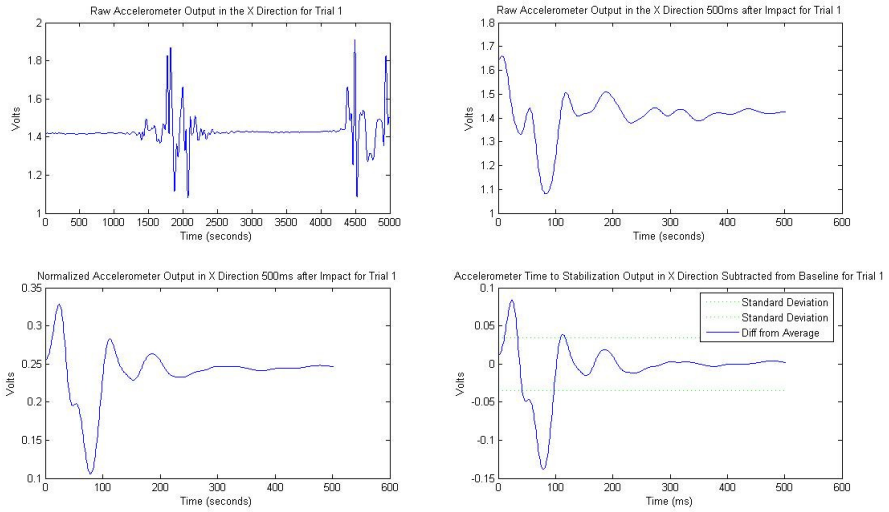

Figures 3a-d: Raw Data Transformation Seqeunce

Second Order Polynomial and Normalized Time

Each subject performed the three squats /one jump sequence until they could no longer land without falling. Establishing this criterion as the stopping point ensured that each subject reached a roughly equivalent state of fatigued. Because the protocol ended based on a subjective decision, trial lengths varied from a minimum number of jumps (13) to a maximum number of jumps (70). These data were normalized from 0 (unfatigued) to 1 (fatigued) in 10% intervals by fitting raw data with a second order polynomial routine ((MATLAB™) and re-sampling, this was consistent with previous research by Madigan and Pidoce[15]. All of the data (forceplate, kinematic sensor, accelerometer) were temporally adjusted using this protocol.

MATLAB™

All of the data analyses were carried out using MATLAB™. Source code is provided in Appendix B.

Statistics

The data interpretations were assessed after fitting all data with a second order polynomial. Appropriate statistic analysis was performed using the Minitab™ software package. Preliminary analysis using Minitab™ produced boxplots of the data that was used to identify outliers in the data. Data plots are shown with 95% confidence intervals encompassing each data value at 0.1 time interval (i.e. 0.1, 0.2, 0.3 etc.) and compared against initial un-fatigued values, to determine if there was a significant difference between the initial and fatigued responses. Correlation between the vGRF magnitude and accelerometer magnitude and foot inversion and accelerometer angular orientation were done.

Chapter 3 – Results

These results summarize the variables used to evaluate the jump landing during the fatigue process. Variables include: vGRF, time to vGRF, vGRF impulse, COP path length, COP area, COP velocity, frontal and sagittal plane kinematic and kinetic, sacral height and time-to-stabilization. Response curves are provided and are compared to like studies. Work by Madigan and Pidoce[15] is used as a primary comparator since this study was performed in the same lab and served as a pilot to current work. The sagittal plane joint response curves from Madigan and Pidcoe's study are overlaid on top of those plots to highlight the results similarity. A statistical comparison of accelerometer data with kinetic and kinematic data is also provided in an effort to provide evidence of validation.

vGRF

Figure 4 displays the average peak vertical Ground Reaction Forces (vGRF) that occurs during the first 200ms after landing on the forceplate. The vGRF values were plotted at every 0.1s time interval and were taken for the entire fatigue protocol for each subject. For the data, the analysis of variance (ANOVA) was used to extend the two-sample t-test for testing the equality of the means of two populations or factor levels to a more general null hypothesis of comparing the equality of more than two means, versus them not all being equal. Specifically, for the one-way analysis of variances conducted in this work, the investigation focused on testing the equality of the mean levels of the response variable (vGRF, hip joint flexion, knee joint flexion, etc.) at the different

normalized time interval levels (0, 0.1, 0.2, 0.3, etc.). The asterisk shown on the bar indicates that mean average peak vGRF at that normalized time was significantly different (p-value <0.5) from the mean average peak vGRF at the normalized time of zero, the un-fatigued state. The maximum peak vGRF decreased from 3.49 to 3.00 times body weight for an average drop of 14.0% as compared to a decrease of 27% for Madigan and Pidcoe's data.[15] This difference was found to be statistically significant (p<0.5).

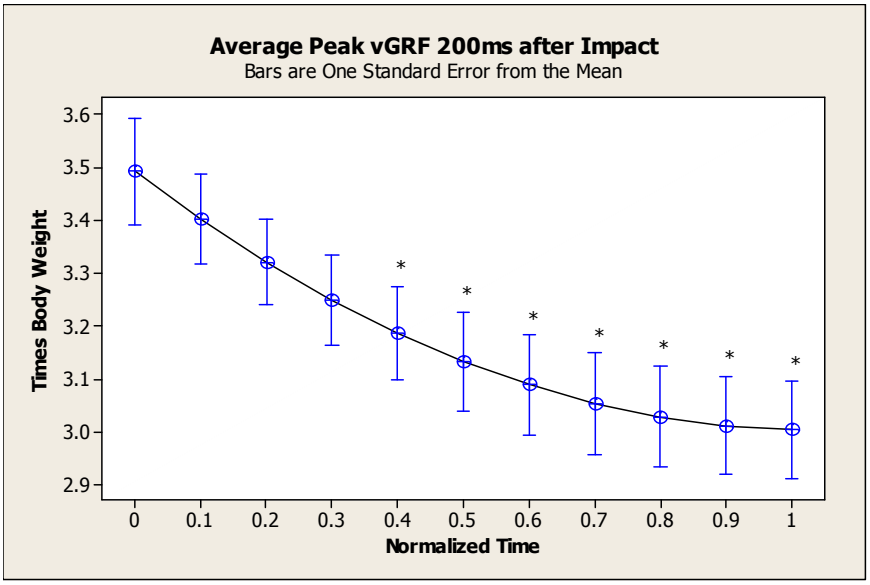

Figure 4: Average Peak vertical Ground Reaction Forces (vGRF)
(* indicates statistical difference from initial value p<0.5)

Figure 5 provides a plot of the average time-to-peak vGRF values for all twelve subjects evaluated in this study. These results exhibit a different pattern than the Madigan and Pidcoe's findings where the time to peak vGRF gradually decreases from 75.2ms to 74ms.[15] With the current investigation a maximum vGRF (74.9 ms) is

observed at a normalized time of 0.4. Unlike the Madigan and Pidcoe data pattern, initially there is a rise in the slope of the current data followed by a relatively sharp drop to a minimum of 70.0 ms at the end of the test period.[15] A total maximum deviation of 3.6ms is noted for this population. This difference is not statistically significant ($p<0.5$).

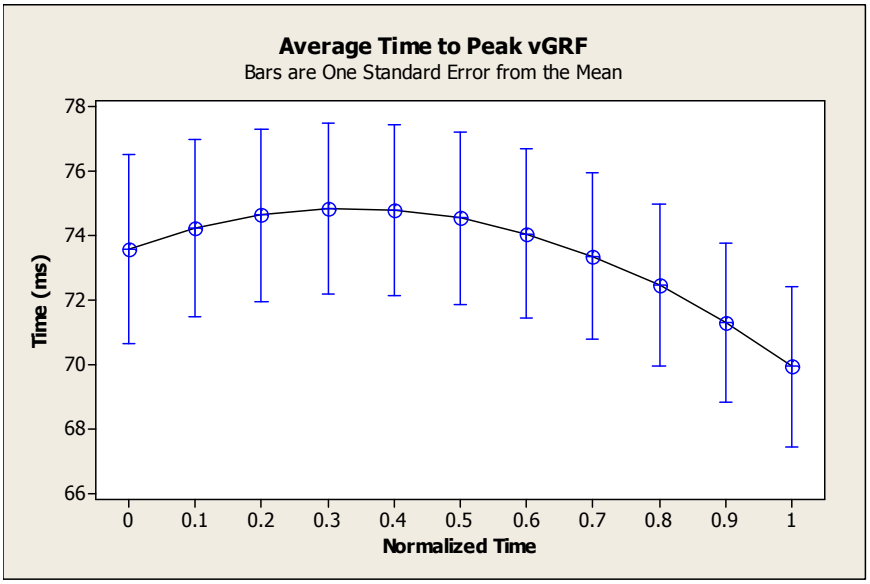

Figure 5: Average Time to Peak vGRF

vGRF Impulse

Figure 6 is a plot of the average vGRF impulse calculated over a 200ms impact period. Both studies (current and Madigan and Pidcoe's study) show a decrease in vGRF impulse with increasing fatigue. The vGRF impulse decreased from 0.378 to 0.356, a drop of 0.022 N-s/kg-m (-5.80%) and is close to the value of 0.023 N-s/kg-m (-5.95%) found by Madigan and Pidcoe .[15] Only the final (fatigued) value in the current study data is significantly different from the initial (unfatigued) value ($p<0.5$).

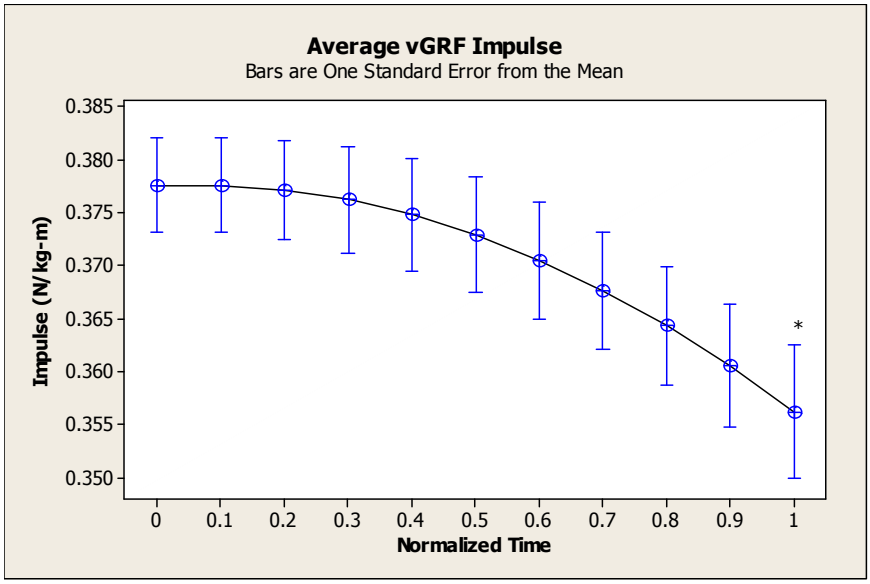

Figure 6: vGRF Impulse
(* indicates statistical difference from initial value $p<0.5$)

Figure 7 shows a plot of a single subjects' vGRF during the first 500ms of the jump/landing event for both an initial (un-fatigued) state and a final (fatigued) state. The plots as shown in Figure 7 are typical of the diminished vGRF responses generated by all the subjects. A drop-off in initial slope with fatigue is noted even-though the maximums are observed at essentially the same time. After the maximum is reached, there is a rapid decay in the dynamics over the next 150 ms and then a relatively steady decay to a common steady state. The net maximum vGRF deviation is 1.5 times the total body weight.

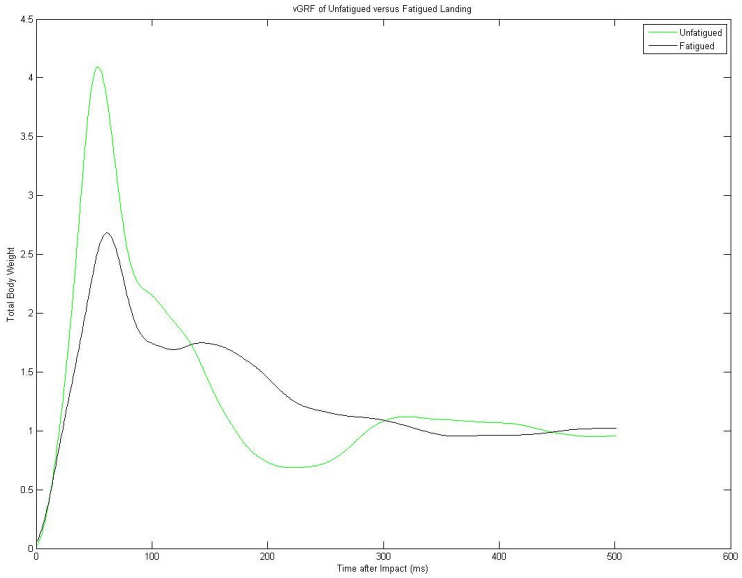

Figure 7: vGRF Unfatigued (green) and Fatigued (black)

COP Path Length

The COP path length movement is captured in Figure 8. The composite COP path length decreased 0.003m (-1.2%). Comparatively, in the study by Alderton and Mortiz where subjects were fatigued through repetitive calf raises, an increase in COP path length with fatigue was observed.[21]

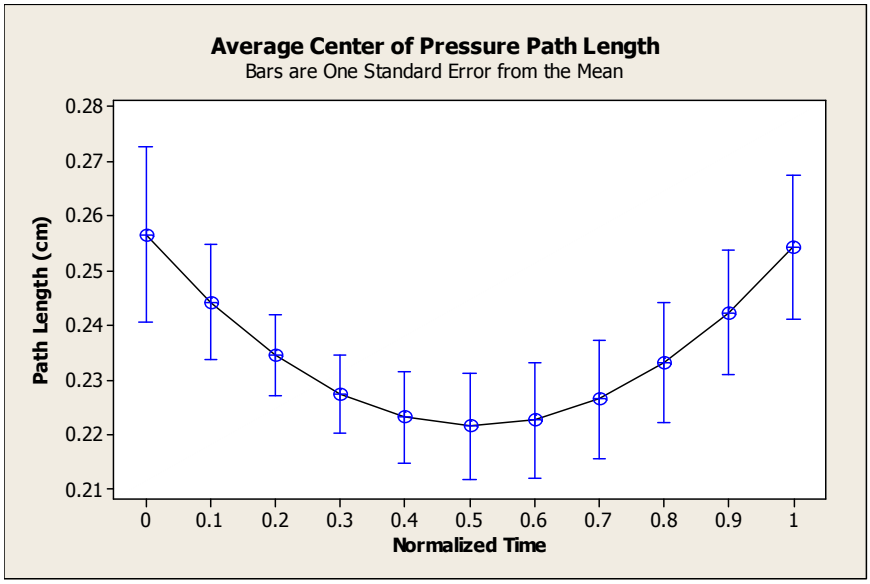

Figure 8: COP Path Length

COP Area

Figure 9 presents the COP area data. This plot initially showed a decrease until about half way through the protocol and then began to increase again. There was an overall decrease of 0.0006 cm^2 from the un-fatigued to the fatigued state. In a similar study on patients with pathology, changes in COP area ranged from 2.07cm^2 in a low back pain group to 0.73cm^2 in a lower extremity injury group.[51] The current COP area results are much smaller, but constitute a normal population.

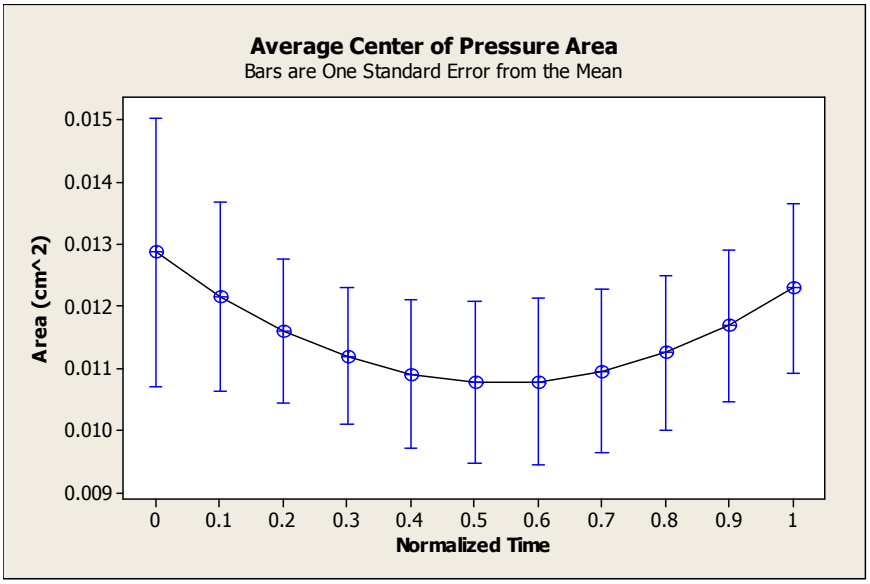

Figure 9: Average COP Area

COP Velocity

The COP velocity data is presented in Figure 10. The COP velocity decreased from 1.28cm/s to 1.27 cm/s as fatigue progressed. This is a decrease of 0.8%. Alderton and Mortiz reported findings of a decrease in COP velocity from approximately 4 mm/s in the anterior/posterior direction and approximately 2 mm/s in the medial/lateral direction.[21]

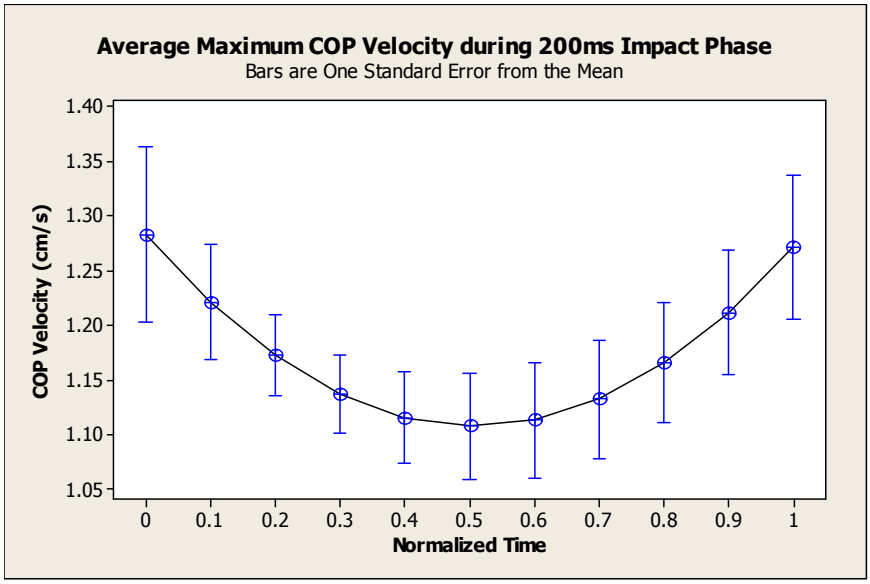

Figure 10: Maximum COP Velocity

Sagittal Plane Kinematics

Figures 11-13 report maximum hip, knee and ankle flexion during the first 500ms of the jump/landing event. These observed results are consistent with the assumption that the lower extremity joint flexion should increase during such events. Figure 11 describes the maximum hip flexion where this value increased 2.9°. These findings are similar to Madigan and Pidcoe's value of 3.9°.[15] The average increase in knee flexion, as shown in Figure 12, was similar to (+6.2°vs. +6.7°) Madigan and Pidcoe's results.[15] Figure 13 indicates essentially equivalent values for the ankle dorsiflexion (+4.6° vs. +4.5°).[15] There is no significant difference between the initial joint flexion and subsequent landings in any of these data ($p<0.5$). Additional plots highlighting the similarities between Madigan and Pidcoe's joint flexion results and this study are included in the discussion.

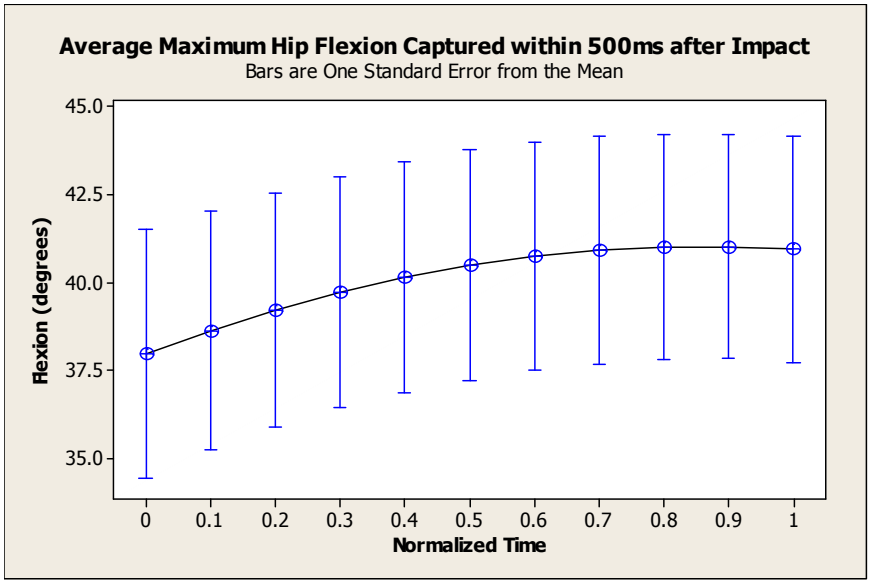

Figure 11: Average Maximum Hip Flexion

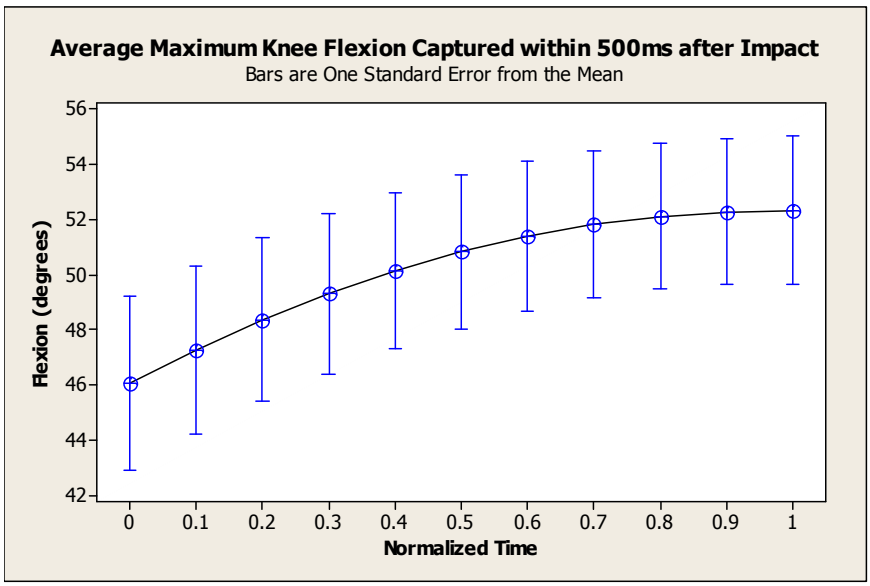

Figure 12: Average Maximum Knee Flexion

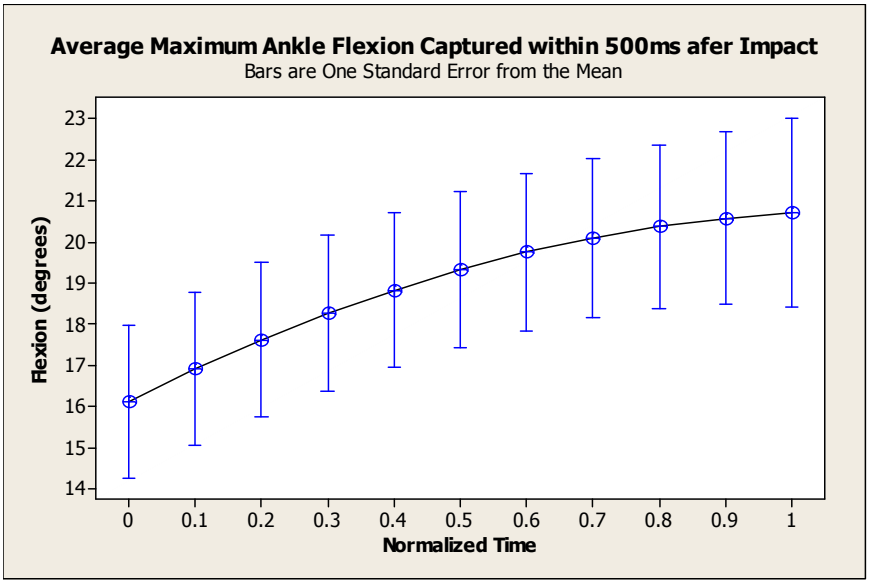

Figure 13: Average Maximum Ankle Flexion

Sagittal Plane Kinetics

Peak sagittal plane joint torques, generated for the initial 200ms impact phase, are plotted in Figures 14-16. Collective results for the hip, knee and ankle are summarized in these figures. With the hip torque data an increase torque of 0.20 Nm (+8.4%) is observed. The sagittal plane knee torque decreased 0.25 Nm (-19.2%) while the peak sagittal plane ankle torque decreased 0.15 Nm (-5.3%). There is no significant difference between the initial joint torque and subsequent landings in any of these data ($p<0.5$).

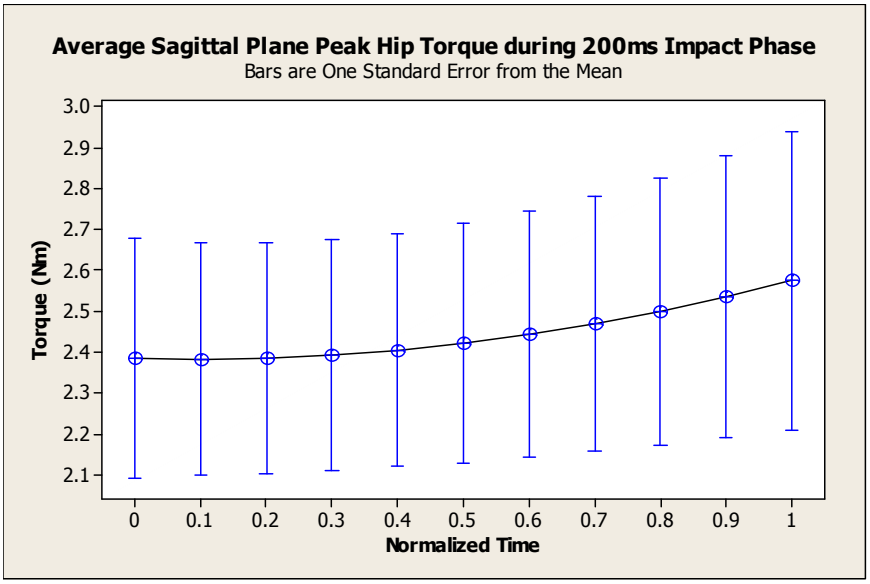

Figure 14: Peak Sagittal Plane Hip Torque during 200ms Impact Phase

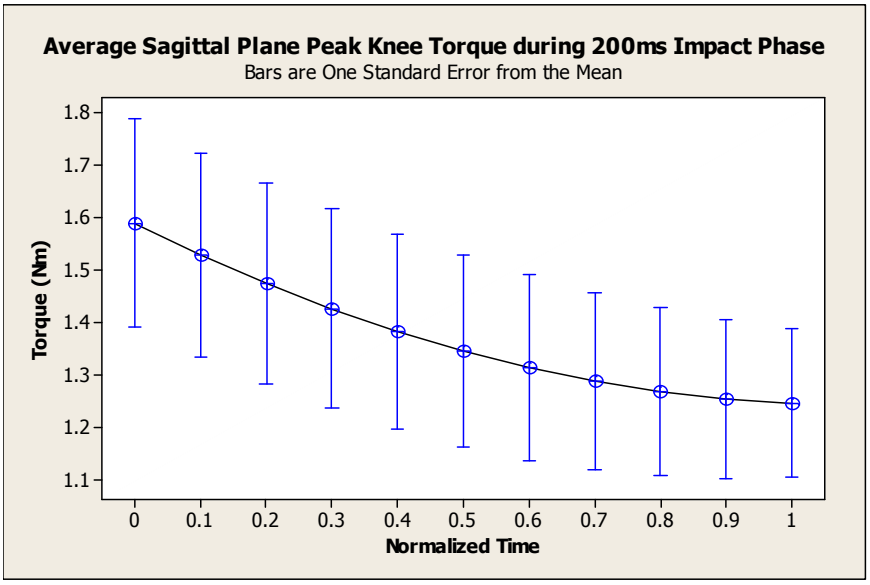

Figure 15: Peak Sagittal Plane Knee Torque during 200ms Impact Phase

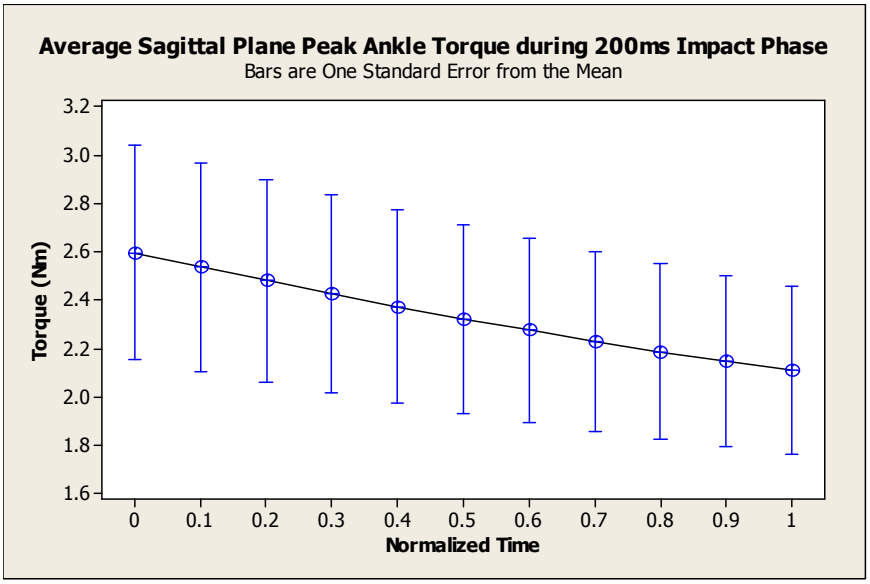

Figure 16: Peak Sagittal Plane Ankle Torque during 200ms Impact Phase

Madigan and Pidcoe found that the sagittal plane joint impulse increased 0.015 Nm-s/kg-m at the hip while decreasing 0.010 Nm-s/kg-m along both the knee and ankle.[15] Those joint impulses were defined as the total integrated values generated over the first 200ms after impact. Based on a similar definition of the impulse, an average decrease of 0.019 Nm-s/kg-m was observed at the hip, an average decrease of 0.025 Nm-s/kg-m at the knee, and an average reduction of 0.015 Nm-s/kg-m at the ankle. All of these average changes in impulse were significantly larger than those reported by Madigan and Pidcoe and suggest that there may be an inherent large variance in such measurements among individuals. There is no significant difference between the initial joint impulse and subsequent landings in any of these data ($p<0.5$).

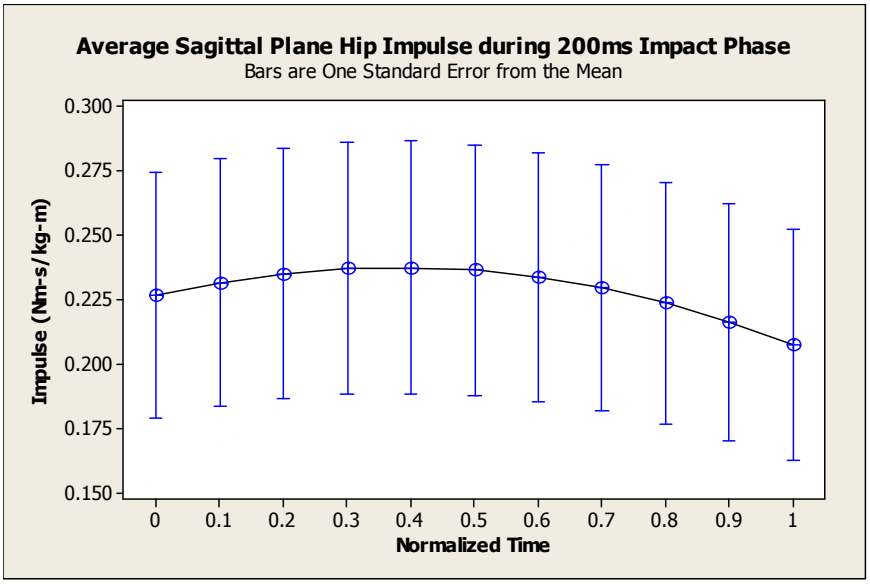

Figure 17: Average Sagittal Plane Hip Impulse

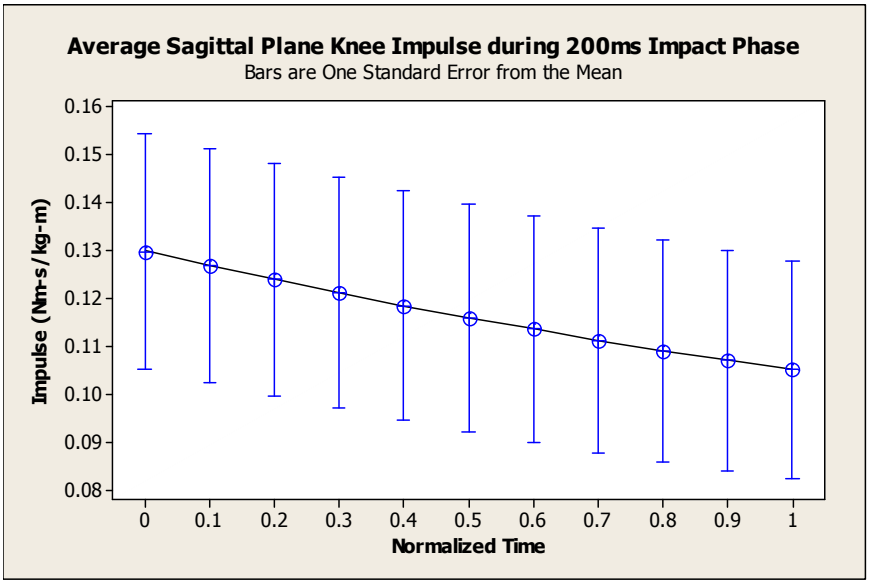

Figure 18: Sagittal Plane Knee Impulse

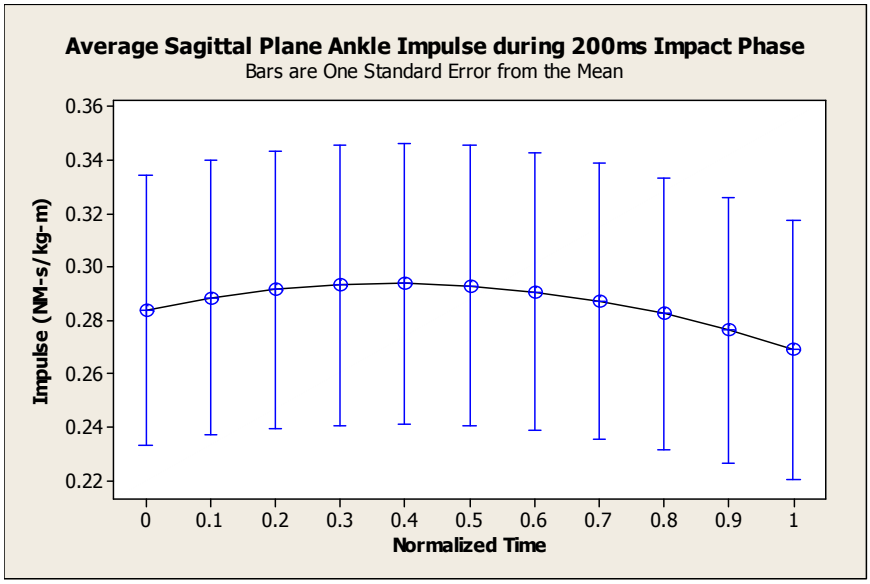

Figure 19: Sagittal Plane Ankle Impulse

Frontal Plane Kinematics

Figure 20 represents the average maximum foot inversion during the impact phase. Maximum foot inversion increased in a nearly linear fashion increasing from 5.5° to 6.2° (+12.7%). There is no significant difference between the initial foot inversion and subsequent landings in any of these data ($p<0.5$).

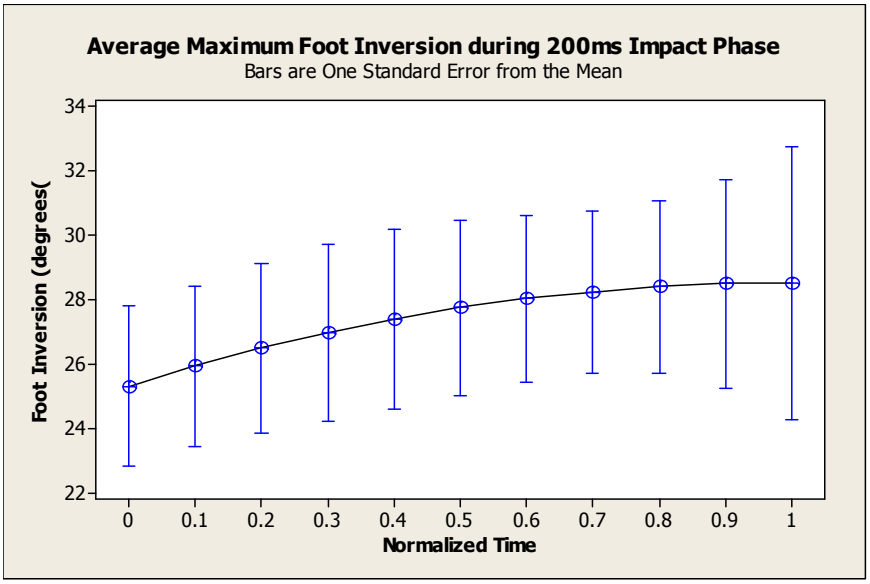

Figure 20: Average Maximum Foot Inversion during Impact Phase

Frontal Plane Kinetics

Frontal plane joint torques generated during the first 200ms after contact are summarized in Figure 21-23. The peak hip and knee torque were found to increase with increasing fatigue, while ankle torque tended to decrease with increasing fatigue. The average peak hip torque increased from 0.632 to 1.045 Nm-s/kg-m (+65.0%) The average peak frontal knee torque increased from 1.19 to 1.25 Nm-s/kg-m (+5.0%). The average peak ankle torque dropped 0.49 Nm-s/kg-m (-13.6%). There is no significant difference between the initial joint torque and subsequent landings in any of these data ($p<0.5$).

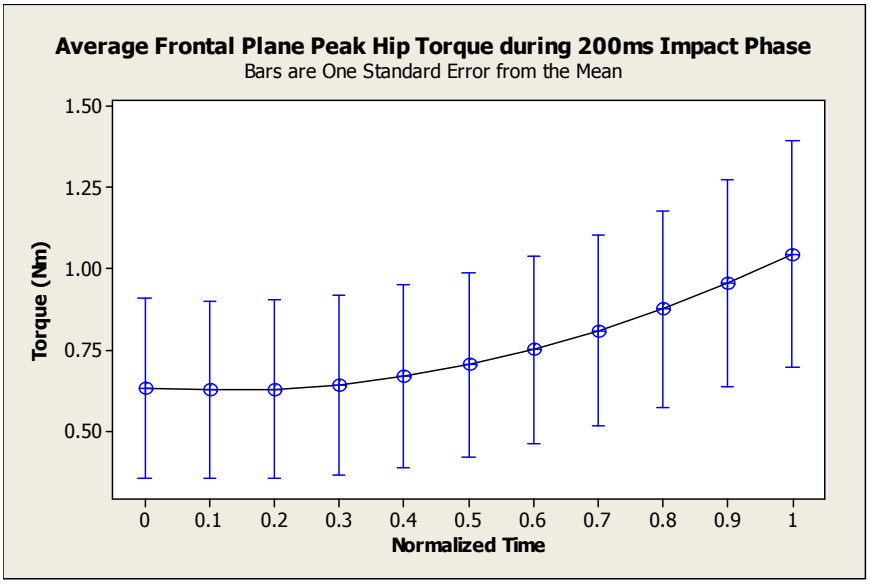

Figure 21: Peak Frontal Plane Hip Torque

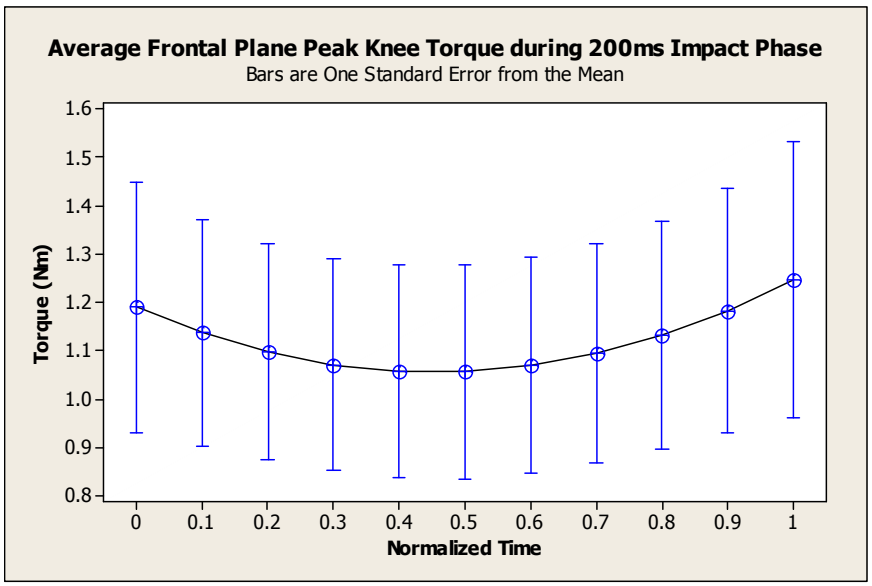

Figure 22: Peak Frontal Plane Knee Torque

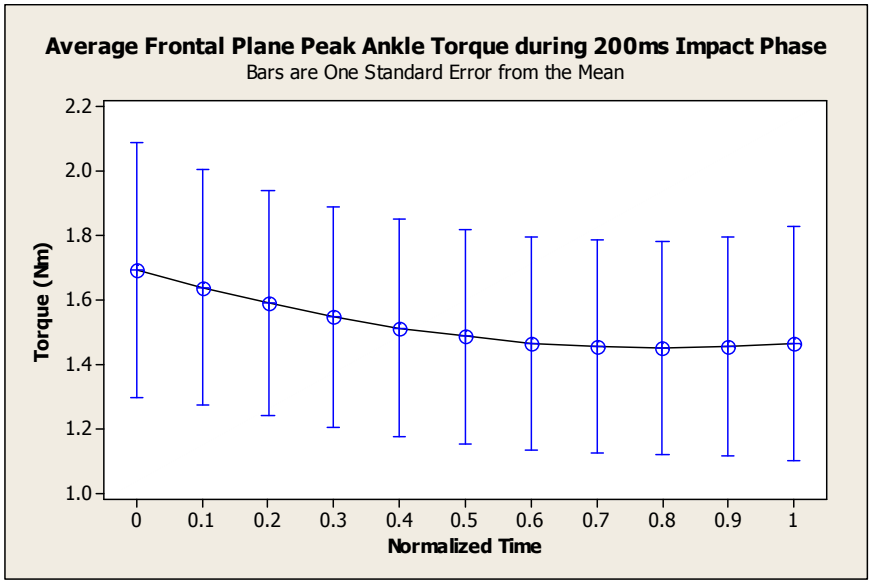

Figure 23: Peak Frontal Plane Ankle Torque

Frontal plane joint impulse increased 0.020 Nm-s/kg-m at the hip (+10.3 %) and 0.020 Nm-s/kg-m (+ 133.3 %) along at the knee while decreasing 0.004Nm-s/kg-m (-5.2%) at the ankle. Those joint impulses were defined as the total integrated values generated over the first 200ms after impact. There is no significant difference between the initial joint impulse and subsequent landings in any of these data ($p<0.5$).

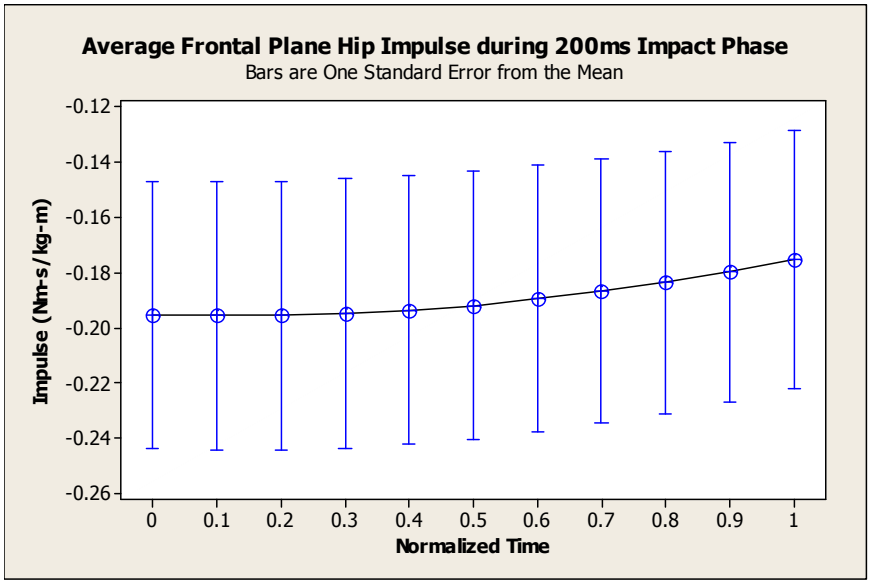

Figure 24: Average Frontal Plane Hip Impulse during 200ms Impact Phase

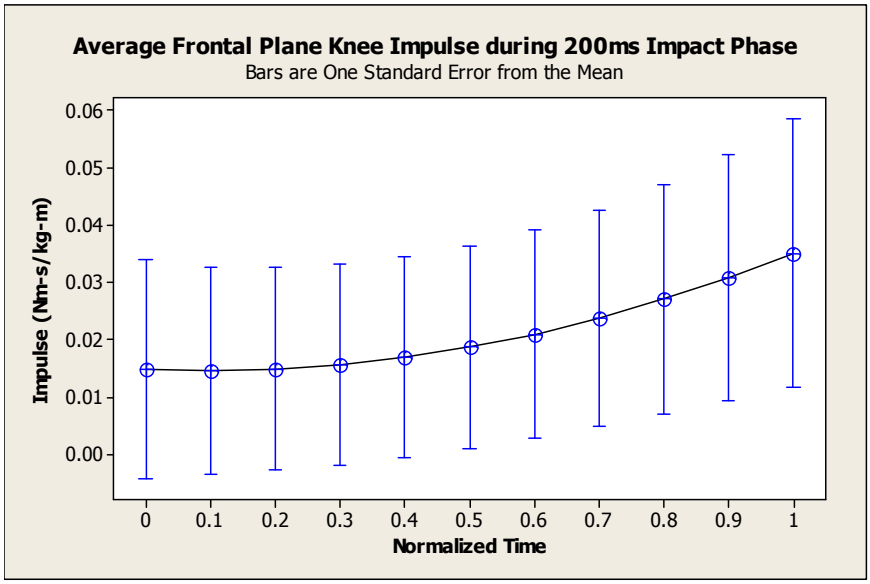

Figure 25: Average Frontal Plane Knee Impulse during 200ms Impact Phase

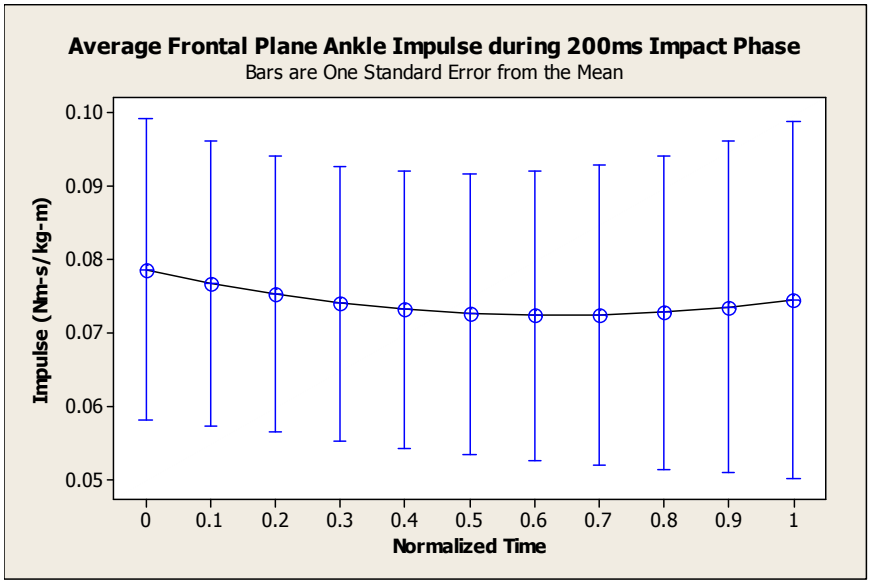

Figure 26: Average Frontal Plane Ankle Impulse during 200ms Impact Phase

Sacral Height

The maximum sacral heights were plotted to ensure that changes observed in landing biomechanics were not a result of the subjects jumping from lower heights with the onset of fatigue. Sacral heights range from 1.147m in the un-fatigued state to 1.145m in the fatigued state. This is a decrease of 0.002m (-0.17 %). There is no significant difference between the initial sacral height and subsequent jump heights in any of these data ($p<0.5$).

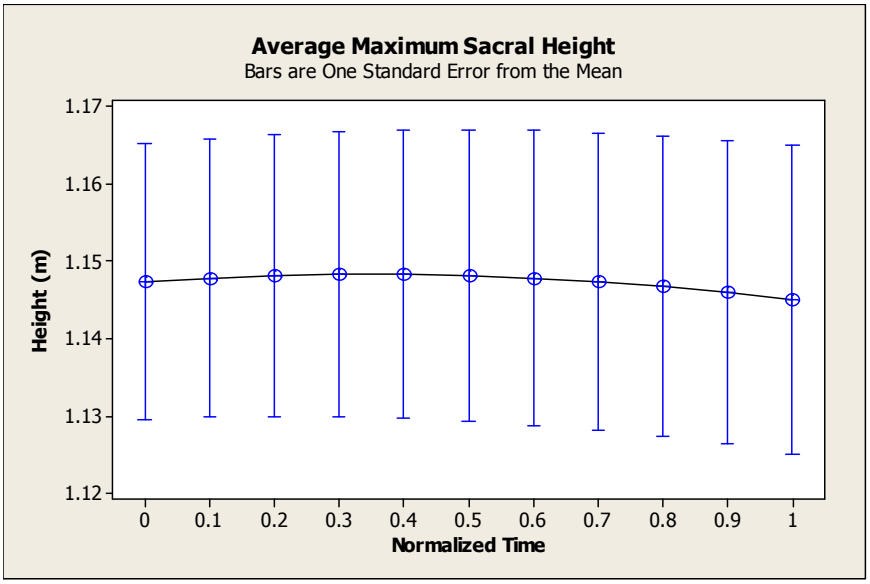

Figure 27: Average Maximum Sacral Height

Accelerometer

Figure 28 shows the maximum acceleration magnitude recorded during the 200ms Impact Phase. Maximum acceleration magnitude increased from 3.55m/s^2 to 3.57m/s^2 (+ 0.6%). There is no significant difference between the initial accelerometer magnitude and subsequent landings in any of these data ($p<0.5$).

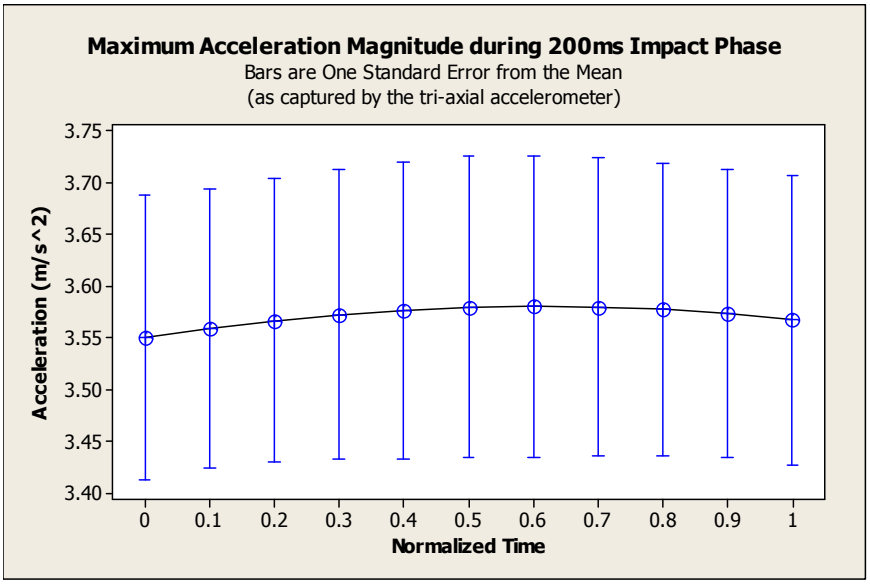

Figure 28: Maximum Accelerometer Acceleration Magnitude during 200ms Impact Phase

Figure 29 represents the average maximum accelerometer angular orientation during the impact phase (0 to 200ms). The overall change shows an decrease of 16.8%. There is no significant difference between the initial accelerometer angular orientation and subsequent landing measures in any of these data ($p<0.5$).

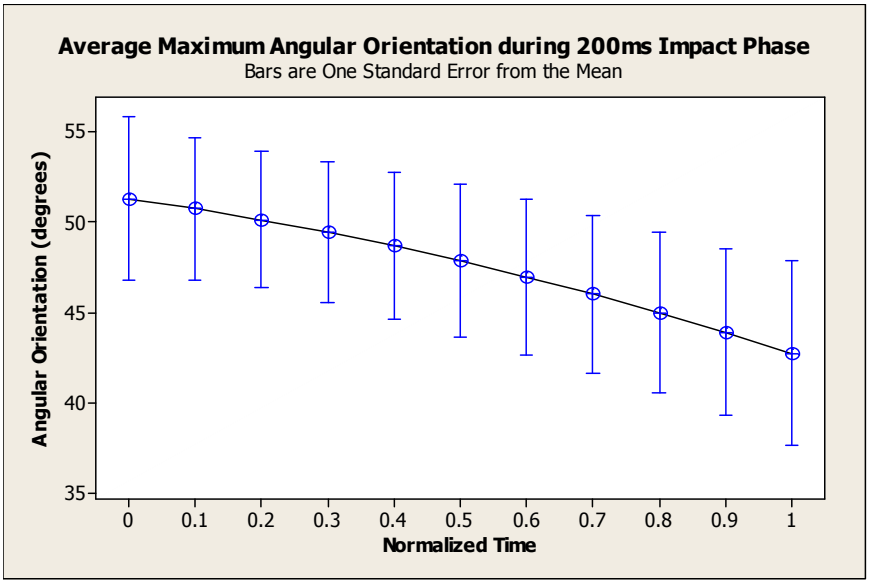

Figure 29: Average Maximum Accelerometer Angular Orientation during Impact Phase

Time-to-Stabilization

Time-to-stabilization was used to assess the dynamic stability of the ankle. Values were determined for both the medial/lateral and anterior/posterior directions. The results show a decrease in time-to-stabilization in both the medial/lateral and anterior/posterior directions of 32.5ms (-15.0%) and 5.5ms (-3.2%) respectively as subjects progressed from the un-fatigued to fatigued state. There is no significant difference between the initial time-to-stabilization and subsequent landing measures in any of these data ($p<0.5$).

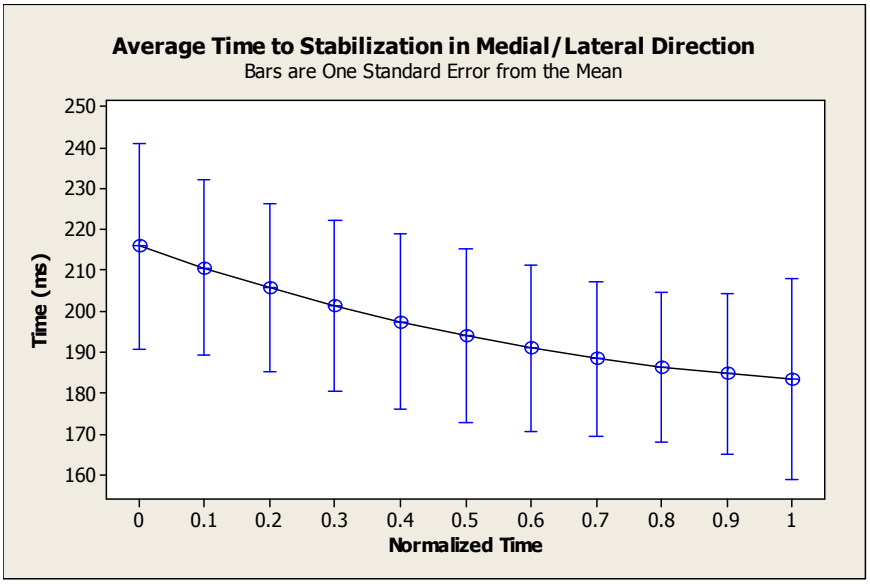

Figure 30: Average Time to Stabilization in the Medial/Lateral Direction

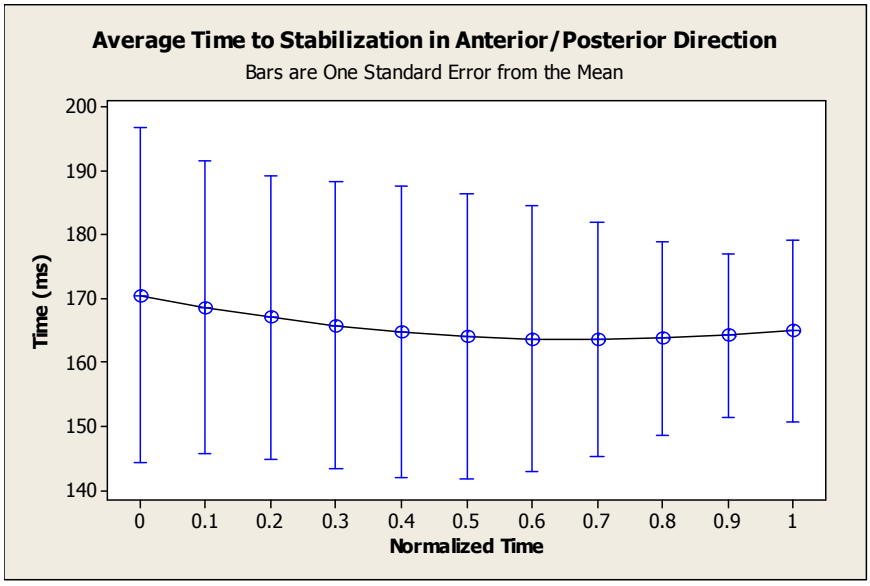

Figure 31: Average Time to Stabilization in Anterior/Posterior Direction

Figure 32 represents the Time to Stabilization in the medial/lateral direction collected by the forceplate. The Forceplate also reported a decrease in Time to Stabilization of 54.7ms, a change of -14.0%.

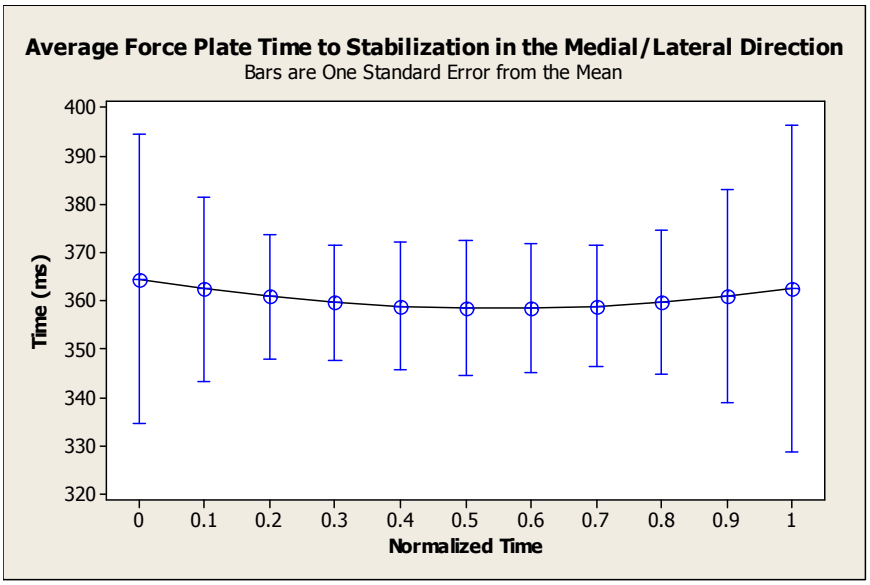

Figure 32: Average Forceplate Time to Stabilization in the Medial/Lateral Direction

Statistical Validation of the Tri-axial Accelerometer

An analysis of the vGRF and the accelerometer magnitude data was used to establish a (kinetic) correlation between the two devices (forceplate and accelerometer). Visual inspection shows the magnitude of the peaks between the two data sets are comparable (Figure 33).

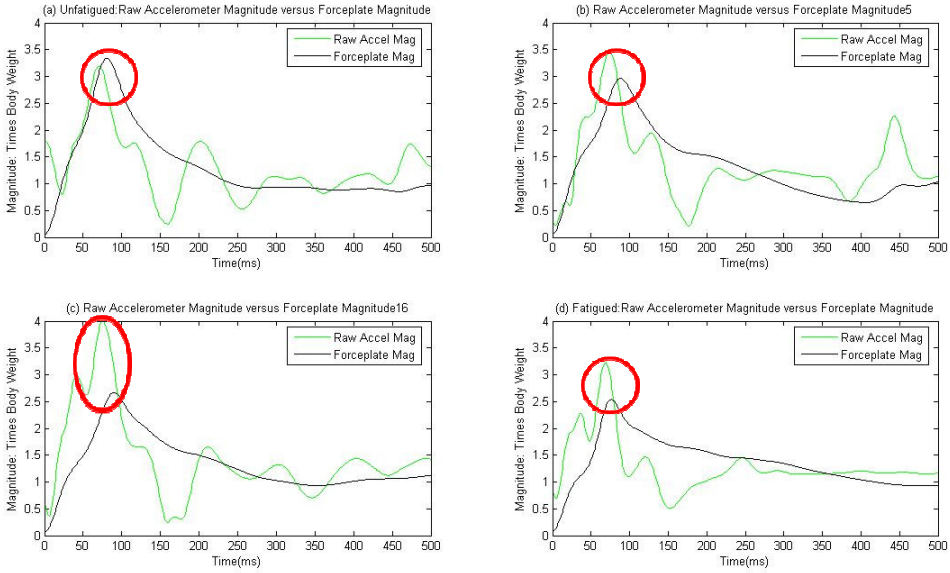

Figure 33: Raw Accelerometer Magnitude versus Forceplate Magnitude Response Curves for a Single Subject taken at Various Intervals during the Fatiguing Protocol

To model the curvature in the relationship between the accelerometer magnitude values (Y) and the forceplate magnitude values (X) a quadratic regression model were used. The "s" value is an estimate of the standard deviation about the regression line. The R-square (r^2 or coefficient of determination) measures the proportion of variability in the Y variable accounted for the X, predictor variable(s). An R-square value of 100% is

considered excellent. This analysis provided in Figure 36 identified an $r^2 = 90.1\%$ for the regression model.

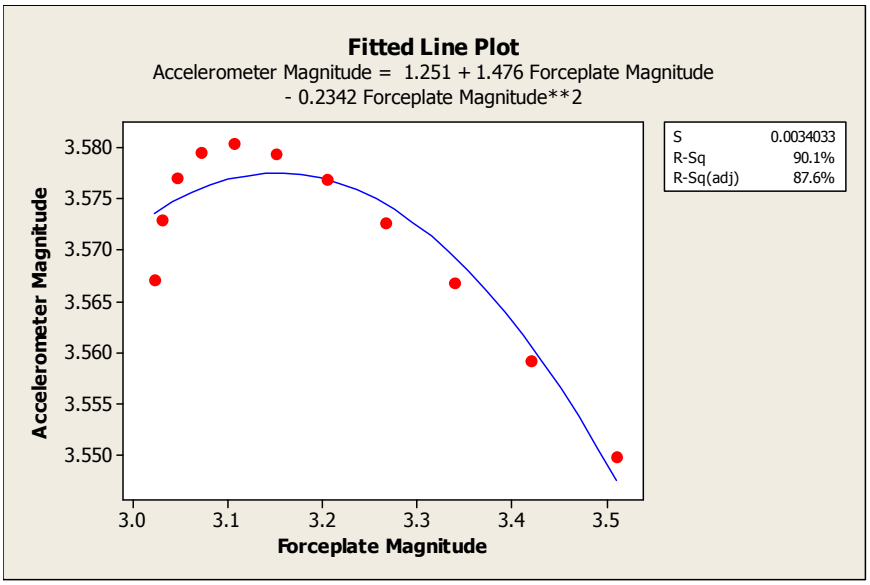

Figure 34: Fitted Regression Relationship between Accelerometer and Forceplate Magnitude Data

The resulting regression model is shown below in Equation 4.

$$\text{Max. Accelerometer Magnitude} = (-0.234 * \text{Max.Forceplate Magnitude})^2 + 1.47 * \text{Max.Forceplate Magnitude} + 1.25 \quad \text{(Equation 4)}$$

Further analysis was performed to identify a link between kinetic data recorded by the accelerometer and forceplate. This analysis involved comparing the time to stabilization in the medial/lateral direction by both devices. Again, a quadratic regression was used to fit the data and an $r^2 = 100.0\%$ was reported as seen in Figure 35.

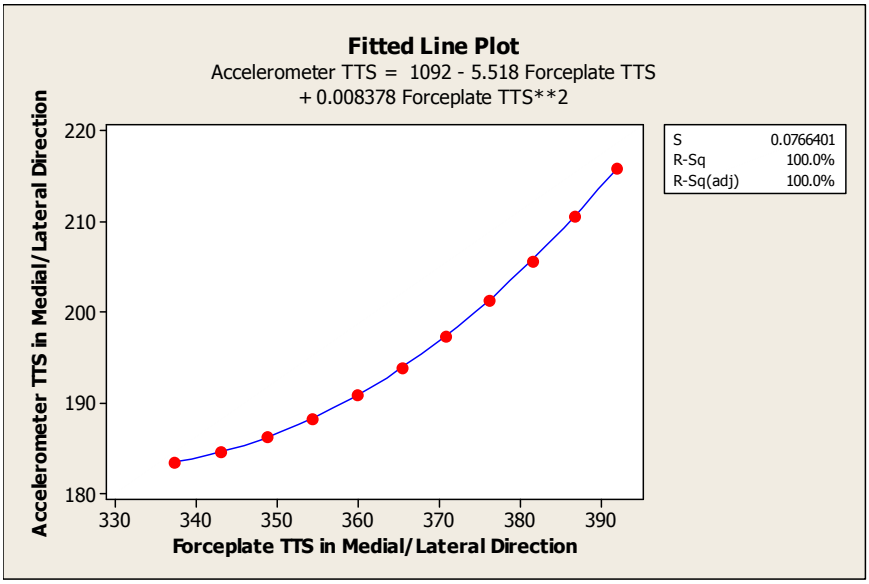

Figure 35: Fitted Regression Relationship of the Time to Stabilization in the Medial/Lateral Direction between Accelerometer and Forceplate Data

The resulting regression model is shown below in Equation 5.

$$\text{Accelerometer TTS}=(0.008^{*}\ \text{Forceplate TTS})^{2}-5.52^{*}\text{Forceplate TTS}+1092 \quad \text{(Equation 5)}$$

Both temporal and positional analyses were done to model the curvature in the relationship between the Medial/Lateral Accelerometer Angular Orientation and Foot Inversion a quadratic regression models were used. The analysis of the positional data identified an $r^2 = 37.2\%$ (Figure 39). Thus further analysis was performed on the temporal Accelerometer Angular Orientation and Foot Inversion and that analysis identified an $r^2 = 86.8\%$ for the regression model (Figure 40).

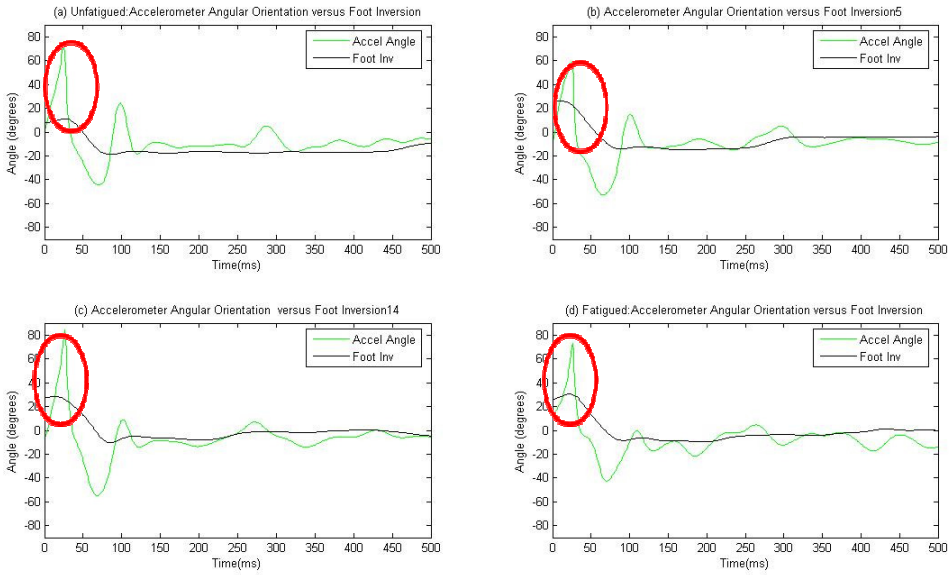

Figure 36: Medial/Lateral Accelerometer Angular Orientation versus Foot Inversion Response Curves for a Single Subject taken at Various Intervals during the Fatiguing Protocol

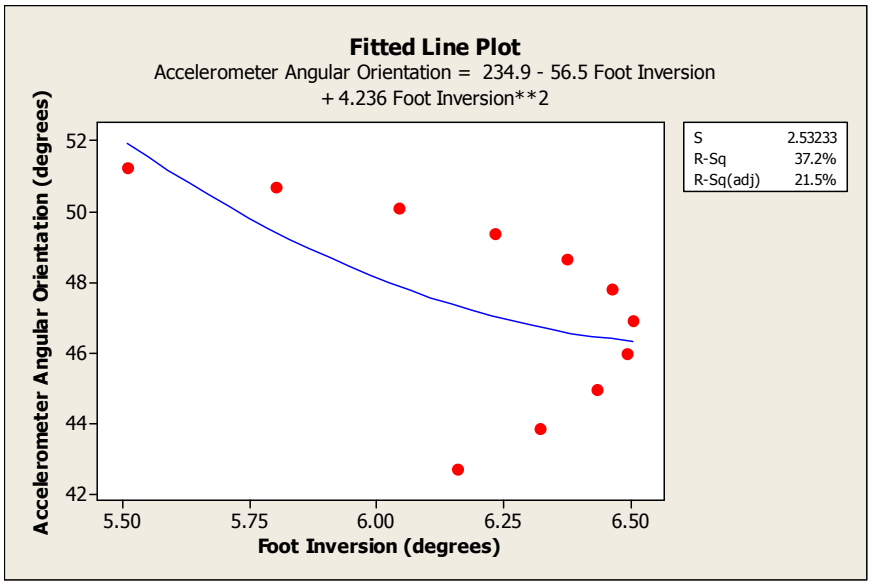

Figure 37: Fitted Regression Relationship between Medial/Lateral Accelerometer Angular Orientation versus Foot Inversion Data

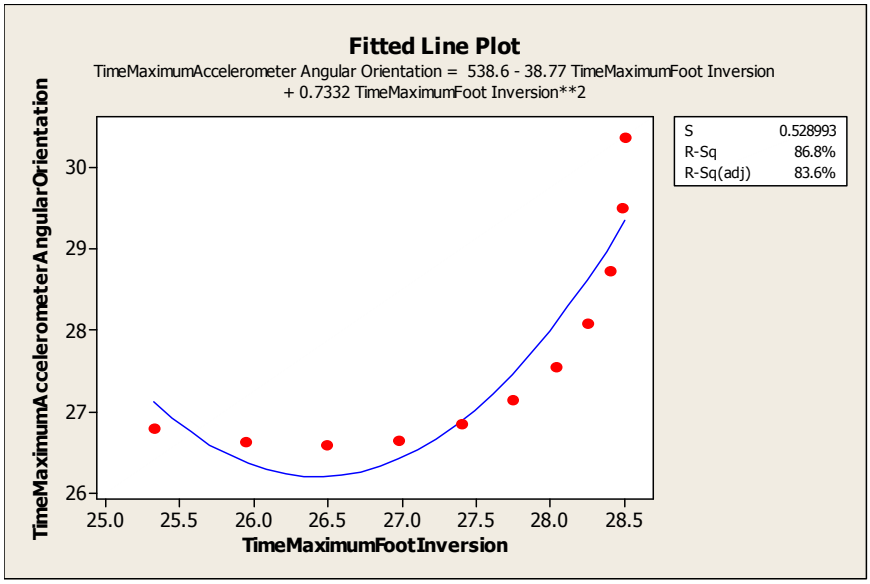

Figure 38: Fitted Regression of the Temporal Relationship between Medial/Lateral Accelerometer Angular Orientation versus Foot Inversion Data

The resulting quadratic regression model is shown below in Equation 6.

$$\text{Time}_{\text{Max.Angular Orientation}} = (0.7332 * \text{Time}_{\text{Foot Inversion}})^2 - 38.77 * \text{Time}_{\text{Foot Inversion}} + 538.6 \quad \text{(Equation 6)}$$

Table 1a: Summary of Biomechanical Changes from Unfatigued to Fatigued State

Peak vGRF	**Unfatigued**	**Fatigued**	**Change**	**% Change**
Current Study (N=12)	3.49 BW	3.00 BW	0.49	-14.0%
Madigan Study (N=12)	3.69 BW	3.24 BW	0.45	-12.2%
Time to Peak vGRF	**Unfatigued**	**Fatigued**	**Change**	**% Change**
Current Study(N=12)	73.6 ms	70.3 ms	3.6	-5.0%
Madigan Study (N=12)	75.4 ms	74.2 ms	1.2	-1.6%
Impulse (N-s/kg-m)	**Unfatigued**	**Fatigued**	**Change**	**% Change**
vGRF Impulse (N=12)	0.378	0.356	0.022	-5.8%
Madigan vGRF Impulse (N=12)	0.392	0.369	0.023	-5.9%
Peak Accelerometer Magnitude	**Unfatigued**	**Fatigued**	**Change**	**% Change**
Current Study (N=9)	3.55 g's	3.57g's	0.02	+0.6%
Time to Stabilization	**Unfatigued**	**Fatigued**	**Change**	**% Change**
Medial/Lateral (N=9)	216.0ms	183.5ms	32.5	-15.0%
Anterior/Posterior (N=9)	170.5ms	165.0ms	5.5	-3.2%
Forceplate Medial/Lateral (N=13)	391.9ms	337.2	54.7	-14.0%
Sagittal Hip Flexion (500ms Post Impact)	**Unfatigued**	**Fatigued**	**Change**	**% Change**
Current Study (N=12)	38.0°	40.9°	2.9	+7.6%
Madigan Study (N=12)	29.0°	32.9°	3.9	+13.4%
Sagittal Knee Flexion (500ms Post Impact)	**Unfatigued**	**Fatigued**	**Change**	**% Change**
Current Study (N=12)	46.1°	52.3°	6.2	+13.4%
Madigan Study (N=12)	42.6°	49.3°	6.7	+15.7%
Sagittal Ankle Dorsiflexion (500ms Post Impact)	**Unfatigued**	**Fatigued**	**Change**	**% Change**
Current Study (N=12)	16.1°	20.7°	4.6	+28.6%
Madigan Study	13.3°	17.8°	4.5	+33.8%
Frontal Plane Foot Inversion (Impact Phase)	**Unfatigued**	**Fatigued**	**Change**	**% Change**
Current Study (N=12)	5.5°	6.2°	0.7	+12.7%
Peak Accelerometer Angular Orientations (200ms Impact Phase)	**Unfatigued**	**Fatigued**	**Change**	**% Change**
Current Study (N=9)	51.3°	42.7°	8.6	-16.8%
COP Path Length	**Unfatigued**	**Fatigued**	**Change**	**% Change**
Current Study (N=12)	0.257cm	0.254cm	0.003	-1.2%

Table 1b: Summary of Biomechanical Changes from Unfatigued to Fatigued

COP Area	**Unfatigued**	**Fatigued**	**Change**	**% Change**
Current Study (N=12)	0.011 cm^2	0.010 cm^2	0.001	-9.1%
COP Velocity	**Unfatigued**	**Fatigued**	**Change**	**% Change**
Current Study (N=12)	1.28cm/s	1.27cm/s	0.01	-0.8%
Sagittal Hip Impulse (Nm-s/kg-m)	**Unfatigued**	**Fatigued**	**Change**	**% Change**
Current Study (N=12)	0.227	0.208	0.019	-8.4%
Madigan Study (N=12)	0.102	0.117	0.015	+14.7%
Sagittal Knee Impulse (Nm-s/kg-m)	**Unfatigued**	**Fatigued**	**Change**	**% Change**
Current Study (N=12)	0.130	0.105	0.025	-19.2%
Madigan Study (N=12)	0.183	0.173	0.01	-5.5%
Sagittal Ankle Impulse (Nm-s/kg-m)	**Unfatigued**	**Fatigued**	**Change**	**% Change**
Current Study (N=12)	0.284	0.269	0.015	-5.3%
Madigan Study (N=12)	0.076	0.066	0.010	-13.2%
Sagittal Hip Torque	**Unfatigued**	**Fatigued**	**Change**	**%Change**
Current Study (N=12)	2.38 Nm	2.58Nm	0.20	+8.4%
Sagittal Knee Torque	**Unfatigued**	**Fatigued**	**Change**	**%Change**
Current Study (N=12)	1.59 Nm	1.24 Nm	0.35	-22.0%
Sagittal Ankle Torque	**Unfatigued**	**Fatigued**	**Change**	**%Change**
Current Study (N=12)	2.50 Nm	2.11 Nm	0.49	-18.8%
Frontal Hip Impulse (Nm-s/kg-m)	**Unfatigued**	**Fatigued**	**Change**	**%Change**
Current Study (N=12)	-0.195	-0.175	0.02	+10.3%
Frontal Knee Impulse (Nm-s/kg-m)	**Unfatigued**	**Fatigued**	**Change**	**%Change**
Current Study (N=12)	0.015	0.035	0.02	+133.3%
Frontal Anklee Impulse (Nm-s/kg-m)	**Unfatigued**	**Fatigued**	**Change**	**%Change**
Current Study (N=12)	0.079	0.075	0.004	5.2%
Frontal Hip Torque	**Unfatigued**	**Fatigued**	**Change**	**% Change**
Current Study (N=12)	0.632 Nm	1.045Nm	0.413	+65.0%
Frontal Knee Torque	**Unfatigued**	**Fatigued**	**Change**	**% Change**
Current Study (N=12)	1.19 Nm	1.25 Nm	0.06	+5.0%
Frontal Ankle Torque	**Unfatigued**	**Fatigued**	**Change**	**% Change**
Current Study (N=12)	1.69 Nm	1.46 Nm	0.23	-13.6%

Table 1c: Summary of Biomechanical Changes from Unfatigued to Fatigued

Time to Peak Magnitude	**Unfatigued**	**Fatigued**	**Change**	**% Change**
Accelerometer (N=9)	71.1ms	57.9ms	13.2	-18.6%
Forceplate (N=12)	73.7ms	70.1ms	3.6	-5.0%
Time to Peak Medial/Lateral Rotations	**Unfatigued**	**Fatigued**	**Change**	**% Change**
Angular Orientation (N=9)	26.8ms	30.3ms	3.5	+13.1%
Foot Inversion (N=12)	25.3ms	28.5ms	3.2	+12.6%

Chapter 4 - Discussion

The analysis of sagittal and frontal plane kinetics, kinematics, and center of pressure provides descriptive details regarding performance changes associated with lower extremity fatigue. These results compare closely with previous research performed in this lab (Madigan and Pidcoe, 2003) and demonstrate the reliability of these data. A new twist to this research is the addition of a tri-axial accelerometer in the landing shoe of the subject. Data from this device was correlated with known kinematic and kinetic standards with hopes that accelerometer features could be used as a simpler metric in the measurement of lower extremity fatigue. Accelerometer magnitudes and angular orientations were analyzed with respect to forceplate magnitude and foot frontal plane motion (inversion/eversion) measurements to validate accelerometer readings. A discussion of all associated variables follows.

vGRF variables

There was an observed decrease in the peak vGRF as fatigue progressed. The peak vGRF is related to subject deceleration since kinetic energy has to be dissipated. That deceleration is controlled though LE joint flexion. If a moving body is slowed over a longer period of time, the forces at the foot-floor interface will be less than if the body is slowed abruptly. These types of landings have been described by others as “stiff” and “soft”.[54,55] Coventry performed similar research on jump landings and induced fatigue with a sequence of drop jumps, maximal counter-movement jumps, and five

squats.[56] He reported a decrease in peak vGRF from 3.90 to 3.62 times body weight (-7.2%) secondary to a "soft" landing technique. Madigan and Pidcoe's work showed similar results. The percent decrease in vGRF was 27% in Madigan and Pidcoe's study and 14% in the current study (Figure 4). The fatigued vGRF is smaller (significantly different, $p<0.5$) from the initial unfatigued vGRF. It appears that as subjects fatigue, they perform "softer" landings. This is consistent with Madigan and Pidcoe's findings that found fatigued vGRF were significantly less than the initial, unfatigued state (Figure 39).

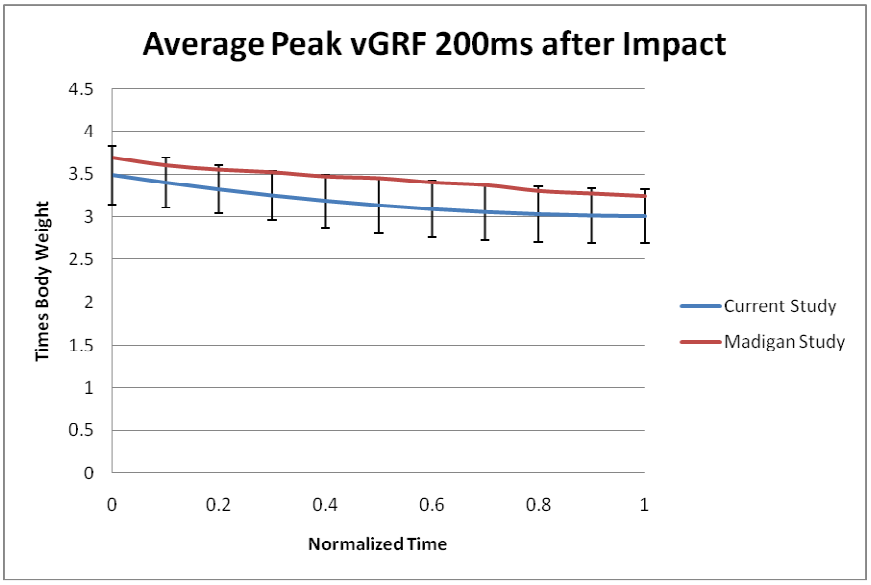

Figure 39: Comparison of current study vGRF data with Madigan data.

TTP vGRF data had a second order trend (Figure 5), increasing to the midpoint of the collection and then decreasing. An increase in TTP force is associated with fatigue and a decline in muscle force generation capacity. Muscle force generation is delayed.

This change may indicate a change in landing strategy as the subjects' are compensating for a continued progression of fatigue.

The vGRF Impulse decreased with fatigue (Figure 6). Impulse is an integrated function of vGRF over time, therefore it is more indicative of the power produced by the muscles. These data, again, follow the vGRF data trend and support the influence of a change in landing biomechanics. There is a significant change in this variable ($p<0.5$) when the fatigue state is reached and are consistent with previous results (figure 40). To rule out that these changes were a result of a change in take-off strategy, peak sacral height was monitored (Figure 27).

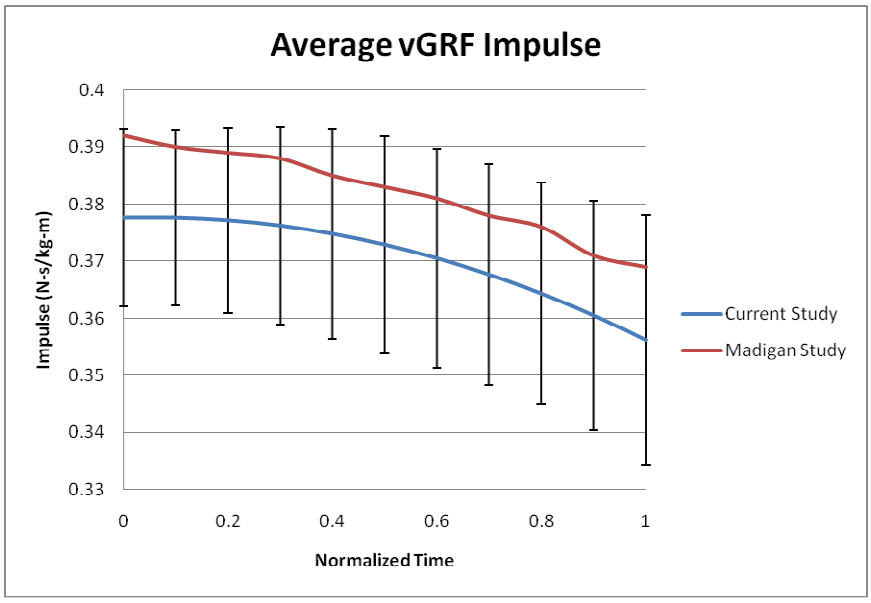

Figure 40: Comparison of current study average vGRF Impulse data with Madigan data.

The average maximum sacral height of all subjects ranged between 1.147m and 1.145m, a deviation of 0.002m. There was little to no change in jump height with fatigue. Since jump height was constant, changes in peak vGRF and vGRF impulse had to be a result of changes in landing kinematics. The wide 95% confidence interval bands for the maximum sacral height are a result of the fact that the jump heights were not normalized for each subjects' height.

Accelerometer measurements increased in peak acceleration magnitude from 3.55 to 3.57 g's (Figure 28). This was not statistically significant ($p<0.5$). It was expected that the accelerometer data would correlate closely with the vGRF data since both are recording the kinetics of the same event and are recording it from nearly the same location (in the shoe as compared to at the foot-floor interface). The current study does demonstrate a correlation, but it is inverse. From the forceplate data, the subjects appear to "soften" their landings and from the accelerometer data, the subjects appear to have the same peak acceleration (changing only slightly in the positive direction). This may have been due to the materials characteristics of the shoe or movement of the accelerometer in the heel cutout of the shoe.

There are conflicting data in other studies. Coventry employed a fatiguing jump landing protocol and reported decreases in acceleration with fatigue from 13.4 to 12.2 g's.[56] This change was larger than the current study, but may have been due to differences in protocol. In addition, the accelerometer was mounted on the tibia.

Not all LE acceleration studies report this decrease. Teramoto et al. used accelerometers to study shock attenuation at the head and leg of female runners. During

the application of a fatiguing protocol, peak head accelerations increased from 1.12g's to 1.47g's and peak leg acceleration increased from 3.96g's to 4.95g's.[31] Both the largest accelerations and largest increase in accelerations were experienced at the leg, which is known to serve a major role in shock attenuation during landing impact. This increase in acceleration (and therefore vGRF) was most likely due to the difference between a landing activity and a running activity. The landing kinetics/kinematics during heel strikes experienced during running are different from those experienced in a jump landing. During running, when the heel strikes, the knee is extended and the ankle is neutral. During jump landings, both the knee and ankle are flexed.[57]These differences can have a dramatic effect on both landing biomechanics and the forces a subject generates during impact. Additionally, there were variations in fatigue protocols that might help explain these differences. First, Teramoto et al. study focused on ankle fatigue and not quadriceps fatigue.[31] Second, the accelerometer was place at the subjects' tibia and data was collected during the stance phase of running (stride), specifically heel strike.[31]

Since both the studies by Coventry and Teramoto involved measuring tibial acceleration under fatigue and different trends were found it is likely that this difference arose because they involved different activities (jump landing versus running heel-strike). Coventry noted the inconsistencies in tibial peak acceleration with fatigue in prior studies and found that others attributed this difference to the level and type of fatigue experienced.

These results suggest that the accelerometer data does correlate with vGRF (r^2=0.90), but it does not mimic it (Figure 36). These finding may be different if the accelerometer is embedded in the heel of the shoe and movement is minimized.

Sagittal Plane Joint Flexion

Sagittal kinematic data from LE joints (hip, knee, and ankle) was consistent with previous studies[15] (Figure 11-13). The amount of joint flexion during landing represents the amount of bending at the joints. This study found maximum hip, knee and ankle flexions increased linearly with fatigue. Previous discussion about vGRF described initial decreases in this variable as connected to kinematic joint changes. In short, to decrease the vGRF, the body must decelerate over a longer period of time. This results in larger joint excursions (larger maximum flexion values). The maximum joint flexion is measured during the first 500ms after impact (entire landing phase). It appears that as fatigue progresses, the subjects' continue to decelerate for a longer period of time (reaching a larger maximum joint angle). These data are consistent with previous work (Figures 41-43).

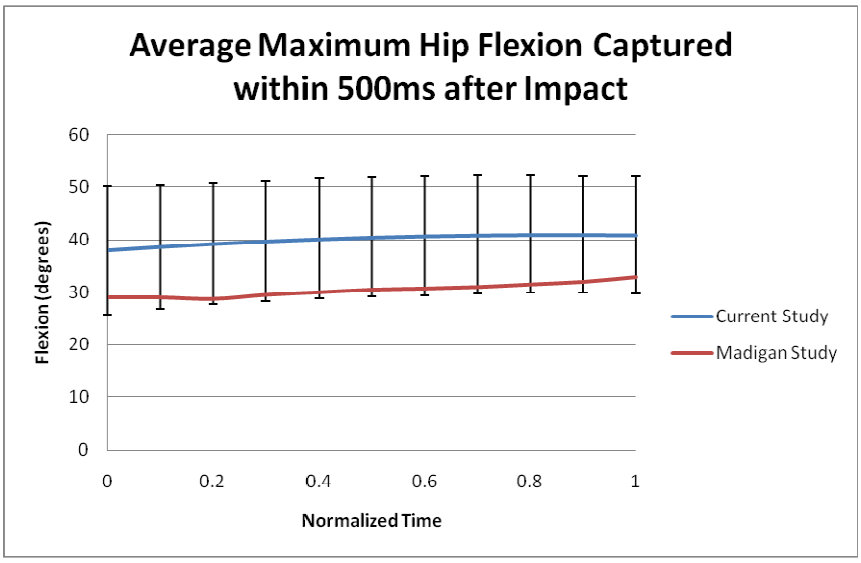

Figure 41: Comparison of current study hip flexion data with Madigan data.

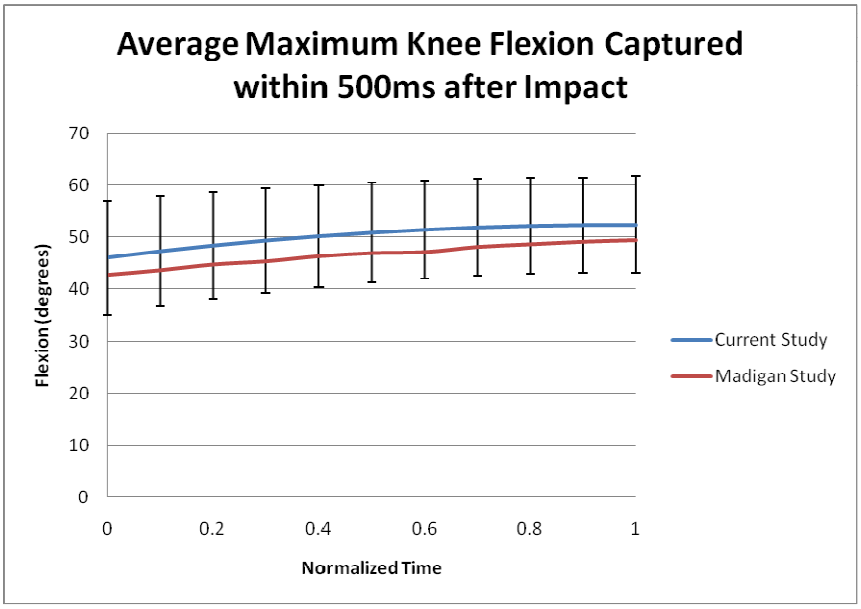

Figure 42: Comparison of current study knee flexion data with Madigan data.

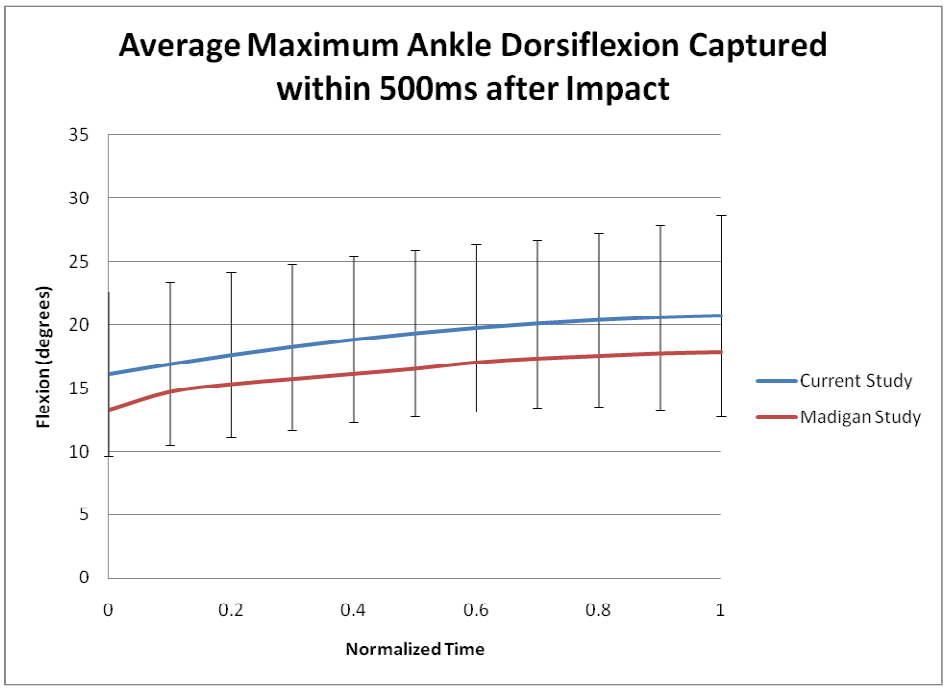

Figure 43: Comparison of current study ankle flexion data with Madigan data.

Center of Pressure

The COP data provides information about postural control strategies. The COP path length, area, and velocity were the three variables assess in this study and were measured during the impact phase of the landing (0 to 200ms). All three were found to decrease as fatigue progressed (Figures 8-10). None of the changes were statistically significant ($p<0.5$).

Alderton and Mortiz also studied the COP path length and velocity in an attempt to understand the effect of fatigue on single legged postural control.[21] After fatiguing their subjects with repeated calf raises they saw COP path length increased with fatigue while the COP velocity decreased. They associated increased COP path length, velocity

and amplitudes with decreased stability, indicating poor balance control when attempting to stand still.[21] Conversely, decreases in these variables imply improved stability and balance. Furthermore, they concluded that these changes were related to changes in postural control strategy. They stated that, "If a change from an ankle strategy towards a hip strategy takes place after fatiguing exercise it can be hypothesized that COP frequency decreases because of increased mass involved in controlling balance, and that trunk acceleration increases because of the more active role of the hip and trunk (control)."[21] Figure 7 shows a difference in vGRF amplitude as a function of fatigue, but also shows a decrease in settling time (or oscillation frequency) with fatigue. This is consistent with progression toward a hip control strategy during landings.

In the current study, the decrease in COP path length and area are also consistent with the idea that the control strategy switches from the ankle to the hip. While accelerometers were not placed at the subjects' trunk and hips, sensors were placed at the hip to measure joint flexion and peak moment data. The data from these sensors recorded increases in hip flexion torque suggesting increased compensation about the hip and a change to hip strategy.

The COP results appear to support previous findings in the following way. As the knee extensor muscles fatigue, the hip and ankle are responsible for controlling more of the landing load. Proximal muscles tend to have larger motor units. As the hip becomes more active (hip strategy), these larger motor units would have less fine control ability and the joints would appear stiffer causing vGRF to increase near the end of each trial.

Frontal Plane Foot Inversion

Frontal plane foot inversion increased with increasing fatigue (Figure 20). The absolute angle changed from 5.5° to 6.2°, an increase of 12.7%. The majority of ankle sprains (85%) are due to lateral ankle inversions.[12] Ankle inversions are often the end result of exaggerated, overextensions of the ankle that lead to damage of the ankle ligaments. It is unknown if a 12.7% increase in ankle inversion is enough to precipitate a sprain. It is interesting to note that this increase in frontal plane movement is associated with a decrease in frontal plane ankle torque. Impulse and torque results will be discussed in the following sections.

Sagittal Plane Torque

Torque is a biomechanical property defined as the tendency of a force to rotate an object around an axis. In the body, the forces are created by muscle contraction and a joint creates the axis. So torque is the tendency of a muscle force to cause rotation around a joint center.[58] This study was designed to fatigue the quadriceps muscle. This muscle produces an extension torque at the knee. It was expected that this torque would decrease as the fatigue state increased. The sagittal plane knee data showed a 19.2% decrease in torque (Figure 15). In order to continue landing successfully, proximal and distal joints would be responsible for replacing this loss in knee torque. Data from this study showed that the hip increased torque production by 8.4% (Figure 14) and the ankle decreased by 5.3% (Figure 16). There is no statistically significant difference in these data ($p<0.5$), but the trends in these findings are consistent with the shift to a hip strategy during landing. In a similar study, Coventry et al. found contrasting hip torque data and reporting a

decrease of 8.9%. [56] They did, however, report similar trends in the knee and ankle torques with respective decreases of 7.1% and 13.0%.[56] The differences in the hip data may have been due to fatigue protocol differences.

Sagittal Plane Impulse

Hip extension, knee extension, and ankle plantar flexion impulse all decreased with fatigue. Joint impulse is an integration of joint torque information over time and represents the power produced by a joint. The sign of this value correlates with the direction of torque production. Joint impulses were computed and reported since they can be directly compared to Madigan and Pidcoe's data (Figures 17, 18, and 19). Madigan and Pidcoe reported decreases in knee extension and ankle plantar flexion impulse as well. A decrease in knee extension was expected because quadriceps muscles are responsible for knee extension. The overall higher impulse values, reported by Madigan and Pidcoe, were most likely attributed to the difference in jump height. The subjects in this study jumped from a lower jump height than Madigan's subjects thus leading to decreased knee impulses. [15] Like Madigan and Pidcoe's study ankle plantar flexion also decreased with fatigued and it was believed that this too was a result of increased plantar flexor fatigue.[15] Ankle impulse results were larger than those reported by Madigan and Pidcoe. [15] In Madigan and Pidcoe's study subjects were asked to land using a toe-heel strategy, whereas no landing strategies were specified in this study. Thus differences in ankle impulse may be a result of the variations in ankle landing strategies carried out by the subjects. The only subtle difference between these two studies was the opposing

trends in hip extension where Madigan and Pidcoe's observed an increase, but these trends are small.

Frontal Plane Torque

Frontal plane hip torque increased (+65.0%), knee increased (+5.0%), and ankle torque decreased (-13.6%) with fatigue (Figures 21-23). None of these changes were statistically significant ($p<0.5$). The hip data implies a trend towards an decreased in hip adduction during landing. The knee data implies no real change in frontal plane knee angle. These data are consistent with previous research. A study by Mclean et al. compared peak jump landing frontal plane joint torques pre and post fatigue in populations of females and males.[59] The study saw decreases in hip adduction by 9.6% in females and 3.7% in males. Both females and males saw a decrease in knee torque for a respective change of 30.0% and 42.9%.[59] The only gender difference was seen in ankle torque where females demonstrated a decrease of 75.0% and the males had an increase of 12.5%.[59] The decrease in knee torque was attributed to quadriceps muslce fatigue. The finding that only the females demonstrated decreases in ankle torque highlights possible performance differences due to gender and is consistent with reports of higher levels of ankle injuries among women.[59]

Time to Stabilization

The time to stabilization values from the accelerometer data were found to decrease with increasing fatigue. It decreased 32.5ms in the medial/lateral direction and 5.5ms in the anterior/posterior direction (Figures 32 and 33). A study by Brown and Mynark found that time to stabilization in the medial/lateral direction was larger in

groups with chronic ankle instability.[40] Mixed results were reported by Shaw who found that the TTS in the medial/lateral direction increased in individuals who did not wear a brace while the two braced groups reported decreased times to stabilization.[40] However, in a study by Wikstrom who performed a fatiguing protocol similar to ours they too found time to stabilization decreased with increasing fatigue .[41] Wikstrom acknowledge that the time to stabilization is a recent measure of neuromuscular control that incorporates both sensory and mechanical systems and thus can be used to assess the effects of fatigue on neuromuscular control and dynamic stability .[41] David et al. believed that chronic ankle instability (CAI) was a constraint in the sensorimotor system and that it interacted with other constraints in limiting the biological systems' attempt to organize optimally (i.e. effecting its balance) .[60] Balance is necessary when an external perturbation is applied. In response to external perturbation the components of the self-organizing network react to the influence of the higher brain center and peripheral inputs .[60] Individuals with CAI may not possess the ability to develop patterns in the presence of an external perturbation.[41] Thus the inability of the sensorimotor system to re-organize after an external perturbation in individuals with CAI leads to their increased TTS. Yet, the ability of healthy individuals to properly reorganize in a timely fashion keeps their TTS from increasing. Furthermore, a healthy individuals' ability to sense the onset of fatigue may enable them to adjust for delays in sensorimotor system reorganization leading to the decrease in TTS. An adjustment seen in this study was the increase in "stiffness" during the landing. Medial-lateral TTS measured from the forceplate correlated with these results (Figure 34).

Accelerometer Methodology Validation

Accelerometer temporal and spatial characteristics of magnitude and angular orientation were used to test the validity of the device as a dynamic measurement tool. As mentioned before, the correlation between vGRF and accelerometer magnitude was high (r^2=0.90), but the inverse relationship makes the accelerometer data unusable as a metric for monitoring fatigue (Figure 36).

The temporal relationship between medial-lateral acceleration and medial-lateral forceplate data was also found to be high (r^2=1.00). The medial-lateral TTS did not have a significant change associated with fatigue (Figure 32), but the trend was consistent with previous research. The accelerometer may be an effective tool for monitoring this variable.

The orientation data had a poor correlation when comparing kinematic data from the shoe with derived angular data from the medial-lateral channel of the accelerometer (Figure 39) (r^2=0.37). This was probably due to the impact of linear (translational) movement on the accelerometer aligned in the medial-lateral direction. It was hoped that this movement would be minimal since the measurement was taken after the foot made contact with the floor. The poor correlation suggests that this was not the case and that the angular orientation data was contaminated by linear translation data.

The temporal relationship of angular movement would not be as sensitive to this linear movement. The correlation of TTP angular accelerometer orientation with kinematic frontal plane foot position (inversion/eversion) is good (Figure 40) (r^2=0.85). This is another variable that may be easily monitored via a shoe mounted accelerometer.

Accelerometer angular orientation and foot inversion were chosen because they represent the rotation occurring at the ankle/foot joint. Increased rotation about this joint puts strain on the lateral ankle ligaments (i.e. the anterior talofibular and calcaneofibular ligaments). This can increase the potential for injury. The time to which the maximum rotations occurred were analyzed and once again a strong correlation was established between the two sets of temporal data.

The fact that there was such a strong correlation between the forceplate, kinematic sensors, and accelerometer, justifies a need for further exploration of this device and perhaps the inclusion of angular rate sensors that are insensitive to linear translations. Due to the strong correlation between the temporal data between the devices and the fact that the changes in time were associated with fatigue it implies that these changes can be used to indicate ankle fatigue in individuals.

Hypotheses

H1: The hypothesis that medial-lateral time-to-stabilization (TTS) during the impact phase of landing (0 to 200ms) will increase with lower extremity fatigue was found to be false. It was postulated that the decrease in TTS associated with fatigue was a result of a change in landing strategy, a shift toward the use of more proximal muscles (a hip strategy).

H2: The hypothesis that ankle and hip joint torque during the impact phase of landing (0 to 200ms) will increase with quadriceps muscle (knee joint) fatigue was found to be false. Hip torque increased and ankle torque decreased. The ankle torque may have

decreased because the fatigue protocol did not isolate the quadriceps muscles. The use of both proximal and distal joints is required when performing a squat. Anecdotally, some subjects did describe a burning sensation in their plantar flexors as the protocol progressed.

H3a: The hypothesis that accelerometer magnitude will be correlated with translational kinetic data during landing was found to be true. However, it was inversely correlated and may not be an appropriate indicator for monitoring fatigue.

H3b: The hypothesis that accelerometer rotational derivatives along an anterior-posterior foot axis will be correlated with rotational kinetic data during landing was found to be true. The temporal relationships may be the most sensitive to changes in fatigue.

Conclusion

The jump landing protocol was successful in inducing quadriceps muscle fatigue. This was confirmed by patterns in the vGRF and the sagittal/ frontal plane kinetics and kinematics data. Additionally, the use of the accelerometer for measuring time to stabilization was also found to be useful since the overall decrease in TTS was consistent with an overall decrease in COP path length, area, and velocity. All of these measurements characterize the dynamic stability at the foot and the ability of the

accelerometer to capture this measurement highlights its roles as a dynamic measurement device.

This research demonstrates that a tri-axial accelerometer mounted in the heel of a shoe can monitor some of the parameters known to change with lower extremity fatigue. Although spatial correlations are not high, the temporal correlations may be sufficient to warrant further exploration of the device. The addition of angular rate sensors may be the next logical step in the development of the device.

References

1. Mohammadi F. Comparison of 3 preventive methods to reduce the recurrence of ankle inversion sprains in male soccer players. *Am J Sports Med.* 2007;35(6):922-926.

2. Konradsen L, Bech L, Ehrenbjerg M, Nickelsen T. Seven years follow-up after ankle inversion trauma. *Scan J Med Sci Sports.* 2002;12(3):129-135.

3. Evans G, Hardcastle P, Frenyo A. Acute rupture of the lateral ligament of the ankle: to suture or not to suture? *J Bone Joint Surg Br.* 1984;66:209-212.

4. Anandacoomarasamy A, Barnsley L. Long term outcomes of inversion ankle injuries. *Br J Sports Med.* 2005;39(3).

5. Torg J. Athletic footwear and orthotic appliances. *Clin Sports Med.* 1982;1:157-175.

6. Smith R, Reischl S. Treatment of ankle sprains in young athletes. *Am J Sports Med.* 1986;14:465-471.

7. Freeman MAR, Dean MRE, Hanham IMF. The etiology and prevention of functional instability of the foot. *J Bone Joint Surg.* 1965;47B:678-685.

8. Harrington KD. Degenerative arthritis of the ankle secondary to longstanding lateral ligament instability. *J Bone Joint Surg Am.* 1979;61:354-361.

9. Gross P, Marti B. Risk of degenerative ankle joint disease in volleyball players: study of former elite athletes. *Int J Sports Med.* 1999;20:58-63.

10. Verhagen RAW, de Keizer G, van Dijk CN. Long-term follow-up of inversion trauma of the ankle. *Arch Orthop Trauma Surg.* 1995;114:92-96.

11. Schaap GR, de Keizer G, Marti K. Inversion trauma of the ankle. *Arch Orthop Trauma Surg.* 1989;108:272-275.

12. Injury Surveillance System. Sport specific injury data. Available at: <http://www1.ncaa.org/membership/ed_outreach/health-safety/iss/Reports2003-04>.Accessed April 3, 2004.

13. Shaw MY, Gribble PA, Frye JL. Ankle Bracing, Fatigue, and Time to Stabilization
in Collegiate Volleyball Athletes. *J. of Athletic Training*, 2008; 43(2): 164-71.

14. Salavanti M, Moghadam M, Ebrahimi, Arab AM. Changes in Postural Stability with Fatigue of Lower Extremity Frontal and Sagittal Plane Movers. *Gait & Posture*. 2007; 26: 214-218.

15. Madigan ML., Pidcoe P. Changes in Landing Biomechanics during a Fatiguing Landing Activity. *Journal of Electromyography and Kinesiology* 2003; 13:491-498.

16. DiStefano LJ, Padua DA, Brown CN, Guskiewicz KM. Lower Extremity Kinematics and Ground Reaction Forces after Prophylactic Lace-Up Ankle Bracing. *J. Athletic Training*. 2008; 43(3): 234-241.

17. Salci Y, Kentel BB, Heycan C, Akin S, Korkusuz F. Comparison of Landing Maneuvers between Male and Female College Volleyball Players. *Clin. Biomech*. 2004; 19 (6): 622-628.

18. Myers JB, Riemann BL, Hwang J, Fu FU, and Lephart SM. Effect of Peripheral Afferent Alteration of the Lateral Ankle Ligaments on Dynamic Stability. *Am. J. Sports Med.* 2003; 31(4): 498-506.

19. Dubin J. Ankle Sprain/Twisted Ankle. Dubin Chiropractic 2003; 1(14).

20. Emedicine Cite: Craig C Young: Foot and Ankle.Emedicine.medscape.com

21. Alderton AK., Mortiz U. and R. Moe-Nilssen. Forceplate and Accelerometer Measures for Evaluating the Effect of Muscle Fatigue on Postural Control During One-Legged Stance. *Physiotherapy Research International* 2003; 8(4): 187-199.

22. Winter DA. Human Balance and Posture Control during Standing and Walking. *Gait*
& Posture 1995; 3: 193-214.

23. Onell A. Quantifying Human Balance. Analysis of Forceplate Data. Uppsala: Uppsala University, dissertation, 1999.

24. Weinhandl, J.T., Smith, J.D., Finch, W.H., & Dugan, E.L. Effects of repetitive drop jumps on lower extremity landing mechanics. *American Society of Biomechanics Annual Meeting*, Palo Alto, CA, August, 2007.

25. Benjamise, A. et.al. Fatigue Alters Lower Extremity Kinematics during a Single-

Leg Stop-Jump Task. *Knee Surg Sports Traumatol. Arthrosc.* 2008; 16:400-407.

26. Christina KA., White SC., and L. Gilchrist. Effect of Localized Muscle Fatique on Vertical Ground Reaction Forces and Ankle Joint Motion during Running. *Human Movement Science* 2001; 20: 257-276.

27. Nigg BM, Cole GK & Bruggemann GP. Impact forces during heel-toe running. *Journal of Applied Biomechanics*, 1995; 11: 407-432.

28. Nyland JA, Shapiro R, Carbon DN, Nitz AJ, Malone TR. The Effect of Quadriceps Femoris, Hamstring, and Placebo Eccentric Fatigue on Knee and Ankle Dynamics during Crossover Cutting. *Knee Surgery, Sports Traumatology, Arthroscopy*,_1997; 25: 171-184.

29. Gage H. Accelerographic analysis of Human Gait. Washington DC: American Society for Mechanical Engineers, 1964.

30. Saunders J, Inman, V, Eberhart H. The Major Determinants in Normal and Pathological Gait. *J Bone Jnt Surg*., 1953; 35A: 543-58.

31. Teramoto K, Dufek J, and John Mercer. The Effects of Local Muscle Fatigue on Shock Attenuation for Female Runners. UNLV.

32. Voloshin A, Wosk J and Brull M. Force Wave Transmission through the Human Locomotor System, Trans. Of the ASME. *J of Biomechanical Eng*., 1981; 100: 48-50.

33. Wosk J and Voloshin A. Wave Attenuation in Skeletons of Young Healthy Persons. *J Biomech*.,1981; 14: 261-267.

34. Henriksen M., et.al. Test-Retest reliability of Trunk Accelerometric Gait Analysis. *Gait and Posture,* 2004; 19: 288-297.

35. Culhane KM, O'Connor M, Lyons D, and G.M. Lyons. Age and Ageing: Accelerometers in Rehabilitation Medicine for Older Adults. *Age and Ageing*, 2005; 34(6): 556-560.

36. Bouten CV, Westerterp KR, Verduin M, and J Janssen.Assessment of Energy Expenditure for Physical Activity using a Triaxial Accelerometer.*Med. Sci. in Sports Exerc.*, 1994; 26 (12): 1516-1523.

37. Bates, Ostering & Sawhill, 1983 (In-shoe measurements article)

38. Oatis, Carol. Kinesiology: The Mechanics and Pathomechanics of Human Movement. Philadelphia: Lippincott Williams & Wilkins, 2009.

39. Billing D. In-shoe Measurement for Biomechanical Monitoring.

40. Brown CA and Mynark R. Balance Deficits in Recreational Athletes with Chronic Ankle Instability. *J. of Athletic Training*, 2007; 42(3):367-73.

41. Wikstrom EA, Powers ME, Tillman MD. Dynamic Stabilization Time After Isokinetic and Functional Fatigue. *J. of Athletic Training*, 2004; 39(3): 247-53.

42. Forestier N, Teasdale N, Nougier V. Alteration of the Position Sense at the Ankle Induced by Muscular Fatigue in Humans. *Med. Sci. Sports Exercise*, 2002; 34(1):117-22.

43. Johnston RB 3rd, Howard ME, Cawley PW, Losse GM. Effect of Lower Extremity Muscular Fatigue on Motor Control Performance. *Med. Sci. Sports Exercise*, 1998; 30(12): 1703-7.

44. Ross SE and KM Guskiewicz. Examination of Static and Dynamic Postural Stability in Individuals with Functionally Stable and Unstable Ankles. *Clin. J. Sports Med.,* 2004; 14(6): 332-338.

45. Freeman M, Dean M, Hanham I. The Etiology and Prevention of Functional Stability of the Foot. *J. Bone Joint Surg. Br*., 1965; 47: 678-684.

46. Cordova ML, Ingersoll CD. Peroneus Longus Stretch Reflex Amplitude Increases after Ankle Brace Application. Br. *J. Sports Med.,* 2003; 37(3): 258-262.

47. Cavanagh, PR. A Technique for Averaging Center of Pressure Paths from a Force Platform. *J Biomech*., 1978; 11: 487-491.

48. Cho WH, Choi H. Center of Pressure (COP) during the Postural Balance Control of High-Heeled Woman. Proceedings of 2005 IEEE. Sept. 2004: 2761-2764.

49. Winter D. A. B. C. (Anatomy, Biomechanics, Control) of Balance during Standing
and Walking. Waterloo, Ontario: Waterloo Biomechanics Publisher; 1995.

50. Opila, KA, Wagner SS, Schiowitz S et. Al. Postural Alignment in Barefoot and High-Heeled Stance. *Spine*, 1988; 13:542-7.

51. Harringe ML, Halvorsen K, Renstrom P,Werner S. Postural Control Measured as the Center of Pressure Excursion in Young Female Gymnasts with Low Back Pain or Lower Extremity Injury. *Gait & Posture*, 2008; 28: 38-45.

52. Robinovitch SN, Heller B, Lui A, and J Cortez. Effect of Strength and Speed on Torque Development on Balance Recovery with the Ankle Strategy. *J. Neurophysiol*. 2002; 88(2): 613-620.

53. Lees A. Methods of Impact Absorption when Landing from a Jump. *Eng. Med*., 1981; 10(4): 207-211.

54. Devita P, Skelly WA. Effect of Landing Stiffness on Joint Kinetics and Energetics in the Lower Extremity. *Med. Sci. Sports Exerc*., 1992; 24: 108-115.

55. Zhang SN, Bates BT, Dufek JS. Contributions of Lower Extremity joints to Energy Dissipation during Landing. *Med. Sci. Sports Exerc*., 2000; 32: 812-819.

56. Coventry, E et. al. The Effect of Lower Extremity Fatigue on Shock Attenuation during Single-Leg Landing. *Clinical Biomechanics*, 2006; 21: 1090-1097.

57. Wheeless, CR. "Stance Phase of Gait." Wheeless Textbook of Orthopaedics. 2009. Data Trace Internet.12 Jul. 2009. <http://www.wheelessonline.com/ortho/stance_phase_of_gait>.

58. LeVeau, BR. Biomechanics of Human Motion.Philadelphia:W.B. Saunders Company, 1992.

59. Mclean et. al. Impact of Fatigue on Gender-Based High-Risk Landing Strategies. *Medicine & Science in Sports & Exercise,* 2007; 39 (3):502-514.

60. David K, Glazier P, Araujo D, Bartlett R. Movement Systems as Dynamical Systems: the Functional Role of Variability and its Implications for Sports Medicine. *Sports Med*., 2003; 33:245-260.

APPENDIX A

Statistical Analyses

Analysis of Variance was used to compare the means of the response variable (vGRF, hip joint flexion, knee joint flexion, etc.) at the eleven different levels of the normalized time (0, 0.1, 0.2, 0.3, etc.) Hence, the analysis of variance (ANOVA) was used to extend the two-sample t-test for testing the equality of the means of two populations or factor levels to a more general null hypothesis of comparing the equality of more than two means versus the alternative hypothesis of them not all being equal.

First, boxplots of the data were generated to explore the mean level of the response variable at each normalized time level as well as the distributional characteristics of the data at each normalized time level. As part of the ANOVA investigation, the boxplots, also called the box-and-whisker plots, of the response variable were generated at each normalized time interval level. In the plot, a line is drawn across the box at the median. The bottom of the box is at Q1, the first quantile (25^{th} percentile) and the top of the box is at Q3, the third quantile (75^{th} percentile). The whiskers are the lines that extend from the top and bottom of the box to the adjacent values. The adjacent values are the lowest and highest observations that are inside the regions defined with the lower limit at Q1- 1.5 *(Q3-Q1) and the upper limit at Q3 + 1.5*(Q3-Q1). Outliers are points outside of the lower and upper limits and are plotted with an asterick. If the data is normally distributed, the median line is in the middle of

the box and and the whiskers extend approximately the same distance from the top and bottom of the box.

For the ANOVA test, the general assumption is that the data at each of the normalized time interval levels are from a normal distribution with equal variances. Hence, the boxplots of the data at each level should be similar in shape. Furthermore, if the means of the data at the different levels are the same, then the median lines of the boxplots should be about the same. Figure A.1 is a boxplot of the peak vGRF 200ms after impact data values at the normalized time levels. The assumption of normality at each of the normalized levels appears to be valid although there are outliers for the normalized levels less than 0.7.

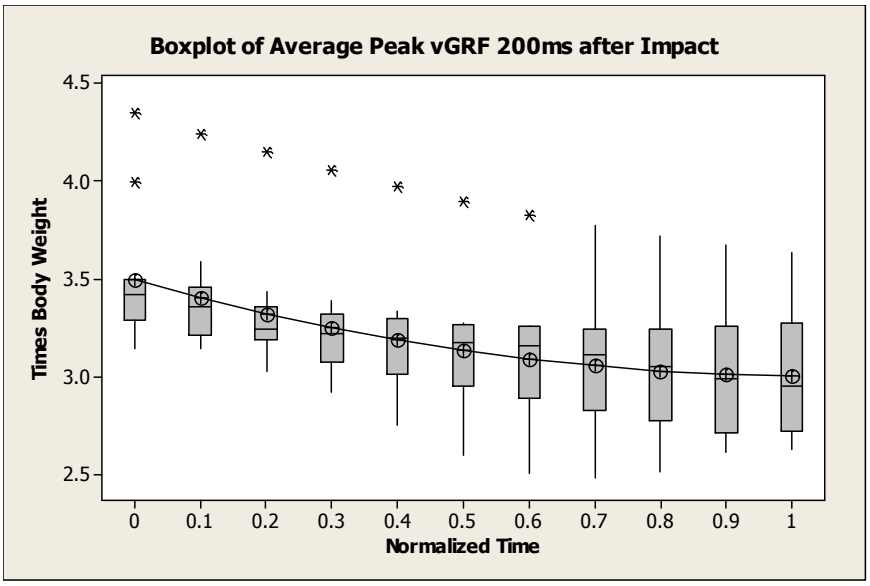

Figure A.1: Boxplot of Maximum vGRF

Interval plots of the data provided a plot of the group means at the normalized time levels with one standard error bar above and below the mean. These plots illustrate

a measure of central tendency and variability of the data. These plots were generated for each of the response variables in the study. The variability between the normalized time levels did not appear to be large relative to the variability within the normalized time levels given that the error bars tend to be similar in width and overlap in the interval plot. Figure A.2 shows the interval plot for the peak vGRF 200ms after impact.

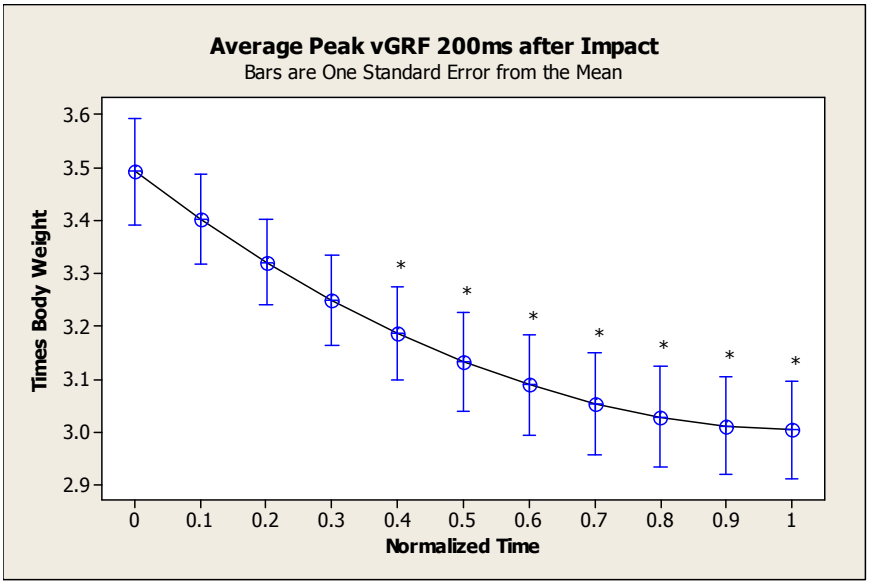

Figure A.2: Plot of Average Peak vGRF 200 ms after Impact

The Minitab 14 statistical software was used to generate the interval plots and boxplots of the data. In the ANOVA analyses of each response variable, all pairwise difference comparisons were performed using Fisher's least significant differences (LSD) to control the individual (comparison-wise) error rate at 5%. All pairwise comparisons of means were conducted using Tukey's method which allowed control of the family (experiment-wise) error rate. This helped to remove the potential of having an

unexpectedly high probability of making at least one Type I error (declaring a difference when there is none) among all the comparisons.

The One-Way ANOVA output consisted of an analysis of variance table, a table of level means, individual 95% confidence intervals, the individual standard deviations and the pooled standard deviation. The null hypothesis of no difference between means is rejected if and only if zero is not contained in the confidence interval. The F-test p-value is provided. Given that the alpha or significance level of the test is 0 .05, a p-value less that 0.05 is an indication that the null hypothesis should be rejected and there is evidence of differences among the means at the different normalized time interval levels.

The "HSU's MCB" output compares each mean with the best of the other means. For this study, the "best" level is the first or "un-fatigued" level. In some instances, the un-fatigued level is the "smallest" mean level and all other levels will be compared with the smallest mean. For others it is the "largest" mean level and all other mean levels with be compared with the largest mean. All of these analyses were conducted for the response variables in the study. The asterisks on the interval plot indicate that the ANOVA results indicated that there was a significant difference in the mean level of the peak vGRF values 200ms after impact at the "un-fatigued" normalized time (0) and the normalized time levels of 0.4 and higher.

TABLE A.1
MINITAB ANOVA OUTPUT FOR PEAK VGRF 200ms AFTER IMPACT

One-way ANOVA: 0, 0.1, 0.2, 0.3, 0.4, 0.5, 0.6, 0.7, 0.8, 0.9, 1

Source	DF	SS	MS	F	P
Factor	10	3.354	0.335	3.34	0.001
Error	121	12.159	0.100		
Total	131	15.512			

S = 0.3170 R-Sq = 21.62% R-Sq(adj) = 15.14%

Individual 95% CIs For Mean Based on Pooled StDev

Level	N	Mean	StDev	----------+---------+---------+---------+--
0	12	3.4912	0.3451	(-------*------)
0.1	12	3.4011	0.2963	(------*------)
0.2	12	3.3202	0.2824	(------*------)
0.3	12	3.2485	0.2914	(------*------)
0.4	12	3.1860	0.3087	(------*-------)
0.5	12	3.1327	0.3243	(------*-------)
0.6	12	3.0885	0.3332	(-------*------)
0.7	12	3.0535	0.3339	(------*------)
0.8	12	3.0277	0.3279	(------*------)
0.9	12	3.0111	0.3198	(------*-------)
1	12	3.0037	0.3179	(------*------)

-------+---------+---------+---------+--
3.00 3.25 3.50 3.75

Pooled StDev = 0.3170

Hsu's MCB (Multiple Comparisons with the Best)

Family error rate = 0.05
Critical value = 2.48

Intervals for level mean minus largest of other level means

Level	Lower	Center	Upper	---+---------+---------+---------+------
0	-0.2306	0.0901	0.4108	(---------*--------)

```
0.1    -0.4108  -0.0901  0.2306           (--------*---------)
0.2    -0.4917  -0.1710  0.1497         (--------*--------)
0.3    -0.5634  -0.2427  0.0781        (--------*--------)
0.4    -0.6259  -0.3052  0.0155       (--------*--------)
0.5    -0.6792  -0.3585  0.0000      (--------*---------)
0.6    -0.7234  -0.4027  0.0000    (--------*----------)
0.7    -0.7584  -0.4376  0.0000   (--------*----------)
0.8    -0.7842  -0.4634  0.0000   (--------*----------)
0.9    -0.8008  -0.4800  0.0000  (--------*----------)
1      -0.8082  -0.4875  0.0000  (--------*----------)
                         ---+---------+---------+---------+------
                         -0.70     -0.35      0.00      0.35
```

Tukey 95% Simultaneous Confidence Intervals
All Pairwise Comparisons

Individual confidence level = 99.86%

0 subtracted from:

```
      Lower   Center    Upper  --------+---------+---------+---------+-
0.1  -0.5147  -0.0901   0.3345         (-------*--------)
0.2  -0.5956  -0.1710   0.2536       (--------*-------)
0.3  -0.6673  -0.2427   0.1819       (--------*--------)
0.4  -0.7298  -0.3052   0.1194     (--------*-------)
0.5  -0.7831  -0.3585   0.0661    (--------*-------)
0.6  -0.8273  -0.4027   0.0219   (--------*-------)
0.7  -0.8622  -0.4376  -0.0131   (-------*--------)
0.8  -0.8880  -0.4634  -0.0388  (--------*-------)
0.9  -0.9046  -0.4800  -0.0554  (-------*--------)
1    -0.9121  -0.4875  -0.0629  (-------*--------)
                        --------+---------+---------+---------+-
                           -0.50      0.00      0.50      1.00
```

0.1 subtracted from:

```
      Lower   Center   Upper  --------+---------+---------+---------+-
0.2  -0.5055  -0.0809  0.3437         (-------*--------)
0.3  -0.5772  -0.1526  0.2720       (--------*-------)
0.4  -0.6397  -0.2151  0.2095      (--------*-------)
0.5  -0.6930  -0.2684  0.1562     (--------*-------)
```

```
0.6  -0.7372  -0.3126  0.1120     (--------*-------)
0.7  -0.7722  -0.3476  0.0770     (-------*--------)
0.8  -0.7980  -0.3734  0.0512    (--------*-------)
0.9  -0.8146  -0.3900  0.0346    (-------*--------)
1    -0.8220  -0.3974  0.0272    (-------*--------)
                        --------+---------+---------+---------+-
                           -0.50      0.00      0.50      1.00
```

0.2 subtracted from:

```
      Lower   Center   Upper  --------+---------+---------+---------+-
0.3  -0.4963  -0.0717  0.3529         (--------*-------)
0.4  -0.5588  -0.1342  0.2904         (-------*--------)
0.5  -0.6121  -0.1875  0.2371        (-------*--------)
0.6  -0.6563  -0.2317  0.1929       (-------*--------)
0.7  -0.6913  -0.2667  0.1579      (--------*-------)
0.8  -0.7171  -0.2925  0.1321      (-------*--------)
0.9  -0.7337  -0.3091  0.1155     (--------*-------)
1    -0.7411  -0.3165  0.1081     (--------*-------)
                        --------+---------+---------+---------+-
                           -0.50      0.00      0.50      1.00
```

0.3 subtracted from:

```
      Lower   Center   Upper  --------+---------+---------+---------+-
0.4  -0.4871  -0.0625  0.3621         (--------*-------)
0.5  -0.5404  -0.1158  0.3088        (--------*-------)
0.6  -0.5846  -0.1600  0.2646        (--------*-------)
0.7  -0.6196  -0.1950  0.2296        (-------*--------)
0.8  -0.6454  -0.2208  0.2038       (--------*-------)
0.9  -0.6620  -0.2374  0.1872       (-------*--------)
1    -0.6694  -0.2448  0.1798       (-------*--------)
                        --------+---------+---------+---------+-
                           -0.50      0.00      0.50      1.00
```

0.4 subtracted from:

```
      Lower   Center   Upper  --------+---------+---------+---------+-
0.5  -0.4779  -0.0533  0.3713         (--------*-------)
0.6  -0.5221  -0.0975  0.3271         (-------*--------)
0.7  -0.5571  -0.1325  0.2921        (-------*--------)
```

```
0.8  -0.5828  -0.1582  0.2663       (--------*-------)
0.9  -0.5995  -0.1749  0.2497       (--------*-------)
1    -0.6069  -0.1823  0.2423       (-------*--------)
                      --------+---------+---------+---------+-
                          -0.50      0.00      0.50      1.00
```

0.5 subtracted from:

```
      Lower   Center   Upper  --------+---------+---------+---------+-
0.6  -0.4688  -0.0442  0.3804         (-------*--------)
0.7  -0.5037  -0.0791  0.3454         (-------*--------)
0.8  -0.5295  -0.1049  0.3197         (--------*-------)
0.9  -0.5461  -0.1215  0.3031         (--------*-------)
1    -0.5536  -0.1290  0.2956         (-------*--------)
                      --------+---------+---------+---------+-
                          -0.50      0.00      0.50      1.00
```

0.6 subtracted from:

```
      Lower   Center   Upper  --------+---------+---------+---------+-
0.7  -0.4596  -0.0350  0.3896         (-------*--------)
0.8  -0.4853  -0.0608  0.3638         (--------*-------)
0.9  -0.5020  -0.0774  0.3472         (-------*--------)
1    -0.5094  -0.0848  0.3398         (-------*--------)
                      --------+---------+---------+---------+-
                          -0.50      0.00      0.50      1.00
```

0.7 subtracted from:

```
      Lower   Center   Upper  --------+---------+---------+---------+-
0.8  -0.4504  -0.0258  0.3988         (-------*--------)
0.9  -0.4670  -0.0424  0.3822         (-------*--------)
1    -0.4744  -0.0498  0.3748         (-------*-------)
                      --------+---------+---------+---------+-
                          -0.50      0.00      0.50      1.00
```

0.8 subtracted from:

```
      Lower   Center   Upper  --------+---------+---------+---------+-
0.9  -0.4412  -0.0166  0.4080         (--------*-------)
```

```
1    -0.4486  -0.0240  0.4006          (--------*-------)
                        --------+---------+---------+---------+-
                              -0.50      0.00      0.50      1.00
```

0.9 subtracted from:

```
    Lower   Center   Upper  --------+---------+---------+---------+-
1  -0.4320  -0.0074  0.4172          (--------*-------)
                      --------+---------+---------+---------+-
                            -0.50      0.00      0.50      1.00
```

Fisher 95% Individual Confidence Intervals
All Pairwise Comparisons

Simultaneous confidence level = 33.69%

0 subtracted from:

```
      Lower   Center    Upper   -+---------+---------+---------+--------
0.1  -0.3463  -0.0901   0.1661            (------*-------)
0.2  -0.4272  -0.1710   0.0852          (------*------)
0.3  -0.4989  -0.2427   0.0135        (------*------)
0.4  -0.5614  -0.3052  -0.0490       (------*-------)
0.5  -0.6147  -0.3585  -0.1023      (-------*------)
0.6  -0.6589  -0.4027  -0.1465     (------*-------)
0.7  -0.6939  -0.4376  -0.1814    (------*-------)
0.8  -0.7196  -0.4634  -0.2072   (-------*------)
0.9  -0.7362  -0.4800  -0.2238   (------*-------)
1    -0.7437  -0.4875  -0.2313   (------*------)
                        -+---------+---------+---------+--------
                      -0.70     -0.35      0.00      0.35
```

0.1 subtracted from:

```
      Lower   Center    Upper   -+---------+---------+---------+--------
0.2  -0.3371  -0.0809   0.1753            (-------*------)
0.3  -0.4088  -0.1526   0.1036          (-------*------)
0.4  -0.4713  -0.2151   0.0411          (------*------)
0.5  -0.5246  -0.2684  -0.0122        (------*-------)
0.6  -0.5688  -0.3126  -0.0564        (------*------)
```

```
0.7  -0.6038  -0.3476  -0.0914       (------*------)
0.8  -0.6296  -0.3734  -0.1172      (------*-------)
0.9  -0.6462  -0.3900  -0.1338      (------*------)
1    -0.6536  -0.3974  -0.1412     (-------*------)
                          -+---------+---------+---------+--------
                        -0.70     -0.35      0.00      0.35
```

0.2 subtracted from:

```
      Lower   Center    Upper    -+---------+---------+---------+--------
0.3  -0.3279  -0.0717   0.1845             (------*------)
0.4  -0.3904  -0.1342   0.1220           (------*------)
0.5  -0.4437  -0.1875   0.0687          (-------*------)
0.6  -0.4879  -0.2317   0.0245         (------*-------)
0.7  -0.5229  -0.2667  -0.0105         (------*-------)
0.8  -0.5487  -0.2925  -0.0363        (-------*------)
0.9  -0.5653  -0.3091  -0.0529        (------*------)
1    -0.5727  -0.3165  -0.0603       (------*------)
                         -+---------+---------+---------+--------
                       -0.70     -0.35      0.00      0.35
```

0.3 subtracted from:

```
      Lower   Center   Upper    -+---------+---------+---------+--------
0.4  -0.3187  -0.0625  0.1937             (------*-------)
0.5  -0.3720  -0.1158  0.1404           (-------*------)
0.6  -0.4162  -0.1600  0.0962          (------*-------)
0.7  -0.4512  -0.1950  0.0612          (------*-------)
0.8  -0.4770  -0.2208  0.0354         (-------*------)
0.9  -0.4936  -0.2374  0.0188         (------*-------)
1    -0.5010  -0.2448  0.0114        (------*------)
                        -+---------+---------+---------+--------
                      -0.70     -0.35      0.00      0.35
```

0.4 subtracted from:

```
      Lower   Center   Upper    -+---------+---------+---------+--------
0.5  -0.3095  -0.0533  0.2029             (------*-------)
0.6  -0.3537  -0.0975  0.1587            (------*-------)
0.7  -0.3887  -0.1325  0.1237           (------*-------)
0.8  -0.4145  -0.1582  0.0980          (------*-------)
```

```
0.9  -0.4311  -0.1749  0.0813          (------*------)
1    -0.4385  -0.1823  0.0739         (-------*------)
                        -+---------+---------+---------+--------
                       -0.70     -0.35      0.00      0.35
```

0.5 subtracted from:

```
      Lower   Center   Upper   -+---------+---------+---------+--------
0.6  -0.3004  -0.0442  0.2120           (-------*------)
0.7  -0.3354  -0.0791  0.1771           (-------*------)
0.8  -0.3611  -0.1049  0.1513           (------*------)
0.9  -0.3777  -0.1215  0.1347           (-------*------)
1    -0.3852  -0.1290  0.1272           (------*-------)
                        -+---------+---------+---------+--------
                       -0.70     -0.35      0.00      0.35
```

0.6 subtracted from:

```
      Lower   Center   Upper   -+---------+---------+---------+--------
0.7  -0.2912  -0.0350  0.2212           (------*------)
0.8  -0.3170  -0.0608  0.1955           (------*-------)
0.9  -0.3336  -0.0774  0.1788           (-------*------)
1    -0.3410  -0.0848  0.1714           (-------*------)
                        -+---------+---------+---------+--------
                       -0.70     -0.35      0.00      0.35
```

0.7 subtracted from:

```
      Lower   Center   Upper   -+---------+---------+---------+--------
0.8  -0.2820  -0.0258  0.2304           (------*-------)
0.9  -0.2986  -0.0424  0.2138           (-------*------)
1    -0.3060  -0.0498  0.2064           (-------*------)
                        -+---------+---------+---------+--------
                       -0.70     -0.35      0.00      0.35
```

0.8 subtracted from:

```
      Lower   Center   Upper   -+---------+---------+---------+--------
0.9  -0.2728  -0.0166  0.2396           (-------*------)
1    -0.2802  -0.0240  0.2322           (------*-------)
```

```
                    -+---------+---------+---------+--------
                   -0.70     -0.35      0.00      0.35
```

0.9 subtracted from:

```
    Lower   Center   Upper    -+---------+---------+---------+--------
1  -0.2636  -0.0074  0.2488              (-------*------)
                    -+---------+---------+---------+--------
                   -0.70     -0.35      0.00      0.35
```

Reference

MINITAB Reference Manual, Release 14, MINITAB Inc., July 2004.

APPENDIX B

The following pages contain a printout of the customized MATLAB™ software used to perform the analysis in this study.

Matlab Code

```
clear
close all
%Baseline Data %%%%%%%%%%%%%%%%%%%%%%%%%%%%%%%%%%%%%%%%%%%%%%%%%%%%%%%%%%%%%%%%
Wt=86.20;    %kg
Ht=1.71;     %meters
tbw=Wt*9.81; %Newtons
WtHt=Wt*Ht;
%%%%%%%%%%%%%%%%%%%%%%%%%%%%%%%%%%%%%%%%%%%%%%%%%%%%%%%%%%%%%%%%%%%%%%%%%%%%%%%%
data0=xlsread('ts050109a_0');
Frame0=data0(:,1); Hip0=data0(:,2); Knee0=data0(:,3); Ankle0=data0(:,4);
Foot0=data0(:,5); SacHt0=data0(:,6); ThighSM0=data0(:,7); ShankSM0=data0(:,8);
FootSM0=data0(:,9);
ThighFP0=data0(:,10); ShankFP0=data0(:,11); FootFP0=data0(:,12);
ThighFM0=data0(:,13); ShankFM0=data0(:,14); FootFM0=data0(:,15);
Accx0=data0(:,16);Accy0=data0(:,17);Accz0=data0(:,18);
fpm0=data0(:,19);fpx0=data0(:,20); fpy0=data0(:,21); fpAPM0=data0(:,22);
fpz0=data0(:,23);
%Orientation
%%%%%%%%%%%%%%%%%%%%%%%%%%%%%%%%%%%%%%%%%%%%%%%%%%%%%%%%%%%%%%%%%%%%%%%%%%%%%%%%
OrientMatrix=[0.865, 0.211,0.453;0.011,0.948,0.317;-0.224,-0.052,0.974];
   AccX0=((Accx0-1.5)./.3).*tbw;
   AccY0=((Accy0-1.5)./.3).*tbw;
   AccZ0=((Accz0-1.5)./.3).*tbw;
   AccMag0=sqrt(((AccX0).^2)+((AccY0).^2)+((AccZ0).^2));
VectorMatrix0=[AccX0,AccY0,AccZ0];
AccXX0=AccX0./tbw;AccYY0=AccY0./tbw;AccZZ0=AccZ0./tbw;
Vector0=VectorMatrix0*OrientMatrix;
VectorX0=Vector0(:,1);VectorY0=Vector0(:,2);VectorZ0=Vector0(:,3);
VecSquared0=sqrt((VectorX0.^2)+(VectorY0.^2)+(VectorZ0.^2));
VecNormX0=VectorX0./VecSquared0;
VecNormY0=VectorY0./VecSquared0;
VecNormZ0=VectorZ0./VecSquared0;
```

```
AngleX0=asind(VecNormX0(1:500));
%Averages %%%%%%%%%%%%%%%%%%%%%%%%%%%%%%%%%%%
AvgHip0=mean(Hip0);
AvgKnee0=mean(Knee0);
```

```
AvgAnkle0=mean(Ankle0);
AvgFoot0=mean(Foot0);
AvgCorVecNormX=mean(VecNormX0);
AvgCorVecNormY=mean(VecNormY0);
AvgCorVecNormZ=mean(VecNormZ0);
%%%%%%%%%%%%%%%%%%%%%%%%%%%%%%%%%%%%%%%%%%%%%%%%%%%%%%%%%%%%%%%%
jump=37;
for i=1:jump
   filename=['ts050109a_',num2str(i)];
   data=xlsread(filename);

Frame=data(:,1); Hip=data(:,2); Knee=data(:,3); Ankle=data(:,4);
Foot=data(:,5); SacHt=data(:,6); ThighSM=data(:,7); ShankSM=data(:,8);
FootSM=data(:,9);
ThighFP=data(:,10); ShankFP=data(:,11); FootFP=data(:,12);
ThighFM=data(:,13); ShankFM=data(:,14); FootFM=data(:,15);
Accx=data(:,16);Accy=data(:,17);Accz=data(:,18);
fpm=data(:,19);fpx=data(:,20); fpy=data(:,21); fpAPM=data(:,22);
fpz=data(:,23);

LF=length(Frame);
for j=1:LF
   AccX(j)=((Accx(j)-1.5)./.3).*tbw;
   AccY(j)=((Accy(j)-1.5)./.3).*tbw;
   AccZ(j)=((Accz(j)-1.5)./.3).*tbw;
   AccMag(j)=sqrt(((AccX(j)).^2)+((AccY(j)).^2)+((AccZ(j)).^2));

    if j>2
      if fpz(j-1)==0 && fpz(j)>1
      contacttime(i)=j;
      end
    end
end
%%%%%%%%%%%%%%%%%%%%%%%%%%%%%%%%%%%%%%%%%%%%%%%%%%%%%%%%%%%%%%%%
range200=contacttime(i):contacttime(i)+200;
range500=contacttime(i):contacttime(i)+500;
range1000=contacttime(i):contacttime(i)+1000;
range1500=contacttime(i):contacttime(i)+1500;
range450=contacttime(i)+55:contacttime(i)+555;
range415=contacttime(i)+15:contacttime(i)+515;
```

```
lr=length(range500);
%%%Accelerometer%%%%%%%%%%%%%%%%%%%%%%%%%%%%%%%%
AccelX(:,i)=((AccX)/tbw)';
AccelY(:,i)=((AccY)/tbw)';
AccelZ(:,i)=((AccZ)/tbw)';
AccelMag(:,i)=sqrt(((AccelX(range415,i)).^2)+((AccelY(range415,i)).^2)+((AccelZ(rang
e415,i)).^2));
[peakAccMag(i),peakAccMagtime(i)]=max(AccelMag(:,i));
%%%%%%%%%%%%%%%%%%%%%%%%%%%%%%%%%%%%%%%%%%%%%
VectorMatrix=[AccelX(range500,i),AccelY(range500,i),AccelZ(range500,i)];
AccelXvec(:,i)=AccelX(range500,i);
AccelYvec(:,i)=AccelY(range500,i);
AccelZvec(:,i)=AccelZ(range500,i);
AccelMagvec(:,i)=AccelMag(:,i);
%VectorMatrix=[Accx(range500),Accy(range500),Accz(range500)]; %original
Vector=VectorMatrix*OrientMatrix;
VectorX=Vector(:,1);
VectorY=Vector(:,2);
VectorZ=Vector(:,3);
VecSquared=sqrt((VectorX.^2)+(VectorY.^2)+(VectorZ.^2));
VecNormX(:,i)=VectorX./VecSquared;
VecNormY(:,i)=VectorY./VecSquared;
VecNormZ(:,i)=VectorZ./VecSquared;
%Vector=VectorMatrix*OrientMatrix;
[peakAccelX(i),timepeakAccelX(i)]=max(AccelX(range500,i)); %G's
[peakVecNormX(i),timepeakVecNormX(i)]=max(VecNormX(:,i)); %G's
NormXVecGs(:,i)=((VecNormX(:,i))-1.5/0.3); %G's
%%%%%%%%%%%%%%%%%%%%%%%%%%%%%%%%%%%%%%%%%%%%%
[MaxangleVecNormXs(i),TimeMaxangleVecNormXs(i)]=max(asind(VecNormX(1:200,i
)));
[MinangleVecNormXs(i),TimeMinangleVecNormXs(i)]=min(asind(VecNormX(1:200,i)
));
AngleX(:,i)=(asind(VecNormX(1:500,i)));
%Accelerometer Derivative/Jerk Calculation%%%%%%%%%%%%%%%%%%%
DiffAccX(:,i)=diff(AccelXvec(:,i));
DiffAccY(:,i)=diff(AccelYvec(:,i));
DiffAccZ(:,i)=diff(AccelZvec(:,i));
DiffAccelX(:,i)=diff(VecNormX(:,i));
DiffAccelY(:,i)=diff(VecNormY(:,i));
DiffAccelZ(:,i)=diff(VecNormZ(:,i));
```

```
ContactTime(i)=contacttime(i);
%Ground Force Reaction(vGRF)Ranges
%%%%%%%%%%%%%%%%%%%%%%%%%%%%%%%%%%%%%%%%%
fpmag(:,i)=fpm(range500)/tbw;
[maxfpmag(i),maxtimefpmag(i)]=max(fpm(range500)/tbw);
[minfpmag(i),mintimefpmag(i)]=min(fpm(range500)/tbw);
fpZ(:,i)=fpz;
fpZ200(:,i)=fpZ(range200);
fpZ500(:,i)=fpZ(range500);
FPZ(:,i)=fpz/tbw;
FPZ200(:,i)=FPZ(range200);
FPZ500(:,i)=FPZ(range500);
%Peak
vGRF%%%%%%%%%%%%%%%%%%%%%%%%%%%%%%%%%%%%%%
[vGRFpeak(i),vGRFpeaktime(i)]=max(FPZ(range200,i));
%Max Loading Rate%%%%%%%%%%%%%%%%%%%%%%%%%%%%%%%
[Rise,Run]=max(fpZ(range200,i));
RiseKN=Rise/1000;
RunS=Run/1000;
maxloadrate(i)=(RiseKN/RunS);
%Impulse: vGRF %%%%%%%%%%%%%%%%%%%%%%%%%%%%%%%%%%%
vGRFImp(i)=trapz((FPZ(range200,i))*0.001);
%Time to Stabilization%%%%%%%%%%%%%%%%%%%%%%%%%%%%%%
AvgCorVecX=mean(VecNormX0);
diffCorVecX(:,i)=(VecNormX(:,i))-AvgCorVecX;%
StdX(i)=std(diffCorVecX(:,i));

AvgCorVecY=mean(VecNormY0);
diffCorVecY(:,i)=(VecNormY(:,i))-AvgCorVecY;
StdY(i)=std(diffCorVecY(:,i));

AvgCorVecZ=mean(VecNormZ0);
diffCorVecZ(:,i)=(VecNormZ(:,i))-AvgCorVecZ;
StdZ(i)=std(diffCorVecZ(:,i));

for m=1:500
   if abs(diffCorVecX(m,i))>=StdX(i)
   ttsoutx(m,i)=1;
      if ttsoutx(m,i)==1
```

```
        ttscountx(i)=m;
       end
   else
   ttsoutx(m,i)=0;
   end
   if abs(diffCorVecY(m,i))>=StdY(i)
   ttsouty(m,i)=1;
      if ttsouty(m,i)==1
      ttscounty(i)=m;
      end
   else
   ttsouty(m,i)=0;
   end
   if abs(diffCorVecZ(m,i))>=StdZ(i)
   ttsoutz(m,i)=1;
      if ttsoutz(m,i)==1
      ttscountz(i)=m;
      end
      else
   ttsoutz(m,i)=0;
   end
end
%Flexion(degrees): Hip, Knee and Ankle%%%%%%%%%%%%%%%%%%%%%%
HipZeroed(:,i)=Hip-AvgHip0;
KneeZeroed(:,i)=Knee-AvgKnee0;
AnkleZeroed(:,i)=Ankle-AvgAnkle0;
FootZeroed(:,i)=Foot-AvgFoot0;
[HipMaxFlex(i),HipMaxFlexTime(i)]=max(HipZeroed(range500,i));
[KneeMaxFlex(i),KneeMaxFlexTime(i)]=max(KneeZeroed(range500,i));
[AnkleMaxFlex(i),AnkleMaxFlexTime(i)]=max(AnkleZeroed(range500,i));
[footMaxInv(i),footMaxInvTime(i)]=max(FootZeroed(range200,i));
[footMinInv(i),footMinInvTime(i)]=min(FootZeroed(range200,i));
HipZ(:,i)=HipZeroed(range500,i);
KneeZ(:,i)=KneeZeroed(range500,i);
AnkleZ(:,i)=AnkleZeroed(range500,i);
FootZ(:,i)=FootZeroed(range500,i);
%Saggital Plane Moments &
Impulses%%%%%%%%%%%%%%%%%%%%%%%%%%%%%%%%%%%%%%%%%%%%%%%%%%%%
%%%
ThighSM(:,i)=ThighSM/WtHt;
```

```
ThighSM500(:,i)=ThighSM(range500,i);
[ThighSMPeak(i),ThighSMTime(i)]=max(ThighSM(range200,i));
ThighSMImp(i)=trapz(ThighSM(range200,i))*0.001;%*0.2;

ShankSM(:,i)=ShankSM/WtHt;
ShankSM500(:,i)=ShankSM(range500,i);
[ShankSMPeak(i),ShankSMTime(i)]=max(ShankSM(range200,i));
ShankSMImp(i)=trapz(ShankSM(range200,i))*0.001;

FootSM(:,i)=FootSM/WtHt;
FootSM500(:,i)=FootSM(range500,i);
[FootSMPeak(i),FootSMTime(i)]=max(FootSM(range200,i));
FootSMImp(i)=trapz(FootSM(range200,i))*0.001;
%Frontal Plane Moments &
Impulses%%%%%%%%%%%%%%%%%%%%%%%%%%%%%%%%
ThighFM(:,i)=ThighFM/WtHt;
ThighFM500(:,i)=ThighFM(range500,i);
[ThighFMPeak(i),ThighFMTime(i)]=max(ThighFM(range200,i));
ThighFMImp(i)=trapz(ThighFM(range200,i))*0.001;

ShankFM(:,i)=ShankFM/WtHt;
ShankFM500(:,i)=ShankFM(range500,i);
[ShankFMPeak(i),ShankFMTime(i)]=max(ShankFM(range200,i));
ShankFMImp(i)=trapz(ShankFM(range200,i))*0.001;

FootFM(:,i)=FootFM/WtHt;
FootFM500(:,i)=FootFM(range500,i);
[FootFMPeak(i),FootFMTime(i)]=max(FootFM(range200,i));
FootFMImp(i)=trapz(FootFM(range200,i))*0.001;
%Sacral Height%%%%%%%%%%%%%%%%%%%%%%%%%%%%%%%%%%
aSacHt(:,i)=abs(SacHt);
[MaxSacHt(i),MaxSacHtTime(i)]=max(aSacHt(:,i));
%Center of Pressure%%%%%%%%%%%%%%%%%%%%%%%%%%%%%%%
copx(:,i)=fpx(range200);
diffx(:,i)=abs(diff(copx(:,i)));
pathlengthx(i)=sum(diffx(:,i));
[maxcopx(i)]=max(copx(:,i));
[mincopx(i)]=min(copx(:,i));
rangex(i)=maxcopx(i)-mincopx(i);
```

```
copy(:,i)=fpy(range200)';
diffy(:,i)=abs(diff(copy(:,i)));
pathlengthy(i)=sum(diffy(:,i));
[maxcopy(i)]=max(copy(:,i));
[mincopy(i)]=min(copy(:,i));
rangey(i)=maxcopy(i)-mincopy(i);

coparea(i)=rangex(i)*rangey(i);
coppathlength(i)=(sqrt(((pathlengthx(i)).^2)+((pathlengthy(i)).^2)));
copvelocity(i)=coppathlength(i)/0.2;
%%Moment
about%%Y%%%%%%%%%%%%%%%%%%%%%%%%%%%%%%%%%%%%%%%
%%%%%%%%%%%%%%%%%%%%%
fPAPM(:,i)=(fpAPM(range500))/tbw;
mm=1:500;
fPAPM500(:,i)=fPAPM(:,i);
StdFP(i)=std(fPAPM500(:,i));
for mm=1:500
    if abs(fPAPM500(mm,i))>=StdFP(i)
    fpapmout(mm,i)=1;
            if fpapmout(mm,i)==1
            fpapmnumber(i)=mm;
              end
     else
        fpapmout(mm,i)=0;
     end
end
%Data Derivatives%%%%%%%%%%%%%%%%%%%%%%%%%%%%%%%%%%%%
diffFPX(:,i)=diff(FPZ500(:,i));
Difffpapm(:,i)=diff(fPAPM(:,i));
%%%%%%%%%%%%%%%%%%%%%%%%%%%%%%%%%%%%%%%%%%%%%%%%%%%%%
normtime(i)=((i-1)/(jump-1));
%%%%%%%%%%%%%%%%%%%%%%%%%%%%%%%%%%%%%%%%%%%%%%%%%%%%%
figure(1)
ylim=[0 70];
for a=i
   x=[HipMaxFlexTime(a) HipMaxFlexTime(a)] ;
   plot(x,ylim)
   hold on
   plot(HipZ(:,a))
```

```
   title(['Hip FlexionTrial',num2str(a)])
   drawnow;
   trial(i)=a;
end

figure(2)
ylim=[0 70];
for a=i
   x=[KneeMaxFlexTime(a) KneeMaxFlexTime(a)] ;
   plot(x,ylim)
   hold on
   plot(KneeZ(:,a))
   title(['Knee Flexion Trial',num2str(a)])
   drawnow;
   trial(i)=a;
end

figure(3)
ylim=[-50 40];
for a=i
   x=[AnkleMaxFlexTime(a) AnkleMaxFlexTime(a)] ;
  plot(x,ylim)
   hold on
   plot(AnkleZ(:,a))
   title(['Ankle Flexion Trial',num2str(a)])
   drawnow;
   trial(i)=a;
end

figure(4)
ylim=[0 2];
for a=i
   x=[MaxSacHtTime(a) MaxSacHtTime(a)] ;
   plot(x,ylim)
   hold on
   plot(aSacHt(:,a))
   title(['Sacral Height Trial',num2str(a)])
   drawnow;
   trial(i)=a;
end
```

```
figure(5)
ylim=[0 6];
for a=i
    x=[peakAccMagtime(a) peakAccMagtime(a)];
    plot(x,ylim)
    hold on
    plot(AccelMag(:,a))
    title(['Peak Accel Mag',num2str(a)])
    drawnow;
    trial(i)=a;
end
figure(6)
PeakVGRF(:,i)=(FPZ(range200,i));
ylim=[0 4];
for a=i
    x=[vGRFpeaktime(a) vGRFpeaktime(a)];
    plot(x,ylim)
    hold on
   plot(PeakVGRF(:,a))
   title(['vGRF Trial',num2str(a)])
   drawnow;
    trial(i)=a;
end
trial(i)=i;
end
vGRF Data%%%%%%%%%%%%%%%%%%%%%%%%%%%%%%%%%%%%%
Trial=trial';
PEAKvGRFtime=vGRFpeaktime';
PEAKvGRF=vGRFpeak';
vPeak=vGRFpeak';
vGRFStoreTrialTimePeak=[Trial,PEAKvGRFtime,PEAKvGRF]
%%%%%%%%%%%%%%%%%%%%%%%%%%%%%%%%%%%%%%%%%%%%%
Trial=trial';
peakAccMag=peakAccMag';
peakAccMagtime=peakAccMagtime';
PeakAccMagStoreTrialTimePeak=[Trial,peakAccMagtime,peakAccMag]
%Hip Flex Data%%%%%%%%%%%%%%%%%%%%%%%%%%%%%%%%%%%%%
Trial=trial';
HipMaxFlexTime=HipMaxFlexTime';
HipMaxFlex=HipMaxFlex';
```

```
HipFlexStoreTrialTimePeak=[Trial,HipMaxFlexTime,HipMaxFlex]
%Knee Flex Data%%%%%%%%%%%%%%%%%%%%%%%%%%%%%%%%%%%%%%
KneeMaxFlexTime=KneeMaxFlexTime';
KneeMaxFlex=KneeMaxFlex';
KneeFlexStoreTrialTimePeak=[Trial,KneeMaxFlexTime,KneeMaxFlex]
%Ankle Flex Data%%%%%%%%%%%%%%%%%%%%%%%%%%%%%%%%%%%%%%%
Trial=trial';
AnkleMaxFlexTime=AnkleMaxFlexTime';
AnkleMaxFlex=AnkleMaxFlex';
AnkleFlexStoreTrialTimePeak=[Trial,AnkleMaxFlexTime,AnkleMaxFlex]
%Sacral Height%%%%%%%%%%%%%%%%%%%%%%%%%%%%%%%%%%%%%%
Trial=trial';
MaxSacHtTime=MaxSacHtTime';
MaxSacHt=MaxSacHt';
MaxSacHtStoreTrialTimePeak=[Trial,MaxSacHtTime,MaxSacHt]
%%%%%%%%%%%%%%%%%%%%%%%%%%%%%%%%%%%%%%%%%%%%%%%%%
AvgHip0=mean(Hip0)
AvgKnee0=mean(Knee0)
AvgAnkle0=mean(Ankle0)
AvgFoot0=mean(Foot0)
%%%%%%%%%%%%%%%%%%%%%%%%%%%%%%%%%%%%%%%%%%%%%%%%%%
initialvPeak=vPeak
figure(7)
NormTime=normtime';
pvPeak=polyfit(NormTime,vPeak,2);
pvalvPeak=polyval(pvPeak,NormTime);
plot(NormTime,vPeak,'g')
hold on
plot(NormTime,pvalvPeak,'k')

pvPeak1=pvPeak(1);
pvPeak2=pvPeak(2);
pvPeak3=pvPeak(3);

j=0;
for n=1:11
yvPeak(n)=(pvPeak1*((j)^2))+(pvPeak2*(j))+(pvPeak3);
xdata(n)=j;
j=j+0.1;
end
```

```
VPEAK=yvPeak'
xlabel('Normalized Time')
ylabel('Times BW')
title('vGRF Peak')
legend('Raw Data','2nd Order Polynomial Fit')
%%%%%%%%%%%%%%%%%%%%%%%%%%%
for g=1:length(vPeak)
   if vPeak(g)>=6
      vPeak(g)=(vPeak(g-1)+vPeak(g+1))/2;
   end
end
newvPeak=vPeak

figure(8)
NormTime=normtime';
pnewvPeak=polyfit(NormTime,newvPeak,2);
pvalnewvPeak=polyval(pnewvPeak,NormTime);
plot(NormTime,newvPeak,'g')
hold on
plot(NormTime,pvalnewvPeak,'k')

pnewvPeak1=pnewvPeak(1);
pnewvPeak2=pnewvPeak(2);
pnewvPeak3=pnewvPeak(3);

j=0;
for n=1:11
ynewvPeak(n)=(pnewvPeak1*((j)^2))+(pnewvPeak2*(j))+(pnewvPeak3);
xdata(n)=j;
j=j+0.1;
end
NEWVPEAK=ynewvPeak'
xlabel('Normalized Time')
ylabel('Times BW')
title('NEW vGRF Peak')
legend('Raw Data','2nd Order Polynomial Fit')
%%%%%%%%%%%%%%%%%%%%%%%%%%%%%%%%%%%%%%%%%%%%%
figure(9)
vGRFImpAll=vGRFImp';
ImpG=vGRFImpAll;
```

```
OldImpG=ImpG
pImpG=polyfit(NormTime,ImpG,2);
pvalImpG=polyval(pImpG,NormTime);
plot(NormTime,ImpG,'b')
hold on
plot(NormTime,pvalImpG,'r')

pImpG1=pImpG(1);
pImpG2=pImpG(2);
pImpG3=pImpG(3);

j=0;
for n=1:11
yImpG(n)=(pImpG1*((j)^2))+(pImpG2*(j))+(pImpG3);
xdata(n)=j;
j=j+0.1;
end
IMPG=yImpG'
%%%%%%%%%%%%%%%%%%%%%%%%%%
figure(10)
for g=1:length(ImpG)
   if ImpG(g)>=1
      ImpG(g)=(ImpG(g-1)+ImpG(g+1))/2;
   end
end
newImpG=ImpG

pnewImpG=polyfit(NormTime,newImpG,2);
pvalnewImpG=polyval(pnewImpG,NormTime);
plot(NormTime,newImpG,'b')
hold on
plot(NormTime,pvalnewImpG,'r')

pnewImpG1=pnewImpG(1);
pnewImpG2=pnewImpG(2);
pnewImpG3=pnewImpG(3);

j=0;
for n=1:11
ynewImpG(n)=(pnewImpG1*((j)^2))+(pnewImpG2*(j))+(pnewImpG3);
```

```
xdata(n)=j;
j=j+0.1;
end
newIMPG=ynewImpG'
%%%%%%%%%%%%%%%%%%%%%%%%%%%%%%%%%%%%%%%%%%%%%%%%%%%%%
figure(11)
HipMaxFlexAll=HipMaxFlex;
HipFlex=HipMaxFlexAll
HipMaxFlexTime=HipMaxFlexTime';

KneeMaxFlexAll=KneeMaxFlex;
KneeFlex=KneeMaxFlexAll
KneeMaxFlexTime=KneeMaxFlexTime';

AnkleMaxFlexAll=AnkleMaxFlex;
AnkleFlex=AnkleMaxFlexAll
AnkleMaxFlexTime=AnkleMaxFlexTime';
%%%%%%%%%%%%%%%%%%%%%%%%%%%%%%%%%%%%%%%%
for g=1:length(HipFlex)
   if HipFlex(g)>=180
      HipFlex(g)=(HipFlex(g-1)+HipFlex(g+1))/2;
   end
end
newHipFlex=HipFlex

subplot(3,1,1)
pnewHipFlex=polyfit(NormTime,newHipFlex,2);
pvalnewHipFlex=polyval(pnewHipFlex,NormTime);
plot(NormTime,pvalnewHipFlex,'g')
hold on
plot(NormTime,pvalnewHipFlex,'k')

pnewHipFlex1=pnewHipFlex(1);
pnewHipFlex2=pnewHipFlex(2);
pnewHipFlex3=pnewHipFlex(3);

j=0;
for n=1:11;
  ynewHipFlex(n)=(pnewHipFlex1*((j)^2))+(pnewHipFlex2*(j))+(pnewHipFlex3);
  xdata(n)=j;
```

```
  j=j+0.1;
end
NEWHIPFLEX=ynewHipFlex'
xlabel('Normalized Time')
ylabel('Hip Flexion (degrees)')
title('Average Hip Flexion')
legend('Raw Data','2nd Order Polynomial Fit')

subplot(3,1,2)
for g=1:length(KneeFlex)
    if KneeFlex(g)>=180
        KneeFlex(g)=(KneeFlex(g-1)+KneeFlex(g+1))/2;
    end
end
newKneeFlex=KneeFlex

pnewKneeFlex=polyfit(NormTime,newKneeFlex,2);
pvalnewKneeFlex=polyval(pnewKneeFlex,NormTime);
plot(NormTime,pvalnewKneeFlex,'g')
hold on
plot(NormTime,pvalnewKneeFlex,'k')

pnewKneeFlex1=pnewKneeFlex(1);
pnewKneeFlex2=pnewKneeFlex(2);
pnewKneeFlex3=pnewKneeFlex(3);

j=0;
for n=1:11;
  ynewKneeFlex(n)=(pnewKneeFlex1*((j)^2))+(pnewKneeFlex2*(j))+(pnewKneeFlex3);
  xdata(n)=j;
  j=j+0.1;
end
NEWKNEEFLEX=ynewKneeFlex'
xlabel('Normalized Time')
ylabel('Knee Flexion (degrees)')
title('Average Knee Flexion')
legend('Raw Data','2nd Order Polynomial Fit')

subplot(3,1,3)
```

```
for g=1:length(AnkleFlex)
   if AnkleFlex(g)>=180
      AnkleFlex(g)=(AnkleFlex(g-1)+AnkleFlex(g+1))/2;
   end
end
newAnkleFlex=AnkleFlex

pnewAnkleFlex=polyfit(NormTime,newAnkleFlex,2);
pvalnewAnkleFlex=polyval(pnewAnkleFlex,NormTime);
plot(NormTime,pvalnewAnkleFlex,'g')
hold on
plot(NormTime,pvalnewAnkleFlex,'k')

pnewAnkleFlex1=pnewAnkleFlex(1);
pnewAnkleFlex2=pnewAnkleFlex(2);
pnewAnkleFlex3=pnewAnkleFlex(3);

j=0;
for n=1:11;

ynewAnkleFlex(n)=(pnewAnkleFlex1*((j)^2))+(pnewAnkleFlex2*(j))+(pnewAnkleFlex
3);
  xdata(n)=j;
  j=j+0.1;
end
NEWANKLEFLEX=ynewAnkleFlex'
xlabel('Normalized Time')
ylabel('Ankle Flexion (degrees)')
title('Average Ankle Flexion')
legend('Raw Data','2nd Order Polynomial Fit')
%%%%%%%%%%%%%%%%%%%%%%%%%%%%%%%%%%%%%%%%%%%%%%%%%%%%%%%%%%%%%%%%%%%%%%%%%%%%
figure(12)
TTStimex=(ttscountx+1)'
TTStimey=(ttscounty+1)'

for g=1:length(TTStimex)
   if TTStimex(g)>=1000
      TTStimex(g)=(TTStimex(g-1)+TTStimex(g+1))/2;
   end
end
```

```
newTTStimex=TTStimex

subplot(3,1,1)
pnewTTStimex=polyfit(NormTime,newTTStimex,2);
pvalnewTTStimex=polyval(pnewTTStimex,NormTime);
plot(NormTime,newTTStimex,'g')
hold on
plot(NormTime,pvalnewTTStimex,'k')

pnewTTStimex1=pnewTTStimex(1);
pnewTTStimex2=pnewTTStimex(2);
pnewTTStimex3=pnewTTStimex(3);

j=0;
for n=1:11
ynewTTStimex(n)=(pnewTTStimex1*((j)^2))+(pnewTTStimex2*(j))+(pnewTTStimex3)
;
xdata(n)=j;
j=j+0.1;
end
NEWTTSTIMEX=ynewTTStimex'
xlabel('Normalized Time')
ylabel('Time (ms)')
title('Time to Stabilization in X Direction')
legend('Raw Data','2nd Order Polynomial Fit')

subplot(3,1,2)
for g=1:length(TTStimey)
   if TTStimey(g)>=1000
      TTStimey(g)=(TTStimey(g-1)+TTStimey(g+1))/2;
   end
end
newTTStimey=TTStimey

pnewTTStimey=polyfit(NormTime,newTTStimey,2);
pvalnewTTStimey=polyval(pnewTTStimey,NormTime);
plot(NormTime,newTTStimey,'g')
hold on
plot(NormTime,pvalnewTTStimey,'k')
```

```
pnewTTStimey1=pnewTTStimey(1);
pnewTTStimey2=pnewTTStimey(2);
pnewTTStimey3=pnewTTStimey(3);

j=0;
for n=1:11
ynewTTStimey(n)=(pnewTTStimey1*((j)^2))+(pnewTTStimey2*(j))+(pnewTTStimey3)
;
xdata(n)=j;
j=j+0.1;
end
NEWTTSTIMEY=ynewTTStimey'
xlabel('Normalized Time')
ylabel('Time (ms)')
title('Time to Stabilization in Y Direction')
legend('Raw Data','2nd Order Polynomial Fit')
%%%%%%%%%%%%%%%%%%%%%%%%%%%%%%%%%%%%%%%%%%%%%%%%%%%%%%%%%%%%%%%%%%%%%%%%%%%%
figure(13)
vGRFPeakTime=PEAKvGRFtime
for g=1:length(vGRFPeakTime)
   if vGRFPeakTime(g)<=2
      vGRFPeakTime(g)=(vGRFPeakTime(g-1)+vGRFPeakTime(g+1))/2;
   end
end
newvGRFPeakTime=vGRFPeakTime

pnewvGRFPeakTime=polyfit(NormTime,newvGRFPeakTime,2);
pvalnewvGRFPeakTime=polyval(pnewvGRFPeakTime,NormTime);
plot(NormTime,pvalnewvGRFPeakTime,'g')
hold on
plot(NormTime,pvalnewvGRFPeakTime,'k')

pnewvGRFPeakTime1=pnewvGRFPeakTime(1);
pnewvGRFPeakTime2=pnewvGRFPeakTime(2);
pnewvGRFPeakTime3=pnewvGRFPeakTime(3);

j=0;
for n=1:11;
```

```
ynewvGRFPeakTime(n)=(pnewvGRFPeakTime1*((j)^2))+(pnewvGRFPeakTime2*(j))+
(pnewvGRFPeakTime3);
  xdata(n)=j;
  j=j+0.1;
end
NEWVGRFPEAKTIME=ynewvGRFPeakTime'
xlabel('Normalized Time')
ylabel('Hip Flexion (degrees)')
title('Average Hip Flexion')
legend('Raw Data','2nd Order Polynomial Fit')
%%%%%%%%%%%%%%%%%%%%%%%%%%%%%%%%%%%%%%%%%%%%%%%%%%%%%%%%%%%%%%%%%%%%%%%%
figure(14)
MaxScHt=MaxSacHt
for g=1:length(MaxScHt)
    if MaxScHt(g)>=2
        MaxScHt(g)=(MaxScHt(g-1)+MaxScHt(g+1))/2;
    end
end
newMaxScHgt=MaxScHt

pnewMaxScHgt=polyfit(NormTime,newMaxScHgt,2);
pvalnewMaxScHgt=polyval(pnewMaxScHgt,NormTime);
plot(NormTime,pvalnewMaxScHgt,'g')
hold on
plot(NormTime,pvalnewMaxScHgt,'k')

pnewMaxScHgt1=pnewMaxScHgt(1);
pnewMaxScHgt2=pnewMaxScHgt(2);
pnewMaxScHgt3=pnewMaxScHgt(3);

j=0;
for n=1:11;

ynewMaxScHgt(n)=(pnewMaxScHgt1*((j)^2))+(pnewMaxScHgt2*(j))+(pnewMaxScHg
t3);
  xdata(n)=j;
  j=j+0.1;
end
NEWMAXSCHGT=ynewMaxScHgt'
```

```
xlabel('Normalized Time')
ylabel('Maximum Sacral Height (cm)')
title('Average Maximum Sacral Height')
legend('Raw Data','2nd Order Polynomial Fit')
%%%%%%%%%%%%%%%%%%%%%%%%%%%%%%%%%%%%%%%%%%%%%%
figure(15)
Maxfpmag=maxfpmag'
for g=1:length(Maxfpmag)
   if Maxfpmag(g)>=6
      Maxfpmag(g)=(Maxfpmag(g-1)+Maxfpmag(g+1))/2;
   end
end
newMaxfpmag=Maxfpmag

subplot(2,1,1)
pnewMaxfpmag=polyfit(NormTime,newMaxfpmag,2);
pvalnewMaxfpmag=polyval(pnewMaxfpmag,NormTime);
plot(NormTime,newMaxfpmag,'g')
hold on
plot(NormTime,pvalnewMaxfpmag,'k')

pnewMaxfpmag1=pnewMaxfpmag(1);
pnewMaxfpmag2=pnewMaxfpmag(2);
pnewMaxfpmag3=pnewMaxfpmag(3);

j=0;
for n=1:11
ynewMaxfpmag(n)=(pnewMaxfpmag1*((j)^2))+(pnewMaxfpmag2*(j))+(pnewMaxfpma
g3);
xdata(n)=j;
j=j+0.1;
end
NEWMAXFPMAG=ynewMaxfpmag'
xlabel('Normalized Time')
ylabel('Times Body Weight')
title('Maximum Forceplate Magnitude')
legend('Raw Data','2nd Order Polynomial Fit')

%%%%%%%%%%%%%%%%%%%%%%
MaxTimefpmag=maxtimefpmag'
```

```
for g=1:length(MaxTimefpmag)
   if MaxTimefpmag(g)<=2
      MaxTimefpmag(g)=(MaxTimefpmag(g-1)+MaxTimefpmag(g+1))/2;
   end
end
newMaxTimefpmag=MaxTimefpmag
subplot(2,1,2)
pnewMaxTimefpmag=polyfit(NormTime,newMaxTimefpmag,2);
pvalnewMaxTimefpmag=polyval(pnewMaxTimefpmag,NormTime);
plot(NormTime,newMaxTimefpmag,'g')
hold on
plot(NormTime,pvalnewMaxTimefpmag,'k')

pnewMaxTimefpmag1=pnewMaxTimefpmag(1);
pnewMaxTimefpmag2=pnewMaxTimefpmag(2);
pnewMaxTimefpmag3=pnewMaxTimefpmag(3);

j=0;
for n=1:11
ynewMaxTimefpmag(n)=(pnewMaxTimefpmag1*((j)^2))+(pnewMaxTimefpmag2*(j))+
(pnewMaxTimefpmag3);
xdata(n)=j;
j=j+0.1;
end
NEWMAXTIMEFPMAG=ynewMaxTimefpmag'
xlabel('Normalized Time')
ylabel('Time(ms)')
title('Time to Maximum Forceplate Magntiude')
legend('Raw Data','2nd Order Polynomial Fit')
%%%%%%%%%%%%%%%%%%%%%%%%%%%%%%%%%%%%%%%%%%%%%%%%%%%%%%%%%%%%%%%%%%%%%%%%%%%%
figure(16)
subplot(2,1,1)
MaxAngleVecNormXs=MaxangleVecNormXs'
for g=1:length(MaxAngleVecNormXs)
   if MaxAngleVecNormXs(g)>=180
      MaxAngleVecNormXs(g)=(MaxAngleVecNormXs(g-
1)+MaxAngleVecNormXs(g+1))/2;
   end
end
newMaxAngleVecNormXs=MaxAngleVecNormXs
```

```
pnewMaxAngleVecNormXs=polyfit(NormTime,newMaxAngleVecNormXs,2);
pvalnewMaxAngleVecNormXs=polyval(pnewMaxAngleVecNormXs,NormTime);
plot(NormTime,newMaxAngleVecNormXs,'g')
hold on
plot(NormTime,pvalnewMaxAngleVecNormXs,'k')

pnewMaxAngleVecNormXs1=pnewMaxAngleVecNormXs(1);
pnewMaxAngleVecNormXs2=pnewMaxAngleVecNormXs(2);
pnewMaxAngleVecNormXs3=pnewMaxAngleVecNormXs(3);

j=0;
for n=1:11
ynewMaxAngleVecNormXs(n)=(pnewMaxAngleVecNormXs1*((j)^2))+(pnewMaxAngl
eVecNormXs2*(j))+(pnewMaxAngleVecNormXs3);
xdata(n)=j;
j=j+0.1;
end
NEWMAXANGLEVECNORMXS=ynewMaxAngleVecNormXs'
xlabel('Normalized Time')
ylabel('Angle (degrees)')
title('Maximum Normalized Accelerometer Angle X')
legend('Raw Data','2nd Order Polynomial Fit')
%%%%%%%%%%%%%%%%%%%%%%%%%%%%%%%%%%%%
subplot(2,1,2)
TimeMaxAngleVecNormXs=TimeMaxangleVecNormXs'
for g=1:length(TimeMaxAngleVecNormXs)
   if TimeMaxAngleVecNormXs(g)<=2
      TimeMaxAngleVecNormXs(g)=(TimeMaxAngleVecNormXs(g-
1)+TimeMaxAngleVecNormXs(g+1))/2;
   end
end
newTimeMaxAngleVecNormXs=TimeMaxAngleVecNormXs

pnewTimeMaxAngleVecNormXs=polyfit(NormTime,newTimeMaxAngleVecNormXs,2
);
pvalnewTimeMaxAngleVecNormXs=polyval(pnewTimeMaxAngleVecNormXs,NormTi
me);
plot(NormTime,newTimeMaxAngleVecNormXs,'g')
hold on
```

```
plot(NormTime,pvalnewTimeMaxAngleVecNormXs,'k')

pnewTimeMaxAngleVecNormXs1=pnewTimeMaxAngleVecNormXs(1);
pnewTimeMaxAngleVecNormXs2=pnewTimeMaxAngleVecNormXs(2);
pnewTimeMaxAngleVecNormXs3=pnewTimeMaxAngleVecNormXs(3);

j=0;
for n=1:11
ynewTimeMaxAngleVecNormXs(n)=(pnewTimeMaxAngleVecNormXs1*((j)^2))+(pne
wTimeMaxAngleVecNormXs2*(j))+(pnewTimeMaxAngleVecNormXs3);
xdata(n)=j;
j=j+0.1;
end
NEWMAXTIMEANGLEVECNORMXS=ynewTimeMaxAngleVecNormXs'
xlabel('Normalized Time')
ylabel('Time (ms)')
title('Time to Maximum Normalized Accelerometer Angle X')
legend('Raw Data','2nd Order Polynomial Fit')
%%%%%%%%%%%%%%%%%%%%%%%%%%%%%%%%%%%%%%%%%%%%%%%%%%%%%%%%%%%%%%%%%%%%
figure(17)
FootMaxInv=footMaxInv'
for g=1:length(FootMaxInv)
   if FootMaxInv(g)>=180
      FootMaxInv(g)=(FootMaxInv(g-1)+FootMaxInv(g+1))/2;
   end
end
newFootMaxInv=FootMaxInv

subplot(2,1,1)
pnewFootMaxInv=polyfit(NormTime,newFootMaxInv,2);
pvalnewFootMaxInv=polyval(pnewFootMaxInv,NormTime);
plot(NormTime,newFootMaxInv,'g')
hold on
plot(NormTime,pvalnewFootMaxInv,'k')

pnewFootMaxInv1=pnewFootMaxInv(1);
pnewFootMaxInv2=pnewFootMaxInv(2);
pnewFootMaxInv3=pnewFootMaxInv(3);

j=0;
```

```
for n=1:11
ynewFootMaxInv(n)=(pnewFootMaxInv1*((j)^2))+(pnewFootMaxInv2*(j))+(pnewFoot
MaxInv3);
xdata(n)=j;
j=j+0.1;
end
NEWFOOTMAXINV=ynewFootMaxInv'
xlabel('Normalized Time')
ylabel('Angle (degrees)')
title('Maximum Foot Inversion')
legend('Raw Data','2nd Order Polynomial Fit')

subplot(2,1,2)
FootMaxInvTime=footMaxInvTime'
for g=1:length(FootMaxInvTime)
   if FootMaxInvTime(g)<=2
      FootMaxInvTime(g)=(FootMaxInvTime(g-1)+FootMaxInvTime(g+1))/2;
   end
end
newFootMaxInvTime=FootMaxInvTime

pnewFootMaxInvTime=polyfit(NormTime,newFootMaxInvTime,2);
pvalnewFootMaxInvTime=polyval(pnewFootMaxInvTime,NormTime);
plot(NormTime,newFootMaxInvTime,'g')
hold on
plot(NormTime,pvalnewFootMaxInvTime,'k')

pnewFootMaxInvTime1=pnewFootMaxInvTime(1);
pnewFootMaxInvTime2=pnewFootMaxInvTime(2);
pnewFootMaxInvTime3=pnewFootMaxInvTime(3);

j=0;
for n=1:11
ynewFootMaxInvTime(n)=(pnewFootMaxInvTime1*((j)^2))+(pnewFootMaxInvTime2*
(j))+(pnewFootMaxInvTime3);
xdata(n)=j;
j=j+0.1;
end
NEWFOOTMAXINVTIME=ynewFootMaxInvTime'
xlabel('Normalized Time')
```

```
ylabel('Time(ms)')
title('Time to Maximum Foot Inversion')
legend('Raw Data','2nd Order Polynomial Fit')
%%%%%%%%%%%%%%%%%%%%%%%%%%%%%%%%%%%%%%%%%
figure(18)
subplot(3,1,1)
ThighSMImpAll=ThighSMImp';
SHipImp=ThighSMImpAll
for g=1:length(SHipImp)
   if SHipImp(g)>=1
      SHipImp(g)=(SHipImp(g-1)+SHipImp(g+1))/2;
   end
end
newSHipImp=SHipImp

pnewSHipImp=polyfit(NormTime,newSHipImp,2);
pvalnewSHipImp=polyval(pnewSHipImp,NormTime);
plot(NormTime,newSHipImp,'g')
hold on
plot(NormTime,newSHipImp,'k')

pnewSHipImp1=pnewSHipImp(1);
pnewSHipImp2=pnewSHipImp(2);
pnewSHipImp3=pnewSHipImp(3);

j=0;
for n=1:11
ynewSHipImp(n)=(pnewSHipImp1*((j)^2))+(pnewSHipImp2*(j))+(pnewSHipImp3);
xdata(n)=j;
j=j+0.1;
end
NEWSHIPIMP=ynewSHipImp'
xlabel('Normalized Time')
ylabel('Time(ms)')
title('Maximum Saggital Plane Hip Impulse')
legend('Raw Data','2nd Order Polynomial Fit')

subplot(3,1,2)
ShankSMImpAll=ShankSMImp';
SKneeImp=ShankSMImpAll
```

```
for g=1:length(SKneeImp)
   if SKneeImp(g)>=1
      SKneeImp(g)=(SKneeImp(g-1)+SKneeImp(g+1))/2;
   end
end
newSKneeImp=SKneeImp

pnewSKneeImp=polyfit(NormTime,newSKneeImp,2);
pvalnewSKneeImp=polyval(pnewSKneeImp,NormTime);
plot(NormTime,newSKneeImp,'g')
hold on
plot(NormTime,newSKneeImp,'k')

pnewSKneeImp1=pnewSKneeImp(1);
pnewSKneeImp2=pnewSKneeImp(2);
pnewSKneeImp3=pnewSKneeImp(3);

j=0;
for n=1:11
ynewSKneeImp(n)=(pnewSKneeImp1*((j)^2))+(pnewSKneeImp2*(j))+(pnewSKneeImp
3);
xdata(n)=j;
j=j+0.1;
end
NEWSKNEEIMP=ynewSKneeImp'
xlabel('Normalized Time')
ylabel('Time(ms)')
title('Maximum Saggital Plane Knee Impulse')
legend('Raw Data','2nd Order Polynomial Fit')

subplot(3,1,3)
FootSMImpAll=FootSMImp';
SAnkleImp=FootSMImpAll
for g=1:length(SAnkleImp)
   if SAnkleImp(g)>=1
      SAnkleImp(g)=(SAnkleImp(g-1)+SAnkleImp(g+1))/2;
   end
end
newSAnkleImp=SAnkleImp
```

```
pnewSAnkleImp=polyfit(NormTime,newSAnkleImp,2);
pvalnewSAnkleImp=polyval(pnewSAnkleImp,NormTime);
plot(NormTime,newSAnkleImp,'g')
hold on
plot(NormTime,newSAnkleImp,'k')

pnewSAnkleImp1=pnewSAnkleImp(1);
pnewSAnkleImp2=pnewSAnkleImp(2);
pnewSAnkleImp3=pnewSAnkleImp(3);

j=0;
for n=1:11
ynewSAnkleImp(n)=(pnewSAnkleImp1*((j)^2))+(pnewSAnkleImp2*(j))+(pnewSAnkleI
mp3);
xdata(n)=j;
j=j+0.1;
end
NEWSAnkleImp=ynewSAnkleImp'
xlabel('Normalized Time')
ylabel('Time(ms)')
title('Maximum Saggital Plane Ankle Impulse')
legend('Raw Data','2nd Order Polynomial Fit')
%%%%%%%%%%%%%%%%%%%%%%%%%%%%%%%%%%%%%%%%%%%%%%%%%%%%%%%%%%%%%%%%%%%%%%%%%%%%
figure(19)
subplot(3,1,1)
ThighFMImpAll=ThighFMImp'
FHipImp=ThighFMImpAll
for g=1:length(FHipImp)
   if FHipImp(g)>=2
      FHipImp(g)=(FHipImp(g-1)+FHipImp(g+1))/2;
   end
end
newFHipImp=FHipImp

pnewFHipImp=polyfit(NormTime,newFHipImp,2);
pvalnewFHipImp=polyval(pnewFHipImp,NormTime);
plot(NormTime,newFHipImp,'g')
hold on
plot(NormTime,newFHipImp,'k')
```

```
pnewFHipImp1=pnewFHipImp(1);
pnewFHipImp2=pnewFHipImp(2);
pnewFHipImp3=pnewFHipImp(3);

j=0;
for n=1:11
ynewFHipImp(n)=(pnewFHipImp1*((j)^2))+(pnewFHipImp2*(j))+(pnewFHipImp3);
xdata(n)=j;
j=j+0.1;
end
NEWFHIPIMP=ynewFHipImp'
xlabel('Normalized Time')
ylabel('Time(ms)')
title('Maximum Frontal Plane Hip Impulse')
legend('Raw Data','2nd Order Polynomial Fit')

subplot(3,1,2)
ShankFMImpAll=ShankFMImp';
FKneeImp=ShankFMImpAll
for g=1:length(FKneeImp)
   if FKneeImp(g)>=2
      FKneeImp(g)=(FKneeImp(g-1)+FKneeImp(g+1))/2;
   end
end
newFKneeImp=FKneeImp

pnewFKneeImp=polyfit(NormTime,newFKneeImp,2);
pvalnewFKneeImp=polyval(pnewFKneeImp,NormTime);
plot(NormTime,newFKneeImp,'g')
hold on
plot(NormTime,newFKneeImp,'k')

pnewFKneeImp1=pnewFKneeImp(1);
pnewFKneeImp2=pnewFKneeImp(2);
pnewFKneeImp3=pnewFKneeImp(3);

j=0;
for n=1:11
ynewFKneeImp(n)=(pnewFKneeImp1*((j)^2))+(pnewFKneeImp2*(j))+(pnewFKneeImp
3);
```

```
xdata(n)=j;
j=j+0.1;
end
NEWFKNEEIMP=ynewFKneeImp'
xlabel('Normalized Time')
ylabel('Time(ms)')
title('Maximum Frontal Plane Knee Impulse')
legend('Raw Data','2nd Order Polynomial Fit')

subplot(3,1,3)
FootFMImpAll=FootFMImp';
FAnkleImp=FootFMImpAll
for g=1:length(FAnkleImp)
   if FAnkleImp(g)>=2
      FAnkleImp(g)=(FAnkleImp(g-1)+FAnkleImp(g+1))/2;
   end
end
newFAnkleImp=FAnkleImp

pnewFAnkleImp=polyfit(NormTime,newFAnkleImp,2);
pvalnewFAnkleImp=polyval(pnewFAnkleImp,NormTime);
plot(NormTime,newFAnkleImp,'g')
hold on
plot(NormTime,newFAnkleImp,'k')

pnewFAnkleImp1=pnewFAnkleImp(1);
pnewFAnkleImp2=pnewFAnkleImp(2);
pnewFAnkleImp3=pnewFAnkleImp(3);

j=0;
for n=1:11
ynewFAnkleImp(n)=(pnewFAnkleImp1*((j)^2))+(pnewFAnkleImp2*(j))+(pnewFAnkleI
mp3);
xdata(n)=j;
j=j+0.1;
end
NEWFAnkleImp=ynewFAnkleImp'
xlabel('Normalized Time')
ylabel('Time(ms)')
title('Maximum Fronital Plane Ankle Impulse')
```

```
legend('Raw Data','2nd Order Polynomial Fit')
%%%%%%%%%%%%%%%%%%%%%%%%%%%%%%%%%%%%%%%%
figure(20)
ThighSMPeakAll=ThighSMPeak';
SHipPeak=ThighSMPeakAll
for g=1:length(SHipPeak)
   if SHipPeak(g)>=10
      SHipPeak(g)=(SHipPeak(g-1)+SHipPeak(g+1))/2;
   end
end
newSHipPeak=SHipPeak

pnewSHipPeak=polyfit(NormTime,newSHipPeak,2);
pvalnewSHipPeak=polyval(pnewSHipPeak,NormTime);
plot(NormTime,newSHipPeak,'g')
hold on
plot(NormTime,newSHipPeak,'k')

pnewSHipPeak1=pnewSHipPeak(1);
pnewSHipPeak2=pnewSHipPeak(2);
pnewSHipPeak3=pnewSHipPeak(3);

j=0;
for n=1:11
ynewSHipPeak(n)=(pnewSHipPeak1*((j)^2))+(pnewSHipPeak2*(j))+(pnewSHipPeak3);
xdata(n)=j;
j=j+0.1;
end
NEWSHIPPEAK=ynewSHipPeak'
xlabel('Normalized Time')
ylabel('Torque(Nm/kg-m))')
title('Maximum Sagittal Plane Hip Torque')
legend('Raw Data','2nd Order Polynomial Fit')

ThighSMTimeAll=ThighSMTime';
SHipPeakTime=ThighSMTimeAll
%%%%%%%%%%%%%%%%%%%%%%%%%%%%%%%%%%%%%%%%
figure(21)
ShankSMPeakAll=ShankSMPeak';
SKneePeak=ShankSMPeakAll
```

```
for g=1:length(SKneePeak)
   if SKneePeak(g)>=10
      SKneePeak(g)=(SKneePeak(g-1)+SKneePeak(g+1))/2;
   end
end
newSKneePeak=SKneePeak

pnewSKneePeak=polyfit(NormTime,newSKneePeak,2);
pvalnewSKneePeak=polyval(pnewSKneePeak,NormTime);
plot(NormTime,newSKneePeak,'g')
hold on
plot(NormTime,newSKneePeak,'k')

pnewSKneePeak1=pnewSKneePeak(1);
pnewSKneePeak2=pnewSKneePeak(2);
pnewSKneePeak3=pnewSKneePeak(3);

j=0;
for n=1:11
ynewSKneePeak(n)=(pnewSKneePeak1*((j)^2))+(pnewSKneePeak2*(j))+(pnewSKneeP
eak3);
xdata(n)=j;
j=j+0.1;
end
NEWSKNEEPEAK=ynewSKneePeak'
xlabel('Normalized Time')
ylabel('Torque(Nm/kg-m))')
title('Maximum Sagittal Plane Knee Torque')
legend('Raw Data','2nd Order Polynomial Fit')
ShankSMTimeAll=ShankSMTime';
SKneePeakTime=ShankSMTimeAll
%%%%%%%%%%%%%%%%%%%%%%%%%%%%%%%%%%%%%%%%%%%%%%%%%%%%%%%%%%%%%%%%%%%%%%%%
figure(22)
FootSMPeakAll=FootSMPeak';
SAnklePeak=FootSMPeakAll
for g=1:length(SAnklePeak)
   if SAnklePeak(g)>=10
      SAnklePeak(g)=(SAnklePeak(g-1)+SAnklePeak(g+1))/2;
   end
end
```

```
newSAnklePeak=SAnklePeak

pnewSAnklePeak=polyfit(NormTime,newSAnklePeak,2);
pvalnewSKneePeak=polyval(pnewSAnklePeak,NormTime);
plot(NormTime,newSAnklePeak,'g')
hold on
plot(NormTime,newSAnklePeak,'k')

pnewSAnklePeak1=pnewSAnklePeak(1);
pnewSAnklePeak2=pnewSAnklePeak(2);
pnewSAnklePeak3=pnewSAnklePeak(3);

j=0;
for n=1:11
ynewSAnklePeak(n)=(pnewSAnklePeak1*((j)^2))+(pnewSAnklePeak2*(j))+(pnewSAnk
lePeak3);
xdata(n)=j;
j=j+0.1;
end
NEWSANKLEPEAK=ynewSAnklePeak'
xlabel('Normalized Time')
ylabel('Torque(Nm/kg-m))')
title('Maximum Sagittal Plane Ankle Torque')
legend('Raw Data','2nd Order Polynomial Fit')
FootSMTimeAll=FootSMTime';
SAnklePeakTime=FootSMTimeAll
%%%%%%%%%%%%%%%%%%%%%%%%%%%%%%%%%%%%%%%%%%%%%%%%%%%%%%%%%%%%%%%%%%%%%%%%%%%%
figure(23)
ThighFMPeakAll=ThighFMPeak';
FHipPeak=ThighFMPeakAll
for g=1:length(FHipPeak)
   if FHipPeak(g)>=10
      FHipPeak(g)=(FHipPeak(g-1)+FHipPeak(g+1))/2;
   end
end
newFHipPeak=FHipPeak

pnewFHipPeak=polyfit(NormTime,newFHipPeak,2);
pvalnewFHipPeak=polyval(pnewFHipPeak,NormTime);
plot(NormTime,newFHipPeak,'g')
```

```
hold on
plot(NormTime,newFHipPeak,'k')

pnewFHipPeak1=pnewFHipPeak(1);
pnewFHipPeak2=pnewFHipPeak(2);
pnewFHipPeak3=pnewFHipPeak(3);

j=0;
for n=1:11
ynewFHipPeak(n)=(pnewFHipPeak1*((j)^2))+(pnewFHipPeak2*(j))+(pnewFHipPeak3);
xdata(n)=j;
j=j+0.1;
end
NEWFHIPPEAK=ynewFHipPeak'
xlabel('Normalized Time')
ylabel('Torque(Nm/kg-m))')
title('Maximum Frontal Plane Hip Torque')
legend('Raw Data','2nd Order Polynomial Fit')
ThighFMTimeAll=ThighFMTime';
FHipPeakTime=ThighFMTimeAll
%%%%%%%%%%%%%%%%%%%%%%%%%%%%%%%%%%%%%%%%%%%%
figure(24)
ShankFMPeakAll=ShankFMPeak';
FKneePeak=ShankFMPeakAll
for g=1:length(FKneePeak)
   if FKneePeak(g)>=10
      FKneePeak(g)=(FKneePeak(g-1)+FKneePeak(g+1))/2;
   end
end
newFKneePeak=FKneePeak

pnewFKneePeak=polyfit(NormTime,newFKneePeak,2);
pvalnewFKneePeak=polyval(pnewFKneePeak,NormTime);
plot(NormTime,newFKneePeak,'g')
hold on
plot(NormTime,newFKneePeak,'k')

pnewFKneePeak1=pnewFKneePeak(1);
pnewFKneePeak2=pnewFKneePeak(2);
pnewFKneePeak3=pnewFKneePeak(3);
```

```
j=0;
for n=1:11
ynewFKneePeak(n)=(pnewFKneePeak1*((j)^2))+(pnewFKneePeak2*(j))+(pnewFKneeP
eak3);
xdata(n)=j;
j=j+0.1;
end
NEWFKNEEPEAK=ynewFKneePeak'
xlabel('Normalized Time')
ylabel('Torque(Nm/kg-m))')
title('Maximum Frontal Plane Knee Torque')
legend('Raw Data','2nd Order Polynomial Fit')

ShankFMTimeAll=ShankFMTime';
FKneePeakTime=ShankFMTimeAll
%%%%%%%%%%%%%%%%%%%%%%%%%%%%%%%%%%%%%%%%%%%%%%%%%%%%%%%%%%%%%%%%%%%%%%%%
figure(25)
FootFMPeakAll=FootFMPeak';
FAnklePeak=FootFMPeakAll
for g=1:length(FAnklePeak)
   if FAnklePeak(g)>=10
      FAnklePeak(g)=(FAnklePeak(g-1)+FAnklePeak(g+1))/2;
   end
end
newFAnklePeak=FAnklePeak

pnewFAnklePeak=polyfit(NormTime,newFAnklePeak,2);
pvalnewFKneePeak=polyval(pnewFAnklePeak,NormTime);
plot(NormTime,newFAnklePeak,'g')
hold on
plot(NormTime,newFAnklePeak,'k')

pnewFAnklePeak1=pnewFAnklePeak(1);
pnewFAnklePeak2=pnewFAnklePeak(2);
pnewFAnklePeak3=pnewFAnklePeak(3);

j=0;
for n=1:11
```

```
ynewFAnklePeak(n)=(pnewFAnklePeak1*((j)^2))+(pnewFAnklePeak2*(j))+(pnewFAnk
lePeak3);
xdata(n)=j;
j=j+0.1;
end
NEWFANKLEPEAK=ynewFAnklePeak'
xlabel('Normalized Time')
ylabel('Torque(Nm/kg-m))')
title('Maximum Frontal Plane Ankle Torque')
legend('Raw Data','2nd Order Polynomial Fit')
FootFMTimeAll=FootFMTime';
FAnklePeakTime=FootFMTimeAll
%%%%%%%%%%%%%%%%%%%%%%%%%%%%%%%%%%%%%%%%%%%%%%%%%%%%%%%%%%%%%%%%%%%%%%%%%%%%
figure(26)
subplot(2,1,1)
peakAccelMag=peakAccMag
for g=1:length(peakAccelMag)
   if peakAccelMag(g)>=10
      peakAccelMag(g)=(peakAccelMag(g-1)+peakAccelMag(g+1))/2;
   end
end
newpeakAccelMag=peakAccelMag

pnewpeakAccelMag=polyfit(NormTime,newpeakAccelMag,2);
pvalnewpeakAccelMag=polyval(pnewpeakAccelMag,NormTime);
plot(NormTime,newpeakAccelMag,'g')
hold on
plot(NormTime,pvalnewpeakAccelMag,'k')

pnewpeakAccelMag1=pnewpeakAccelMag(1);
pnewpeakAccelMag2=pnewpeakAccelMag(2);
pnewpeakAccelMag3=pnewpeakAccelMag(3);

j=0;
for n=1:11
ynewpeakAccelMag(n)=(pnewpeakAccelMag1*((j)^2))+(pnewpeakAccelMag2*(j))+(pn
ewpeakAccelMag3);
xdata(n)=j;
j=j+0.1;
end
```

```
NEWPEAKACCELMAG=ynewpeakAccelMag'
xlabel('Normalized Time')
ylabel('Area (cm2)')
title('Peak Accelerometer Magnitude Acceleration')
legend('Raw Data','2nd Order Polynomial Fit')

subplot(2,1,2)
PeakAccMagtime=peakAccMagtime
for g=1:length(PeakAccMagtime)
   if PeakAccMagtime(g)<=2
      PeakAccMagtime(g)=(PeakAccMagtime(g-1)+PeakAccMagtime(g+1))/2;
   end
end
newPeakAccMagtime=PeakAccMagtime

pnewPeakAccMagtime=polyfit(NormTime,newPeakAccMagtime,2);
pvalnewPeakAccMagtime=polyval(pnewPeakAccMagtime,NormTime);
plot(NormTime,newPeakAccMagtime,'g')
hold on
plot(NormTime,pvalnewPeakAccMagtime,'k')

pnewPeakAccMagtime1=pnewPeakAccMagtime(1);
pnewPeakAccMagtime2=pnewPeakAccMagtime(2);
pnewPeakAccMagtime3=pnewPeakAccMagtime(3);

j=0;
for n=1:11
ynewPeakAccMagtime(n)=(pnewPeakAccMagtime1*((j)^2))+(pnewPeakAccMagtime2*
(j))+(pnewPeakAccMagtime3);
xdata(n)=j;
j=j+0.1;
end
NEWPEAKACCELMAGTIME=ynewPeakAccMagtime'
xlabel('Normalized Time')
ylabel('Area (cm2)')
title('Time to Peak Accelerometer Magnitude Acceleration')
legend('Raw Data','2nd Order Polynomial Fit')
%%%%%%%%%%%%%%%%%%%%%%%%%%%%%%%%%%%%%%%%%%%%%%%%%%%%%%%%%%%%%%%%%%%%%%%%%%%%
figure(27)
CopArea=coparea'
```

```
for g=1:length(CopArea)
   if CopArea(g)==0
      CopArea(g)=(CopArea(g-1)+CopArea(g+1))/2;
   end
end
newCopArea=CopArea

pnewCopArea=polyfit(NormTime,newCopArea,2);
pvalnewCopArea=polyval(pnewCopArea,NormTime);
plot(NormTime,newCopArea,'g')
hold on
plot(NormTime,pvalnewCopArea,'k')

pnewCopArea1=pnewCopArea(1);
pnewCopArea2=pnewCopArea(2);
pnewCopArea3=pnewCopArea(3);

j=0;
for n=1:11
ynewCopArea(n)=(pnewCopArea1*((j)^2))+(pnewCopArea2*(j))+(pnewCopArea3);
xdata(n)=j;
j=j+0.1;
end
NEWCOPAREA=ynewCopArea'
xlabel('Normalized Time')
ylabel('Area (cm2)')
title('Center of Pressure Area')
legend('Raw Data','2nd Order Polynomial Fit')
%%%%%%%%%%%%%%%%%%%%%%%%%%%%%%%%%%%%%%%%%%%%%%%%%%%%%%%%%%%%%%%%%%%%%%%%%%%%%%%%
figure(28)
COPpathlength=coppathlength'
for g=1:length(COPpathlength)
   if COPpathlength(g)==0
      COPpathlength(g)=(COPpathlength(g-1)+COPpathlength(g+1))/2;
   end
end
newCOPpathlength=COPpathlength

pnewCOPpathlength=polyfit(NormTime,newCOPpathlength,2);
pvalnewCOPpathlength=polyval(pnewCOPpathlength,NormTime);
```

```
plot(NormTime,newCOPpathlength,'g')
hold on
plot(NormTime,pvalnewCOPpathlength,'k')

pnewCOPpathlength1=pnewCOPpathlength(1);
pnewCOPpathlength2=pnewCOPpathlength(2);
pnewCOPpathlength3=pnewCOPpathlength(3);

j=0;
for n=1:11
ynewCOPpathlength(n)=(pnewCOPpathlength1*((j)^2))+(pnewCOPpathlength2*(j))+(p
newCOPpathlength3);
xdata(n)=j;
j=j+0.1;
end
NEWCOPPATHLENGTH=ynewCOPpathlength'
xlabel('Normalized Time')
ylabel('Pathlength(cm)')
title('Center of Pressure Pathlength')
legend('Raw Data','2nd Order Polynomial Fit')
%%%%%%%%%%%%%%%%%%%%%%%%%%%%%%%%%%%%%%%%%%%%%%%%%%%%%%%%%%%%%%%%%%%%%%%%%%%%
figure(29)
COPvelocity=copvelocity'
for g=1:length(COPvelocity)
   if COPvelocity(g)==0
      COPvelocity(g)=(COPvelocity(g-1)+COPvelocity(g+1))/2;
   end
end
newCOPvelocity=COPvelocity

pnewCOPvelocity=polyfit(NormTime,newCOPvelocity,2);
pvalnewCOPvelocity=polyval(pnewCOPvelocity,NormTime);
plot(NormTime,newCOPvelocity,'g')
hold on
plot(NormTime,pvalnewCOPvelocity,'k')

pnewCOPvelocity1=pnewCOPvelocity(1);
pnewCOPvelocity2=pnewCOPvelocity(2);
pnewCOPvelocity3=pnewCOPvelocity(3);
```

```
j=0;
for n=1:11
ynewCOPvelocity(n)=(pnewCOPvelocity1*((j)^2))+(pnewCOPvelocity2*(j))+(pnewCO
Pvelocity3);
xdata(n)=j;
j=j+0.1;
end
NEWCOPVELOCITY=ynewCOPvelocity'
xlabel('Normalized Time')
ylabel('Velocity(cm/s)')
title('Center of Pressure Velocity')
legend('Raw Data','2nd Order Polynomial Fit')
%Time to Stabilization%%%%%%%%%%%%%%%%%%%%%%%%%%%%%%%%%%%%
figure(34)
plot(fPAPM(:,1),'b')
hold on
plot(fPAPM(:,jump),'k')
title('Frontal Plane AP Moment')
legend('First' ,'Last')
figure(35)
plot(fpapmout(:,1),'g')
hold on
plot(fpapmout(:,jump),'k')
figure(36)
FPapmnumber=fpapmnumber+1';
plot(FPapmnumber)
figure(37)
Xlim([0 500]);
Xl=Xlim;
Ycb=[StdFP(1) StdFP(1)];
Ycbn=[-StdFP(1) -StdFP(1)];
plot(Xl,Ycb,'g:')
hold on
plot(Xl,Ycbn,'g:')
hold on
plot(fPAPM500(:,1),'k')

figure(38)
FPAPMnumber=FPapmnumber';
for g=1:length(FPAPMnumber)
```

```
   if FPAPMnumber(g)<=2
      FPAPMnumber(g)=(FPAPMnumber(g-1)+FPAPMnumber(g+1))/2;
   end
end
newFPAPMnumber=FPAPMnumber

pnewFPAPMnumber=polyfit(NormTime,newFPAPMnumber,2);
pvalnewFPAPMnumber=polyval(pnewFPAPMnumber,NormTime);
plot(NormTime,newFPAPMnumber,'g')
hold on
plot(NormTime,pvalnewFPAPMnumber,'k')

pnewFPAPMnumber1=pnewFPAPMnumber(1);
pnewFPAPMnumber2=pnewFPAPMnumber(2);
pnewFPAPMnumber3=pnewFPAPMnumber(3);

j=0;
for n=1:11
ynewFPAPMnumber(n)=(pnewFPAPMnumber1*((j)^2))+(pnewFPAPMnumber2*(j))+(
pnewFPAPMnumber3);
xdata(n)=j;
j=j+0.1;
end
NEWFPAPMNUMBER=ynewFPAPMnumber'
xlabel('Normalized Time')
ylabel('Time(ms)')
title('Time to Stabilization for the Moment about Y')
legend('Raw Data','2nd Order Polynomial Fit')
```

VITA

Kristin Denise Morgan was born March 19, 1985 in Albany, New York. She graduated from Hampton Roads Academy, Newport News, Virginia in 2003. She received her Bachelor of Science in Biomedical Engineering from Duke University, Durham, North Carolina in 2007 before pursuing her Masters.